TECHNICAL REPORT No. 35

ENERGY BUDGET CALCULATIONS AT ECMWF

Part 1 Analyses 1980-81

by

E. Oriol

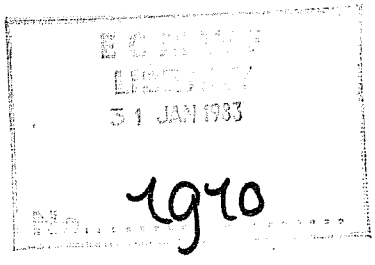

December 1982

C O N T E N T S PAGE

C O N T E N T S PAGE

Abstract

One year of energy budget data derived from ECMWF 12Z analyses for the period August 1980-July 1981 has been studied. Latitude-pressure cross-sections of monthly means, with special emphasis on January and July 1981, are presented and the results are compared with those obtained by other authors. A good agreement is found between them. The daily and seasonal variability of the parameters is discussed in some detail. The energy cycle of the atmosphere is described for this particular period.

1. INTRODUCTION

In recent years there has been increasing interest in the study of atmospheric energetics; in particular available potential energy, kinetic energy and their conversions, in relation to the general circulation of the atmosphere (Oort and Rasmusson 1971, Newell et al 1974, Speth 1975). It has been demonstrated that such calculations provide a useful diagnostic tool for the evaluation of the performance of numerical models (Manabe et al 1970, Tenenbaum 1976, Baker and Kung 1977). It was therefore of considerable interest to carry out such calculations here at ECMWF. The availability of several software packages which use different approaches has meant that it is possible to gain a fairly complete understanding of the behaviour of the energetics of the atmosphere and their simulation in the operational model.

The methodology used is discussed in Section 2. The nature of the data studied is presented in Section 3. In Section 4 the zonally averaged energetics is shown. In Section 5 there is a study of the partition into wavenumber groups using horizontal and vertical integrals. The daily variability of the terms is discussed in Section 6. The diabatic terms are studied in Section 7. The annual cycle of the energetics is shown in Section 8 and the overall energy cycle is discussed in Section 9. The conclusion with a brief summary are set out in Section 10.

2. METHODOLOGY

The data assimilation procedure used at ECMWF has been described by Lorenc et al (1977) and Lorenc (1981). Briefly, it is a 3-dimensional multivariate optimum interpolation scheme which uses a 6 hour forecast as a first guess, except above 50 mb where persistence and climatology are used. Analysed, pressure-level fields are interpolated to the ECMWF model grid on σ-levels, and initialized using a nonlinear normal mode technique (Temperton and Williamson 1981, Williamson and Temperton, 1981).

The present diagnostic scheme was introduced operationally in July 1980 and has been running almost without interruption since then. More than two years of daily data are available on tapes, together with their monthly means.

Calculations are performed on initialized analyses after their interpolation to the 13 standard pressure levels: 1000, 850, 700, 500, 400, 300, 250 , 200, 150, 100, 70, 50 and 30 mb. Six fields are used: u,v,w,T,q,Z from four analyses and twelve forecast steps every day, each of which is Fourier analysed with a resolution of up to wavenumber 96. Cospectra of these fields are calculated and in addition the values of the various energy terms and conversions (using the formulae given in Appendix A1). The resulting spectra, cospectra and energetics are then re-evaluated on latitude lines separated by 3 degrees.

The amount of data stored daily is summarized in Table 1. For the main fields wave numbers 1-15 are kept separately and waves 16 to 96 are grouped together. The other fields have been stored in wave groups: 1-3 (long waves), 4-9 (medium waves), 10-15 (short waves), 16-96 (very short waves).

Monthly means are calculated from the daily values without separating the standing from the transient part of the eddies. A special study, using data from another source to assess the contributions of the standing and transient

Table 1 **Latitude-pressure cross-section diagnostics.**

1. Spectra (zonal mean, wavenumbers 1 to 15, sum of higher wavenumbers)

   geopotential height
   temperature
   u - zonal wind component
   v - meridional component
   ω - vertical wind component in pressure coordinates
   q - specific humidity

2. Cospectra in four wavenumber groups (1-3, 4-9, 10-15, higher wavenumbers)

   $\omega\phi$ - vertical geopotential flux
   $v\phi$ - meridional geopotential flux
   $v\omega$

3. Cospectra in five wavenumber groups (same as 2 plus zonal mean)

   uv - meridional momentum flux
   $u\omega$ - vertical momentum flux
   Tv - meridional flux of sensible heat
   $T\omega$ - vertical flux of sensible heat
   qv - meridional flux of humidity
   $q\omega$ - vertical flux of humidity

4. Energetics in four or five wavenumber groups (same as 2 or 3)

K - kinetic energy
A - available potential energy
C - conversion between K and A
CK - transfer between eddy and zonal kinetic energy
CA - transfer between eddy and zonal available potential energy
LK - transfer between different wavenumber groups of kinetic energy

components is described in Section 4.2.

The present work concentrates mainly on the results of energy budget calculations for the 12Z analyses for one year of data (August 1980 to July 1981); the most detailed investigations being based on the January and July results.

2.1 Energetics

A convenient and compact way of presenting energy calculations was suggested by Lorenz in 1955. The potential energy which is available to be converted into kinetic energy of motion can be partitioned into AZ, the energy in the zonally averaged state, and AE or energy in non axisymmetric flow. The kinetic energy K can be treated similarly.

The following energy equations are used in this study:

$$\frac{\partial AZ}{\partial t} = -CA - CZ + GZ$$

$$\frac{\partial AE}{\partial t} = CA - CE + GE$$

$$\frac{\partial KZ}{\partial t} = CZ - CK - DZ$$

$$\frac{\partial KE}{\partial t} = CE + CK - DE$$

where CA is the conversion from zonal to eddy available potential energy, CE the conversion from eddy available potential to eddy kinetic energy, CK the conversion from zonal to eddy kinetic energy and CZ the conversion from zonal available potential to zonal kinetic energy, as illustrated in the following diagram:

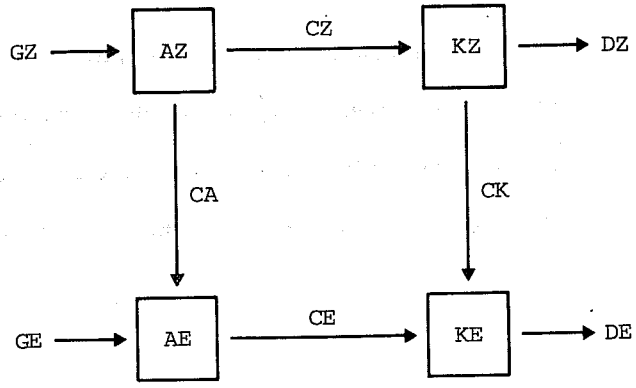

GZ and GE represent generation of zonal and eddy available potential energy, respectively. DZ and DE denote the dissipation of zonal and eddy kinetic energy. These four parameters (GZ,GE,DZ,DE) are calculated as residuals from the conversions.

The energy terms described above can be decomposed into their wave components, as suggested by Saltzmann in 1957. In doing that the redistribution of the eddy components between the different waves should be calculated. Here only the values of LK, corresponding to the nonlinear redistribution of eddy kinetic energy have been evaluated; results are available since November 1980.

3. DATA USED

Some considerations regarding the homogeneity of the data studied and other details are given in this Section.

3.1 Changes in the analyses scheme

When considering at the annual cycle of the terms calculated here, two main problems arise; the fluctuation in the synoptic situation (which could be smoothed out only by a large sample) and changes in the operational analysis scheme during the year under consideration. Some changes have little or no impact on the results but others do, as will be shown later on.

3.1.1 Virtual temperature

The first significant correction introduced during the period of this study took place in November 1980. It removed an error in the treatment of virtual temperature throughout the analysis/initialization/forecast sequence. Prior to the change, temperatures were too warm notably in the tropical troposphere.

3.1.2 Smoothing of analysis across box boundaries

The analysis is done in 6° x 6° boxes. On the 25 November 1980, a scheme to smooth the analysis across the box boundaries was introduced. It consists of extending the central analysis box half a box length in each direction so, on average, each gridpoint is analysed 4 times from different box-clusters. This resulted in a reduction in the noise of the initialized data, particularly for the eddy part of the flow.

3.1.3 Revision of vertical interpolation

The data assimilation scheme consists of 3 main steps: a 6 hour forecast - the first guess - an analyis of the deviations between the first guess and the observed data, and a normal mode initialization. The first and last step are done on σ levels whereas the analyses is carried out on pressure levels, this necessitates interpolations between σ and p co-ordinates. A considerable reduction of the interpolation error was obtained by interpolating the analysed increment instead of the full fields. This was implemented in December 1980. The boundary layer structure and stratospheric temperatures were improved as a result. However, a further correction was needed in the stratosphere (introduced in May 1981). The impact of this modification will be discussed in more detail in Sect.4.5.

3.1.4 Use of Australian surface pressure analysis

In March 1981 the use of PAOBS (pseudo observations) was introduced. These are manually derived surface pressure observations. The digitized reports are treated as synoptic observations.

3.1.5 Reintroduction of humidity analysis

In March objective analysis of humidity was re-introduced, prior to this the humidity analysis was the first guess - a six hour forecast.

3.1.6 Revised specification of orography

The last change which may have an important impact in the data presented here is the introduction of a new, more realistic, orography in April 1981 (Tibaldi and Geleyn, 1981). Some problems occurred regarding convective precipitation in mountaineous areas; these were corrected in October 1981 with a better diffusion scheme. This change did not affect the results of this investigation.

3.2 Initialized and uninitialized analyses

The data used here are based on initialized analyses which are known to undergo a damping of the zonally averaged divergent flow in the tropics (Temperton 1980). The normal mode initialization method affects all the terms related to vertical eddy fluxes such as CA, CE and in particular CZ, which experience a noticeable smoothing both in the tropics and mid-latitudes (see Appendix A2 for a case study). This damping should be taken into account especially when initialized analyses are compared with forecasts. Diabatic forcing was included in the initialization scheme introduced in September 1982 to overcome this problem.

3.3 Comparisons between the daily analyses

The most common analysis time used in climatological studies is 12Z and the majority of this report deals with these. However since there are daily 4 analyses available, each separated by 6 hours, comparisons have been made between them. In principle, differences between the analyses can be due either to the quantity or type of data received (Miller and Hayden 1978) or to a dynamical response to the diurnal cycle. It is difficult to separate these aspects.

Since the model providing the first guess for the analysis scheme does not have an explicit diurnal cycle, it is possible that this is underestimated in the analysis. The best data coverage usually occurs at 12Z, when the greatest number of synops are received, and 00Z. Satellite data are well spread out in time so that in the Southern Hemisphere, which has large spatial gaps in conventional data, the results should be less dependent on the time of the day.

Annual means of energetic terms for the different times are presented in Table 2, for Northern and Southern Hemispheres. There is not much difference between them. The values for 12Z are generally slightly higher than the rest; only the KZ term has higher values at 18Z in both hemispheres; AZ and CE are variable; minima are usually found at 6Z. The differences between values at 12Z and the rest are fairly small with a maximum variability of 15% in CZ. AE has a variability of 6% and CK of 4%.

From these considerations it can be concluded that for the purposes of this report it is sufficient to use only the 12Z analyses.

Table 2 **One year means of integrated Northern and Southern Hemisphere energy modes and conversions for 4 different analysis steps. Units: KJ/m^2 and W/m^2.**

	TIME	AZ	AE	KZ	KE	CA	CK	CZ	CE
NH	00Z	3644	500	580	699	1.74	-.45	-.20	1.88
	06Z	3617	485	580	704	1.71	-.46	-.23	1.89
	12Z	3654	516	577	707	1.75	-.47	-.20	1.90
	18Z	3646	492	585	703	1.74	-.47	-.20	1.95
SH	00Z	4798	334	913	668	2.03	-.70	-.38	1.69
	06Z	4789	327	934	659	1.99	-.69	-.38	1.87
	12Z	4833	346	929	669	2.06	-.71	-.38	1.95
	18Z	4938	341	941	659	2.03	-.68	-.38	1.91

4. ZONAL MEANS OF ENERGETICS

A convenient way of studying the energetics is by means of North-South cross sections of zonal means. The two months January and July 1981 will be discussed. Data from other sources have been included in the plots; comparisons will be made in Sect. 4.3.

4.1 Latitude-pressure cross-sections

4.1.1 Zonal kinetic energy

The maximum values of the zonal kinetic energy KZ (Fig. 1) coincide with the position of the jets. These maxima amount to 50 and 107 $J/m^2/P$ at 50°S and 30°N around 200 mb for January; the polar night jet is also indicated at 65°N. In July the values have changed to 82 and 22 $J/m^2/P$ at 30°S and 45°N respectively. This exhibits the larger annual variability in the Northern Hemisphere, compared to the Southern Hemisphere, and is seen often in other parameters. The maximumm at 10°N in the July stratosphere corresponds to the easterly flow established in the tropics during the month. The summer mid-latitude stratosphere shows little amplitude in both months due to the weak easterly flow at these levels and times. A connection with the quasi-biennial oscillation in the tropics cannot be found here; this is due to the particular period of study, as shown in Appendix A3.

4.1.2 Zonal available potential energy

The zonal available potential energy AZ represents available potential energy due to the deviation of the zonal mean temperature from its global average (Fig. 2). Maxima occur in the polar regions of both hemispheres at 500 mb in January, indicating a rapid decrease in temperature poleward of latitude 45°. Both maxima have similar values, in excess of 300 $J/m^2/P$. In July higher values are concentrated in southern polar regions where there are values greater than 100 $J/m^2/P$ between 50°S and the Pole; the Northern Hemisphere values are negligible. In both months the mid-latitude 400 mb level shows relatively higher values associated with a minimum in the static stability.

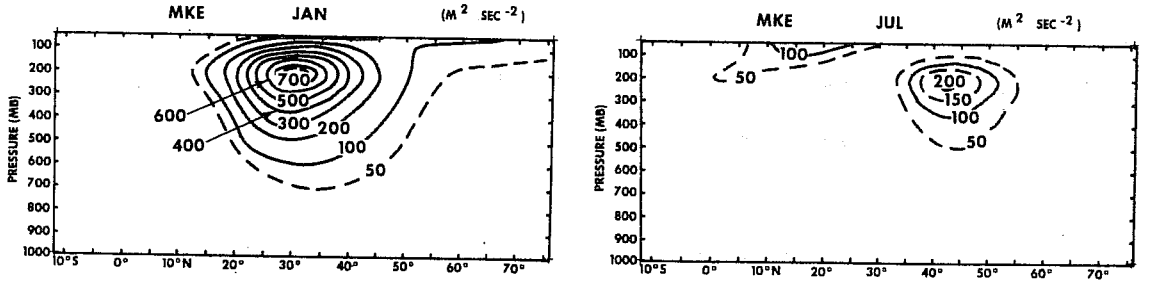

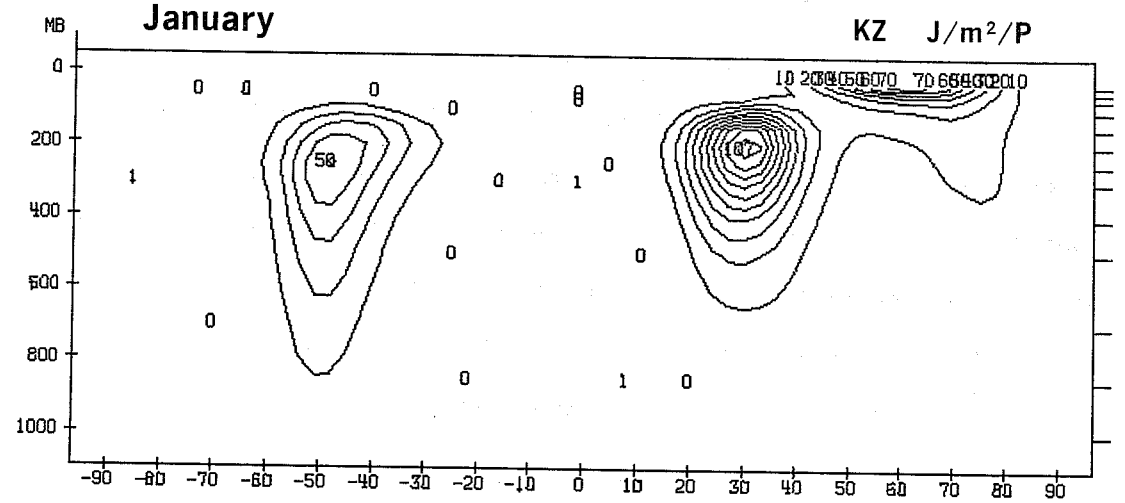

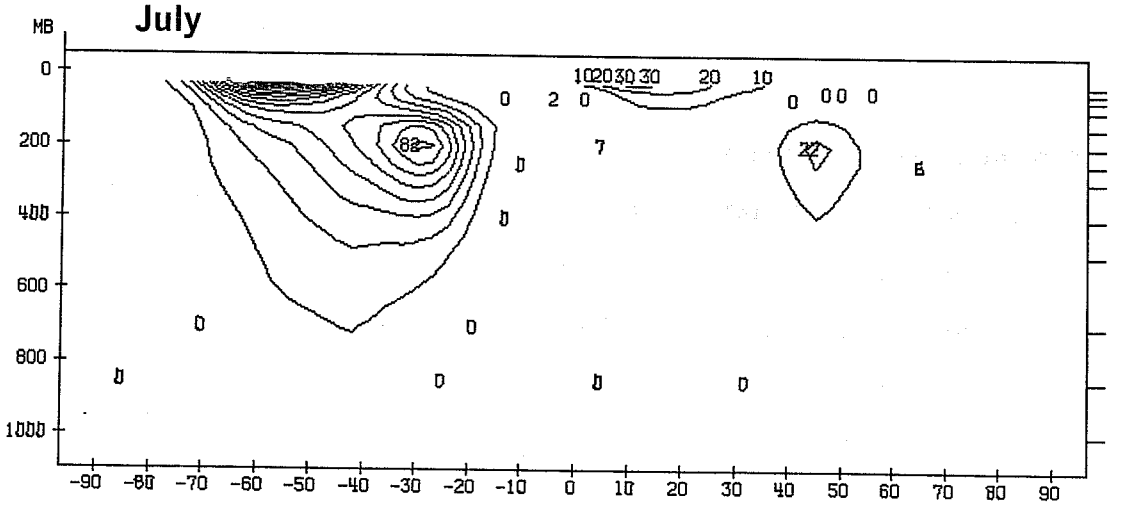

Fig. 1 Cross-sections of monthly mean zonal kinetic energy corresponding to January and July 1981. Unit: $J/m^2/P$.
Top panel: means found by Oort and Rasmusson (1971). Unit: m^2/s^2.

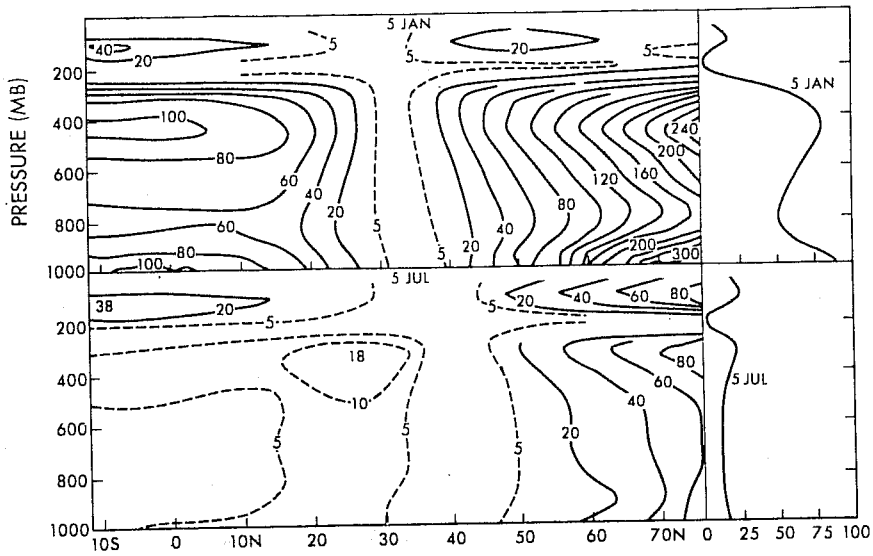

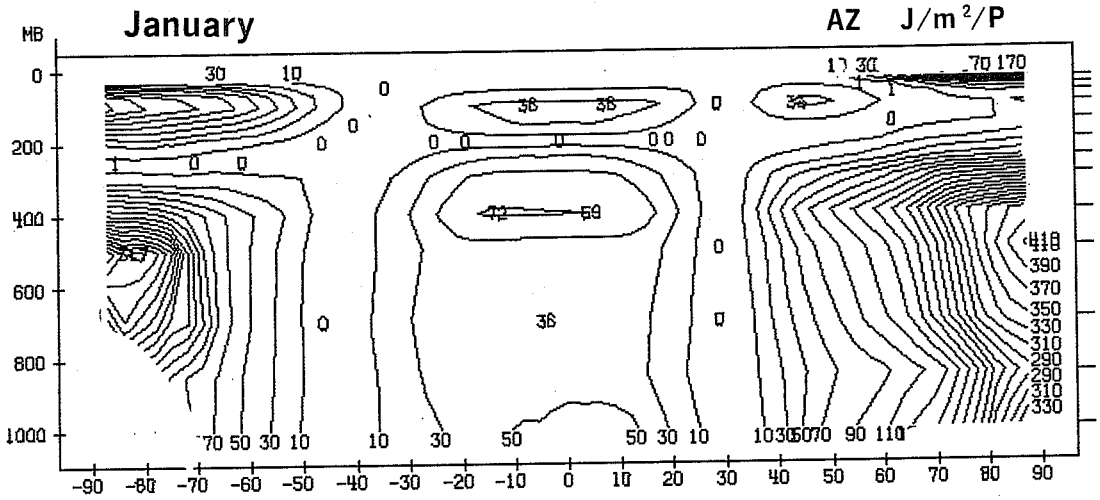

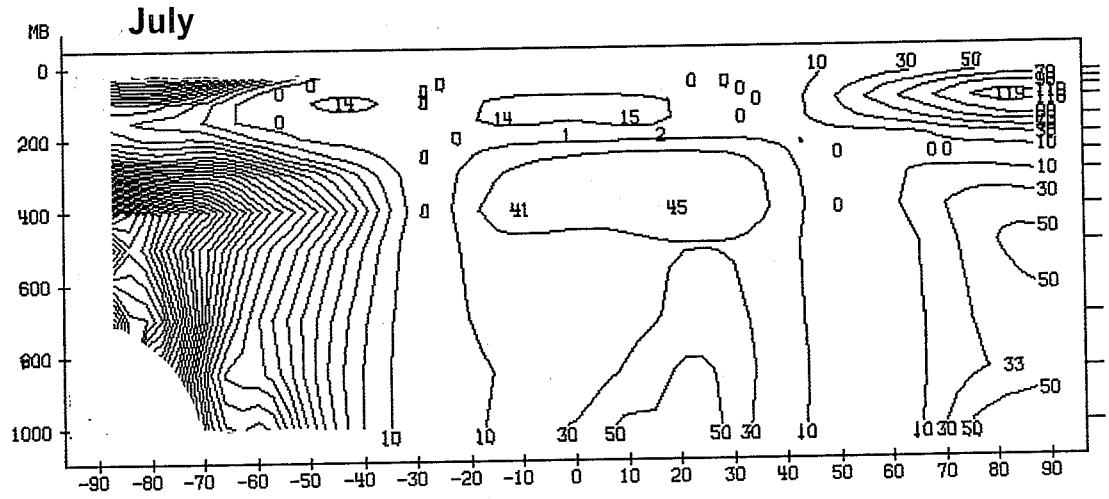

Fig. 2 Cross-sections of monthly mean zonal available potential energy corresponding to January and July 1981. Unit: $J/m^2/P$.
Top panel: means found by Peixoto and Oort (1974)
Unit: $10^5 J/m^2/bar \simeq J/m^2/P$.

Secondary maxima are found at 100 mb in the summer hemispheres, related to relatively warm temperatures near the Pole combined with cooler temperatures near the equator. The minimum values (temperatures equal to the global mean) are found around 30° in the winter hemisphere and 50° in the summer hemisphere. These plots also give a clear indication of the location of the tropopause.

4.1.3 The conversion term CZ

The sign of the conversion from zonal available to zonal kinetic energy CZ provides an indication of the type of zonal mean meridional circulation encountered within a region (see Fig. 3). Positive values are usually associated with a thermodynamically direct circulation whereas negative values with an indirect one. Although this term is very sensitive to the initialization, comparisons can still be made. The Antarctic region is not considered because results there are too noisy, due almost entirely to the large extrapolations below ground.

In January (Fig. 3a) there is a region of strong negative conversion amounting to 0.1 $mW/m^2/P$ between 50° and 70°N, where the rising branch of the Ferrel cell is to be found, as may be seen in the streamlines of the mean meridional circulation shown in Fig. 3c (due to Savijärvi). A rather strong direct circulation occurs at high latitudes coinciding with positive conversions of almost 0.1 $mW/m^2/P$ at around 75°N. In the tropical belt rather low positive and negative values alternate in the vertical, suggesting the two cell structure of the Hadley cell shown in Fig. 3c.The two cell structure in the vertical in the Hadley cell is due to the normal mode initialization of the data. A discussion about the effect of initialization on the tropical circulations can be found in Hollingsworth and Cats (1981). The weak negative conversions at 60°S are again associated with the rising motion in the indirect circulation in this area. There is noise in the CZ results at 30 mb in the Northern Hemisphere due to inaccurate interpolations

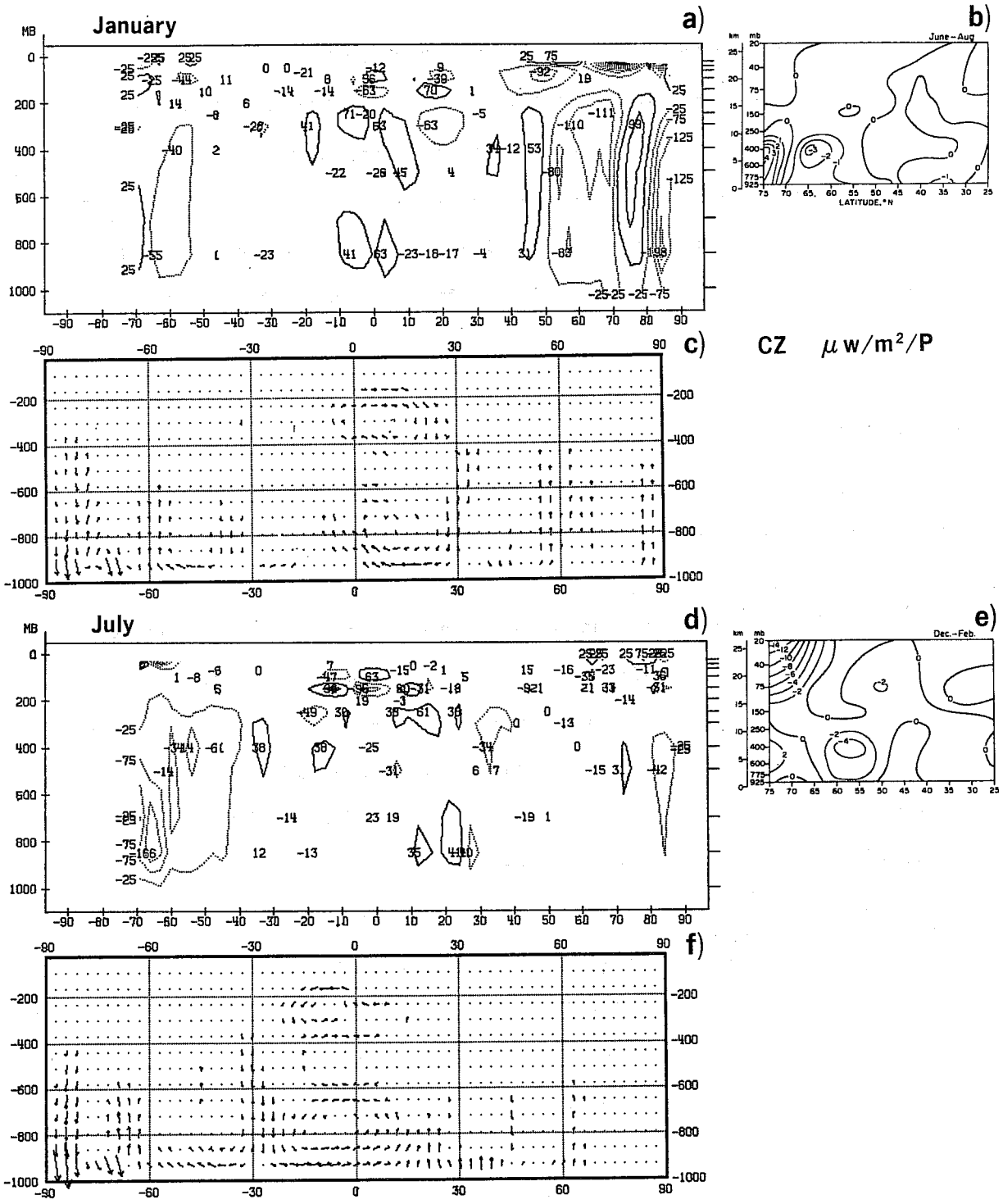

Fig. 3 Cross-sections of monthly mean conversions between zonal components of available and kinetic energy for January (a) and July (d) 1981. Units: $\mu w/m^2/P$. Mean meridional circulation for January (c) and July (f) 1981. Seasonal means found by Tomatsu (1979): b and e. Units: 10^{-3} $w/m^2/mb = 10\mu w/m^2 P$.

at the upper boundary of the model combined with high velociies in the polar night jet.

In July the area of negative conversions (Fig. 3d) is wider in the Southern Hemisphere (70 to 40°S) and stronger than found in the Northern Hemisphere; an indirect circulation dominates most of the extratropical Southern Hemisphere. A two cell structure in the vertical is again very evident in the tropical area; the lower troposphere is responsible for the strongest conversions there. Negative conversions are found in the winter stratosphere for this month.

4.1.4 The eddy kinetic energy

The eddy kinetic energy (Fig. 4), which depends on the zonal variance of the components of the wind, has values of the same order of magnitude as KZ.

In January there are several maxima, most of them situated at levels slightly below the jet; an absolute maximum of 56 $J/m^2/P$ is located at about 30°N and in addition there is a large gradient of KE in a belt of 5° latitude immediately to the south. There is a smaller maximum of 23 $J/m^2/P$ at 60°N and another of 16 $J/m^2/P$ in the tropical upper troposphere. The Southern Hemisphere has lower values presumably because of less standing wave activity due to different land-sea contrasts and mountains. The Southern Hemisphere values do not change very much with the seasons, the maximum increases from 23 to 29 $J/m^2/P$ and shifts slightly towards the equator from summer to winter. The Northern Hemisphere pattern in July shows weaker values shifted towards the pole and to lower levels.

4.1.5 The eddy available potential energy

The values of eddy available potential energy AE (Fig. 5) are very low compared with AZ (Fig. 2) and their distribution is completely different. A more detailed study of the dependency of AE on static stability will be described in Sect.4.4. For January the Northern Hemisphere maximum

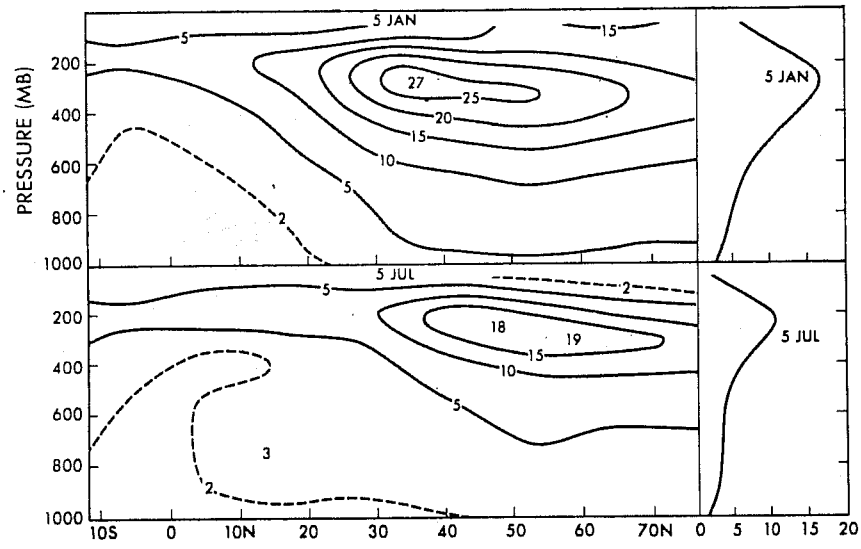

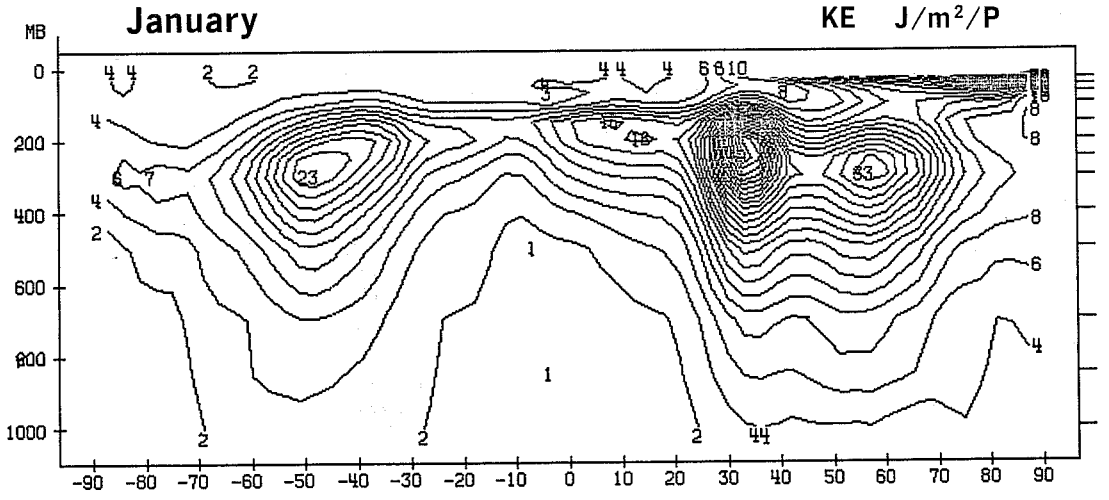

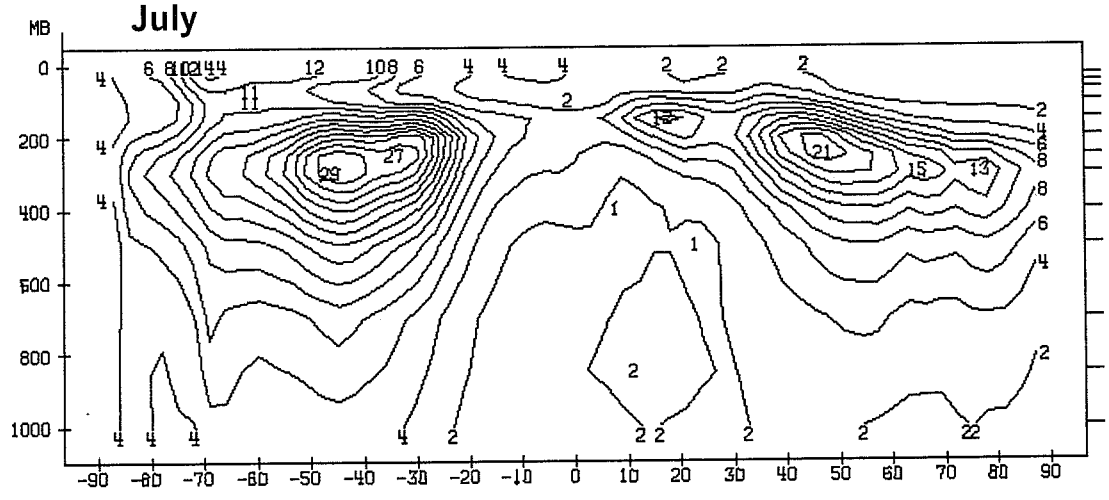

Fig. 4 Cross-sections of monthly mean eddy kinetic energy for January and July 1981. Units: $J/m^2/P$
Top panel: means found by Peixoto and Oort (1974).
Units: $10^5 J/m^2/bar \simeq J/m^2/P$.

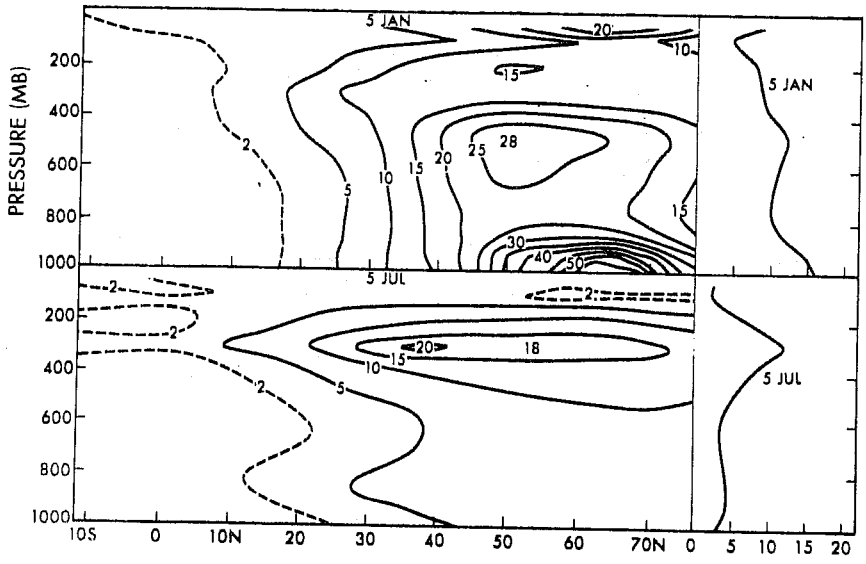

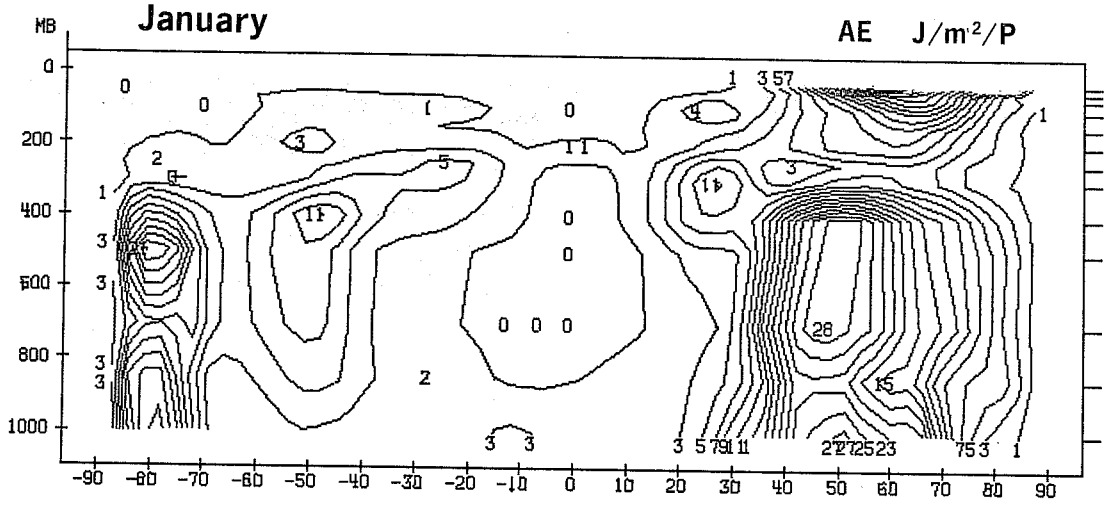

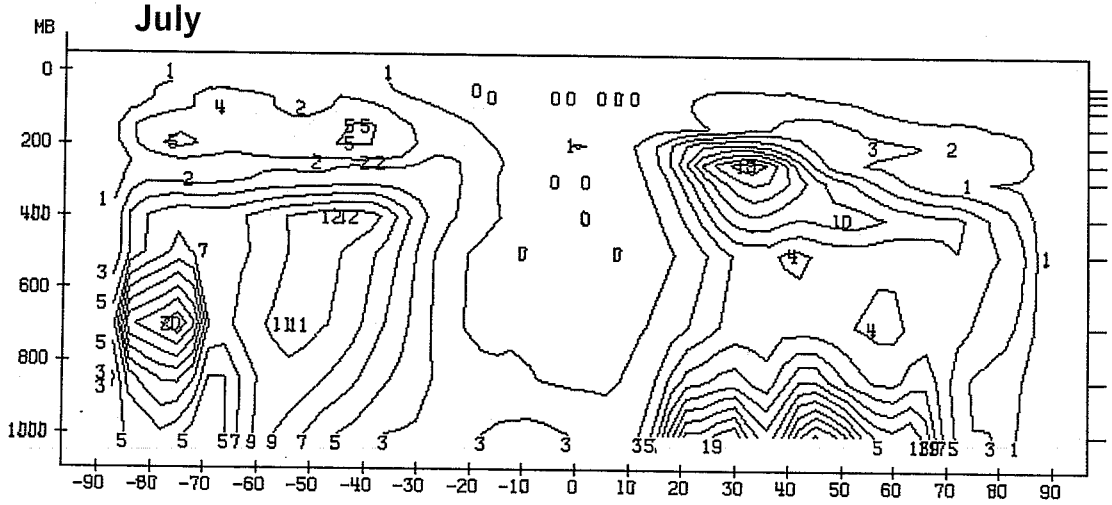

Fig. 5 Cross-sections of monthly mean eddy available potential energy for January and July 1981. Units: $J/m^2/P$.
Top panel: means found by Peixoto and Oort (1974).
Units: $10^5 J/m^2/bar \simeq J/m^2/P$.

corresponds to an area in the upper troposphere of the mid-latitudes, where most non-axisymmetric baroclinicity is found, amounting to 28 $J/m^2/P$.

In the Southern Hemisphere the maximum values occur in the region between 70° and 90°S. The reliability of the calculations in these latitudes is questionable until further investigation of the effect of vertical interpolations in the region is carried out. A reduction in the noise of temperature variances at high latitudes in Southern Hemisphere is evident from March 81 onwards, after the introduction of PAOBS data, giving therefore more confidence in the AE values in that area. Seasonal changes in AE are most marked in the stratosphere.

The annual cycle in the Southern Hemisphere has little amplitude. In the Northern Hemisphere the summer AE values are rather low in the troposphere and zero in the stratosphere. The maxima in AE in the Northern Hemisphere summer are found just below the tropopause, 18 $J/m^2/P$ and near the ground, 23 $J/m^2/P$. The upper tropospheric maximum being due to fairly unstable stratifications whilst the lower one is due to large variances in the temperature.

4.1.6 The conversion CE

The conversion from eddy available to kinetic energy CE is correlated with the vertical transport of sensible heat; the mass redistribution, which occurs when warm air rises or cold air subsides, relaxes the horizontal temperature contrasts; eddy kinetic energy is produced at the expense of eddy potential energy. This term (see Fig. 6) is positive everywhere except in some regions in the stratosphere and tropics. In January there is a high rate of conversion at 500 mb (the level where more activity is found at most latitudes) in the Northern Hemisphere, with amounts up to 0.124 $mW/m^2/P$ in the active baroclinic zones. The July Southern Hemisphere has more intense conversions than January. The July maxima are at slightly lower levels and extend further to the north, with a maximum of 0.112 $mW/m^2/P$ at 40°S and 500

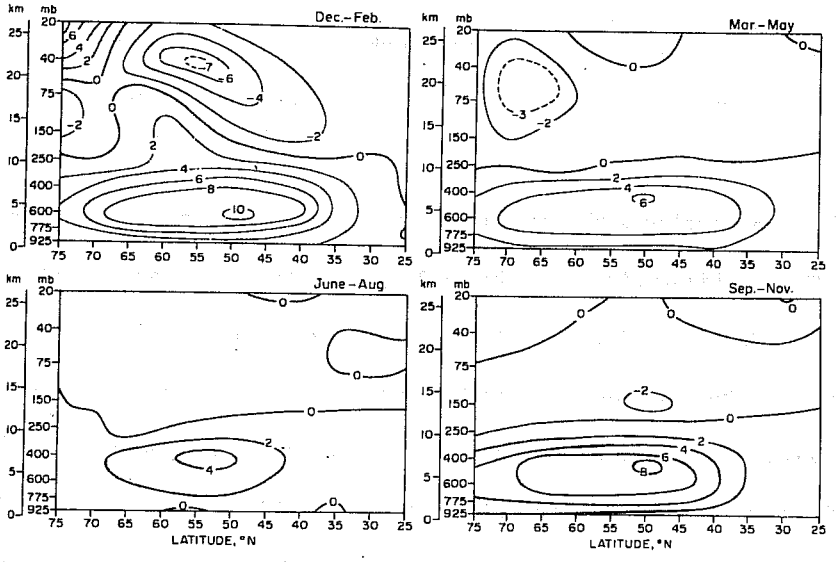

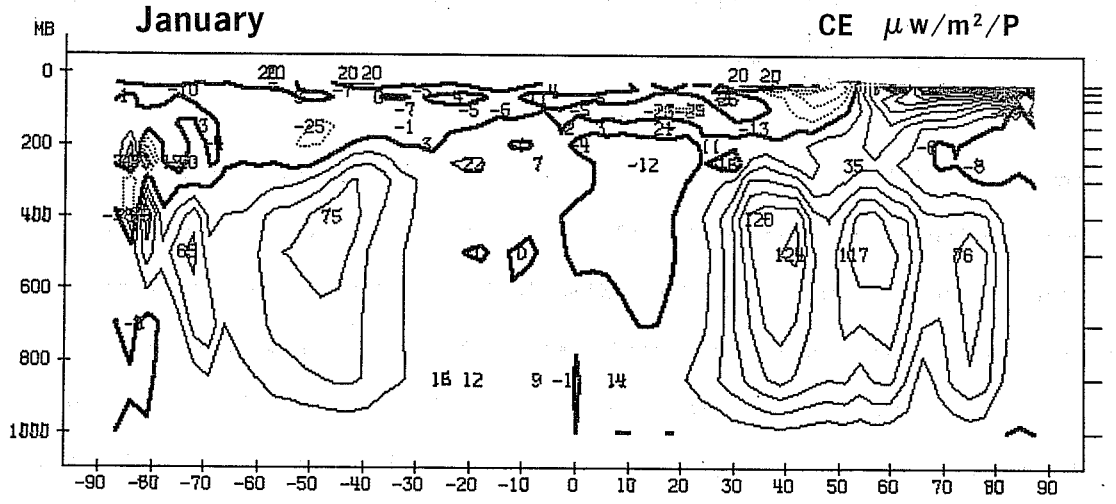

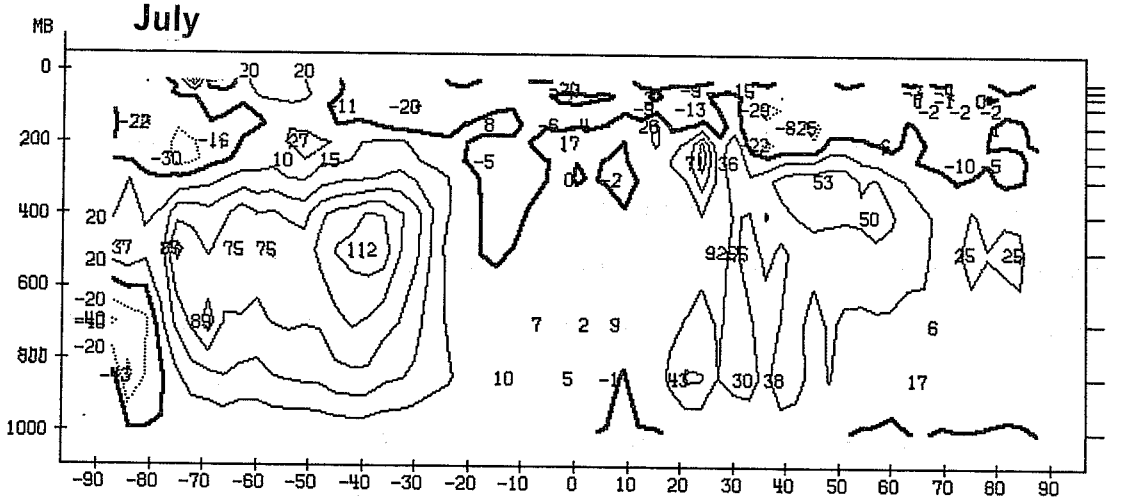

Fig. 6 Cross-sections of monthly mean conversions between eddy available and kinetic energy for January and July 1981. Units: $\mu w/m^2/P$. Top panel: Seasonal means found by Tomatsu (1979). Units: 10^{-3} $w/m^2/mb \simeq 10\mu w/m^2/P$.

mb. The field of CE in the July Northern Hemisphere shows rather low values. There are negative values in the stratosphere and a quite isolated maximum of 0.071 $mW/m^2/P$ at 20°N; a secondary maximum can be found at 850 mb at this latitude, which is now a rather active level in the subtropical areas. There is a suggestion of an influence of the orographic forcing in these conversions.

In Appendix A4 there is an estimate of the impact of the use of the virtual temperature on the CE calculations.

4.1.7 The conversion CA

CA, the conversion from zonal to eddy available potential energy (Fig. 7) is together with CE the most active of the exchanges. A positive transfer is obtained when the meridional eddy sensible heat flux is directed towards lower zonal average temperatures, thus relaxing the existing gradient of temperature. In general, values are positive in the troposphere where one expects a poleward flux of heat. The highest values are found at 700 mbar in January where at 40°N there is a conversion of .185 $mW/m^2/P$. The whole area between 20 and 70°N is very active; high values have sometimes been associated with the persistence of a blocking regime (Schilling, 1981).

In Fig. 8 the mean geopotential height at 1000 mb and 500 mb are represented for January. There was a very intense Azores high with blocking episodes occurring in the Atlantic during most of the month; the Siberian high was also quite pronounced. The 500 mb field reflects the blocking patterns with a marked high centered at (40°N 30°W) and a cyclonic area just to the south. The ridge is much more intense than normal. In the Southern Hemisphere in January, CA is most intense between 40° and 50°, with a secondary maximum of 0.069 $mW/m^2/P$ at 75°S. The tropical values of CA are negligibly small, as is also the case in the stratosphere from 30°N to South Pole. A maximum of 0.210 $mW/m^2/P$ is found at 65°N and 30 mb. The January mean Southern

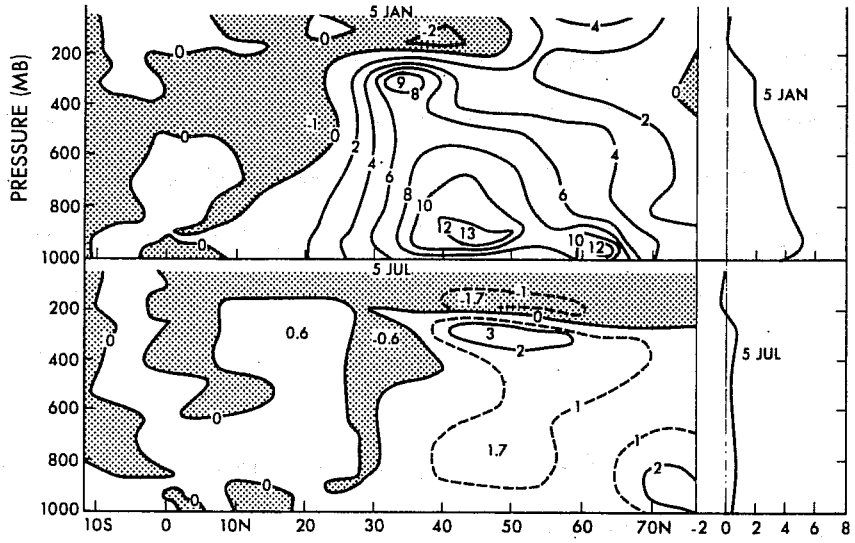

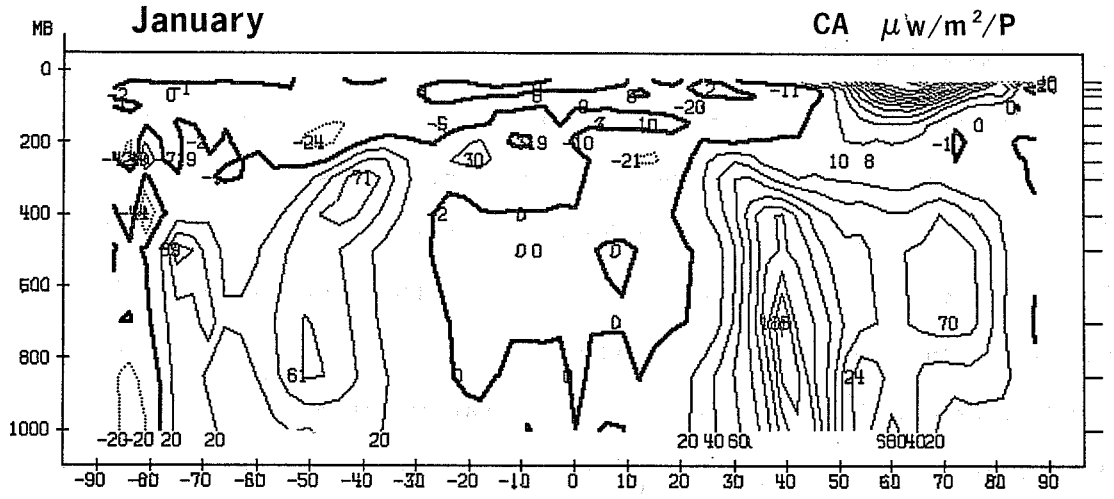

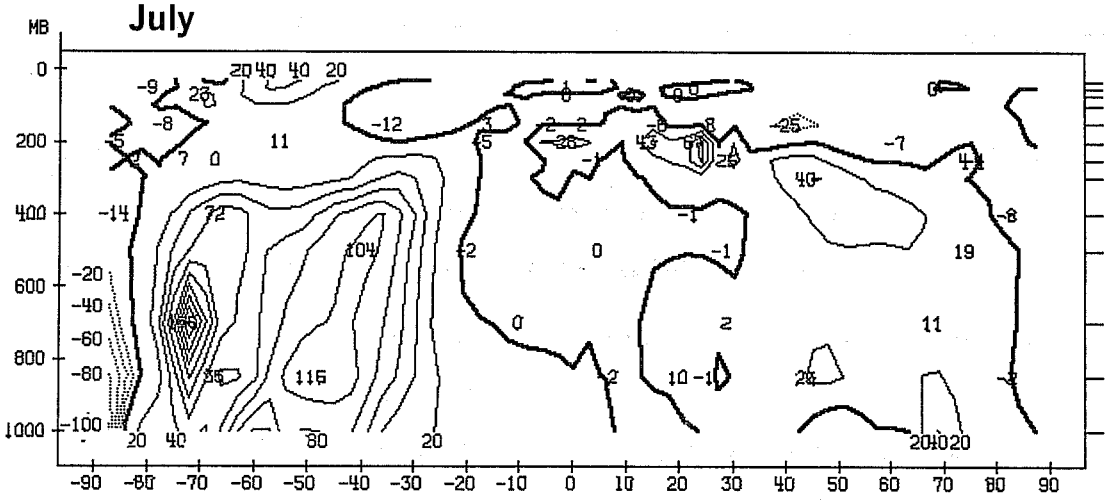

Fig. 7 Cross-sections of monthly mean conversions between zonal and eddy available potential energy for January and July 1981.
Units: $\mu w/m^2/P$.
Top panel: means found by Oort and Peixoto (1974).
Units: $w/m^2/bar \simeq 10\mu w/m^2/P$.

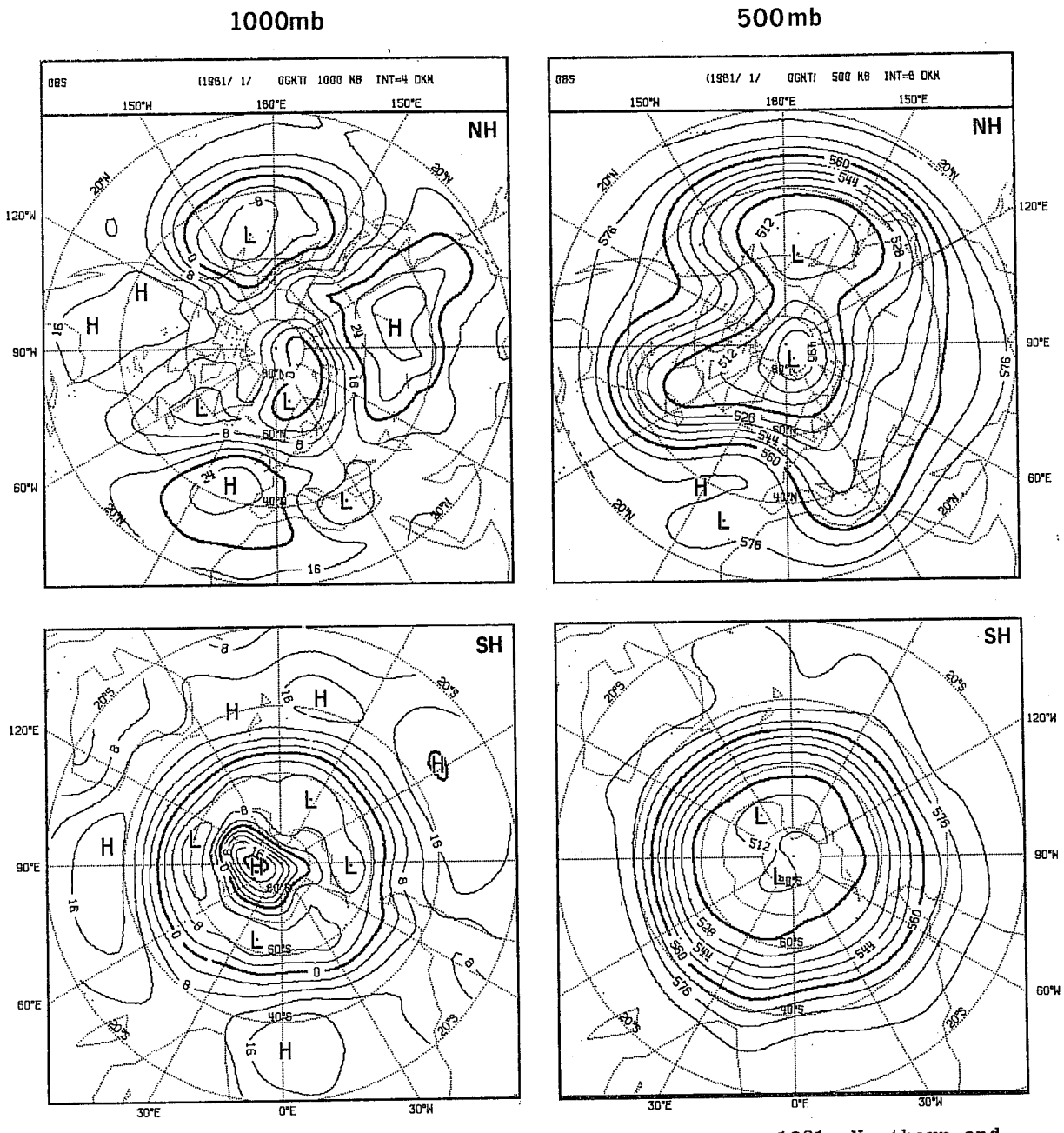

Fig. 8 Mean 1000 and 500 mb map corresponding to January 1981, Northern and Southern Hemisphere.

Hemisphere geopotential maps show an almost zonal circulation at 500 mb, while at 1000 mb level there is a very regular pattern with high pressures in the subtropical belt and no indication of what could be considered a blocking situation in mid-latitudes.

A comparison with the July values shows a much stronger annual cycle in the Northern Hemisphere. The maximum drops from 0.185 in winter to 0.040 $mW/m^2/P$ in summer, while the Southern Hemisphere exhibits only a change from 0.116 to 0.071 $mW/m^2/P$.

4.1.8 The conversion CK

The conversion CK (Fig. 9) from zonal to eddy kinetic energy depends on the correlation between the meridional gradient of $\overline{u}$ and the eddy momentum flux, the latter being due to tilted ridges and troughs. The net forcing on the zonal flow can only be found by taking the global integral of this quantity, and will be discussed later. Maximum values are found in the region of the jets (see Fig. 1). In January there are two maxima in conversions of KE into KZ amounting to 0.081 and 0.116 $mW/m^2/P$ at 250 mb, occurring at 40°S and 25°N with another maximum conversion of 0.053 $mW/m^2/P$ from KZ into KE at 200 mb, 40°N. The occurrence of maxima of opposite sign near the jet has been discussed theoretically by McIntyre (1970) and Simmons and Hoskins (1978). Negative values are predominant except in northern mid-latitudes. In July conversions are weaker but there are still alternating positive and negative columns in the main centres. Negative stratospheric winter values indicate reinforcement of the polar night jet by the eddies in both hemispheres.

CK can give an indication of the transition from high to low index periods. When the zonal westerly polar vortex breaks down into meanders of large amplitude planetary waves, the eddy energy can be drawn from the zonal flow and CK can be positive, but negative values are more normal.

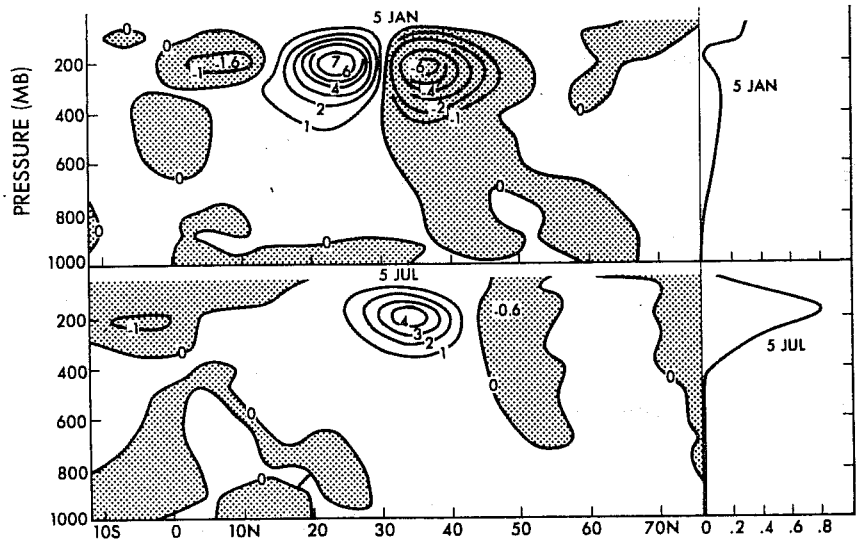

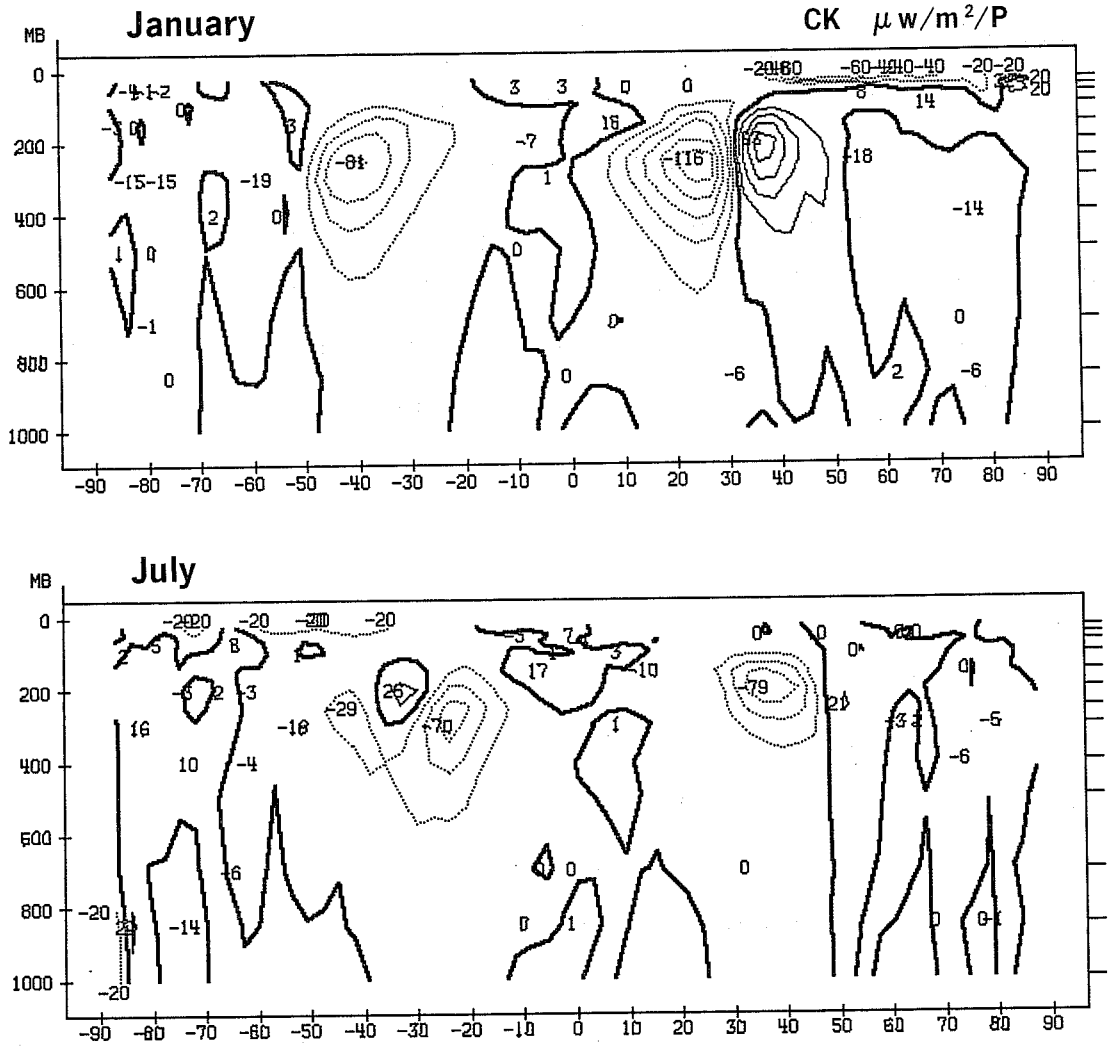

Fig. 9 Cross-sections of monthly mean conversions between zonal and eddy kinetic energy corresponding to January and July 1981.
Units: $\mu w/m^2/P$.
Top panel: means found by Oort and Peixoto (1974)
Units: $w/m^2/bar \simeq 10 \mu w/m^2/P$.

4.1.9 Eddy fluxes of kinetic energy

Fig. 10 shows the zonal mean distribution of $\sum_{n=1}^{96} LK(n)$, which is the convergence of the eddy flux of kinetic energy. The global integral of this term should vanish precisely but does not in fact do so. The values of this convergence have a lot of small scale structure; this may indicate an inconsistency in the method of calculation used and/or to some noise, especially within the boundary layer where there may be interpolation problems. The sum over all waves in this cross-section indicates divergences or convergences of fluxes of KE. In January maximum activity occurs at 250 mb between 20 and 55°N and at 300 mb north of 60°N, with a highest value of 0.108 $mW/m^2/P$; there is another maximum at 70°N in stratospheric levels. The areas of convergence and divergence alternate within each layer. The picture for July is less noisy. Negative and positive values are well spread in successive latitude belts and appear to compensate quite well. The levels of maximum activity in both hemispheres are 300 and 250 mb - similar to January; the stratosphere is far less active than before. There is no indication at present about the net export of kinetic energy being stable from year to year.

To complete the description of the energy budget for KE, cross-sections of vertical and northward eddy fluxes of geopotential are presented for January and July in Fig. 11. In January the maximum upward flux (negative values) occurs at 400 mb in both hemispheres and amounts to around 3 w/m^2 (after dividing by g), being located at 35°N, 55°N and 45°S; the downward flux is found at 850 mb and values are also around 3 w/m^2 at 50°N and some 1 w/m^2 at 60°S. The same levels are significant in July except that the maximum upward flux in the Northern Hemisphere is found, weaker, at 300 mb; in the Southern Hemisphere the distribution of the fluxes has changed but their values are similar. The physical interpretation of this term is that the mid-latitude and mid tropospheric levels (where ω'^2, $\overline{\omega'T'}$ and CE are largest) do work, through the pressure work term $\overline{\omega'\phi'}$, on the boundary layer and on the upper troposphere. Thus one can think of this term as a propagator of kinetic

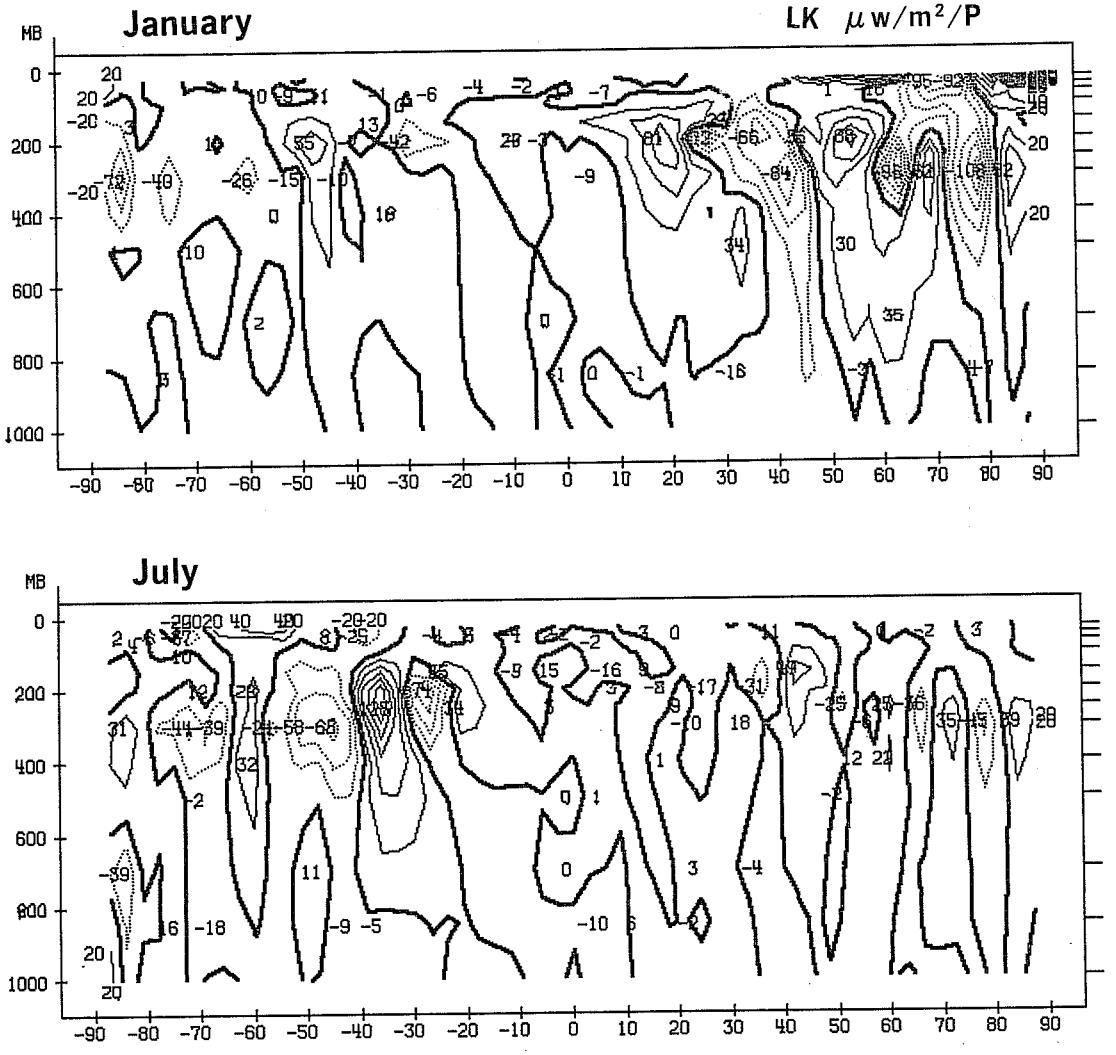

Fig. 10 Non-linear monthly mean redistribution of eddy kinetic energy corresponding to January and July 1981. Units: $\mu w/m^2/P$.

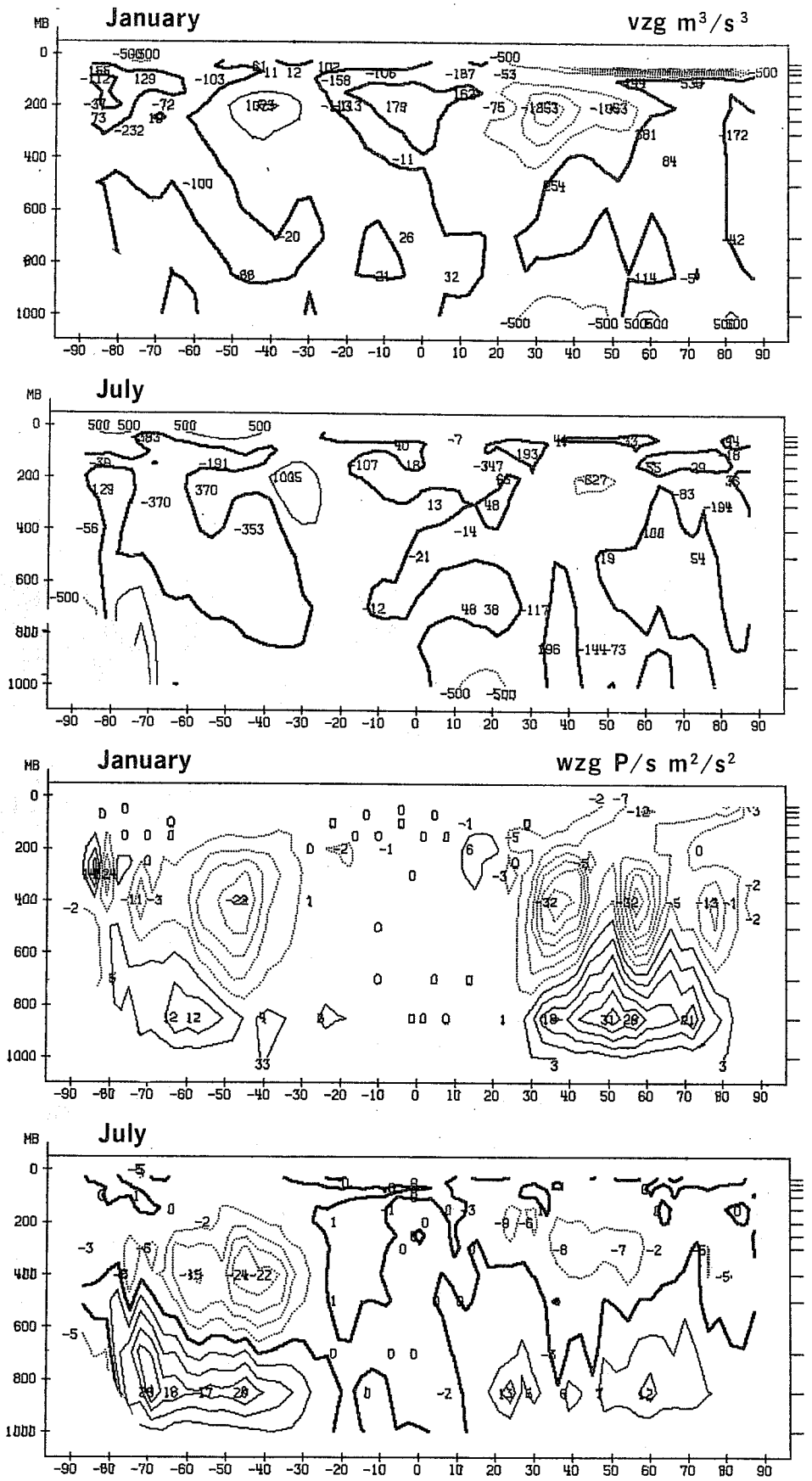

Fig. 11 Monthly mean vertical and horizontal fluxes of geopotential height corresponding to January and July 1981. Units as shown.

energy from the source regions at mid levels to the dissipation regions in the boundary layer and in the jet. The existence of three distinct maxima in the upper troposphere of the Northern Hemisphere may be related to standing waves generated by orography or land-sea contrast. This will be investigated in a later paper.

The vertical flux convergence of eddy geopotential (not shown) is maximum in January and July at the same latitudes indicated before, at 250 or 200 mb amounting at most to 183 $w/m^2/P$, while the largest divergences occur at 500 mbar and imply in one place 127 $w/m^2/P$. The feeding from middle troposphere to the jet levels is a consequence of the above mentioned behaviour, but values are rather small overall.

The distribution of the term $\overline{v'\phi'}$ shows that the mid-latitudes of the Northern Hemisphere, in winter, do work on the tropics. This phenomenon has been discussed by Mak (1969) and Edmon et al (1980). Eliassen and Palm (1961) showed that for steady waves $\overline{v'\phi'} = -\bar{u}.\overline{u'v'}$, so that the geopotential flux is in the opposite direction to the momentum flux. Related results have been obtained for simple baroclinic waves by Hollingsworth et al (1976) and for much more general situations by Andrews and McIntyre (1976).

The main source of eddy kinetic energy has been shown to be CE, with its maxima in the middle troposphere and mid-latitudes. The sinks are the transfer to KZ (CK) and the dissipation which has not been calculated. The principal areas of these sinks are the boundary layer and the jet core for the dissipation, and equatorwards of the jet for CK. The energy transport from the sources to the sinks is mainly done by the eddy geopoential fluxes but eddy fluxes of kinetic energy also contribute, mainly on a smaller scale as shown by $\sum_{n=1}^{96} LK(n)$.

4.2 Stationary and transient part of the eddies

The present calculations do not include a separation into transient and

stationary components of the eddies. A case study was carried out for the month of April 1981 and both parts are presented in Fig. 12 to 15 (transient is assumed to be the total eddy contribution here calculated minus the stationary eddy taken from another source).

Variances of the three components of the wind are shown in Fig. 12. In respect to the zonal component, both stationary and transient variances seem to have the same spatial structure with the transient part contributing most to the total, except at 150 mb in the tropical area, where two stationary maxima are predominant and at 200 mb, and 30°N where both components have the same strength. The meridional wind shows a rather different spatial distribution between the stationary and the transient eddy components, the latter being predominant. In the Northern Hemisphere there are two places of maximum stationary variance, at 30°N and 200 mb, and at 60°N, 300 mb while the transient eddies have their maximum at 45°N, 250 mbar. There is a remarkable symmetry with respect to the equator regarding the transient eddy component, both in magnitude and in location; this could be due to the fact that April is close to the equinox. In the vertical velocity field, the stationary variance is very small compared to the transient except in the Antarctic (where ω values are dubious) and troposphere between 20 and 50°N. It is interesting to notice that the eddy activity in the upper levels around the equator is mainly a stationary feature.

In Fig. 13 the partition of the variances of Z, T and q are considered. Geopotential height does not show marked differences in spatial distribution between both components. In the troposphere the transient variance is more than double that of the stationary; the latter is more important however in the stratosphere. In the temperature variance fields, the stationary part is responsible for almost all variances found over the Antarctic and in the boundary layer of the Northern Hemisphere, while the features found in other areas are due to the transients which have their maximum at 850 mb and 200 mb

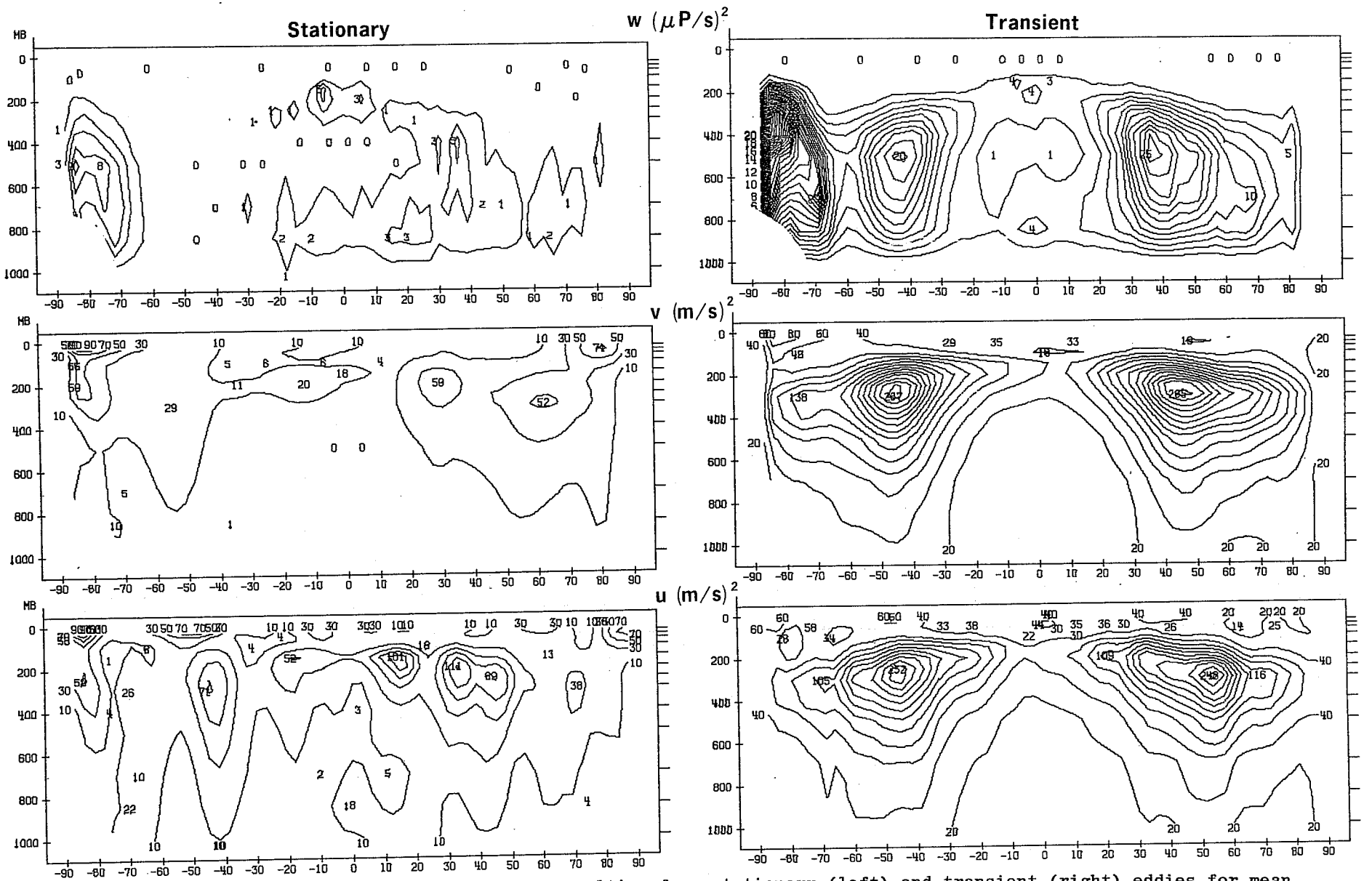

Fig. 12 Variances of the three wind components resulting from stationary (left) and transient (right) eddies for mean April 1981. Units as shown.

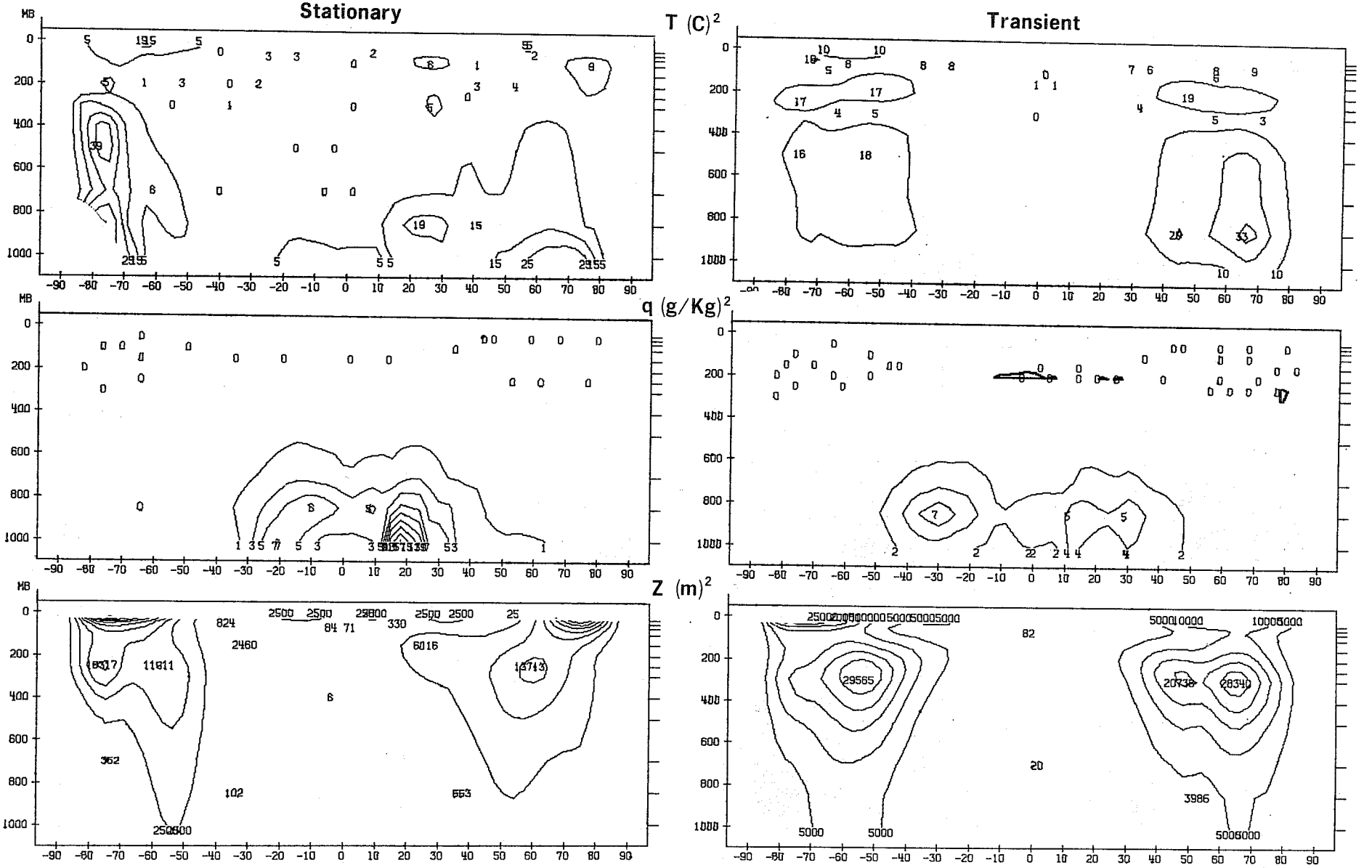

Fig. 13 Variances of temperature, humidity and geopotential resulting from stationary (left) and transient (right) eddies for mean April 1981. Units as shown.

in Northern Hemisphere and at 500 mb and 200 mb in the Southern Hemisphere.

The variances of specific humidity are linked to stationary features mainly in subtropical areas; the maximum at around 20°N is dubious and may be due to an error in the humidity analysis still present in April.

Transports of momentum, temperature and humidity are shown in Figs. 14 to 16. Northward and vertical eddy transports of westward momentum seem to have a rather small contribution from the standing part except at 30°N for the former (21 m^2/s^2 compared to 49 m^2/s^2).

The poleward and upward transports of heat have a large stationary component between 60°S and South Pole; elsewhere transports are due, in the main, to travelling waves. Around 60°N the stationary part of $v'T'$ increases with height reaching maximum values in the stratosphere, which are larger that those of the transient part; unlike the transients which have their maxima at 850 mb they do not show a reduction at the level of the tropopause. The vertical transport of temperature has mainly a stationary component between 10° - 30°N, possibly due to mountain forcing.

The poleward eddy transport of specific humidity is found to be mainly transient except in the trade wind areas in lower levels in Northern Hemisphere. For the upward transport, the stationary component predominates between 30°S and 30°N; in the extratropics transient waves are responsible for the transport. Notice a maximum of 115 g/Kg mP/s at 40°S which is almost entirely transient compared to a maximum of 119 g/Kg mP/s at 25°N which is mainly stationary.

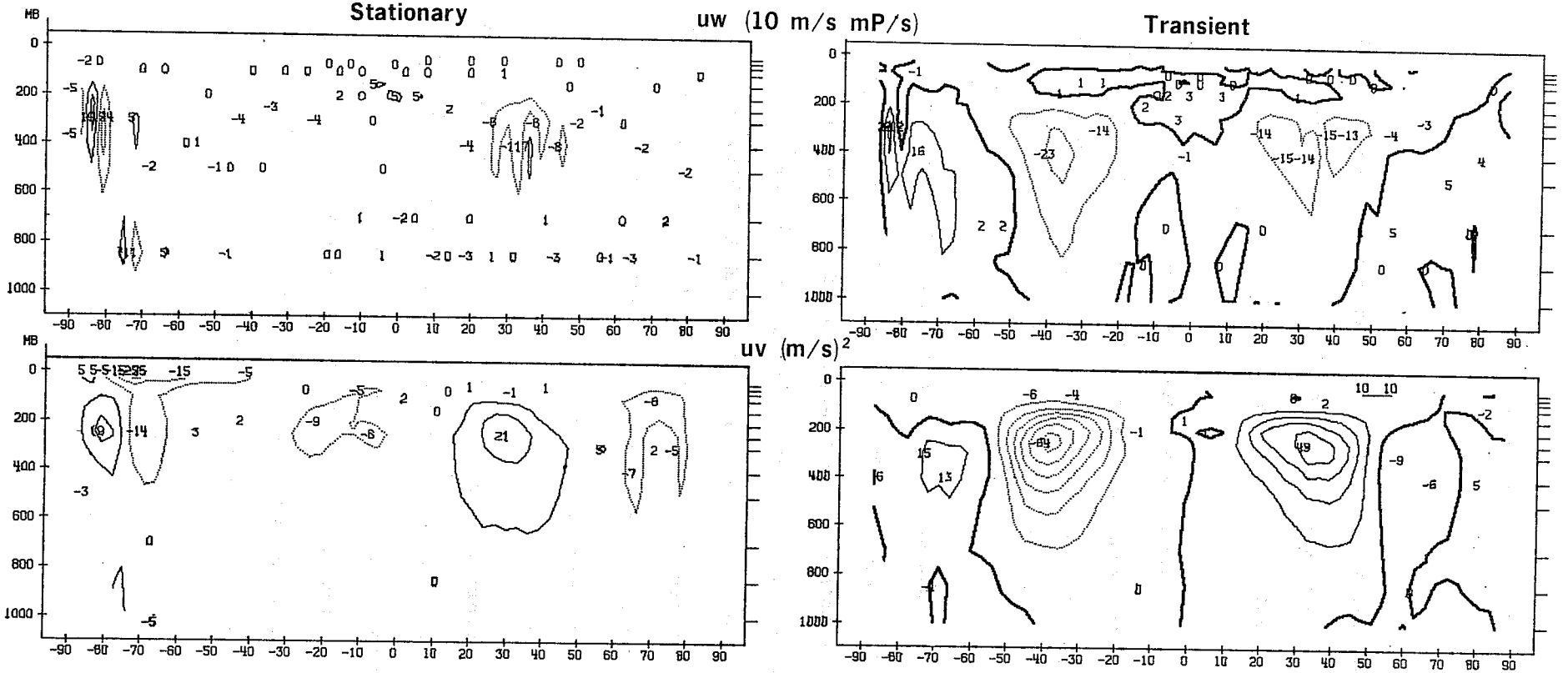

Fig. 14 Northward and upward transport of westerly momentum resulting from stationary (left) and transient (right) eddies for mean April 1981. Units as shown.

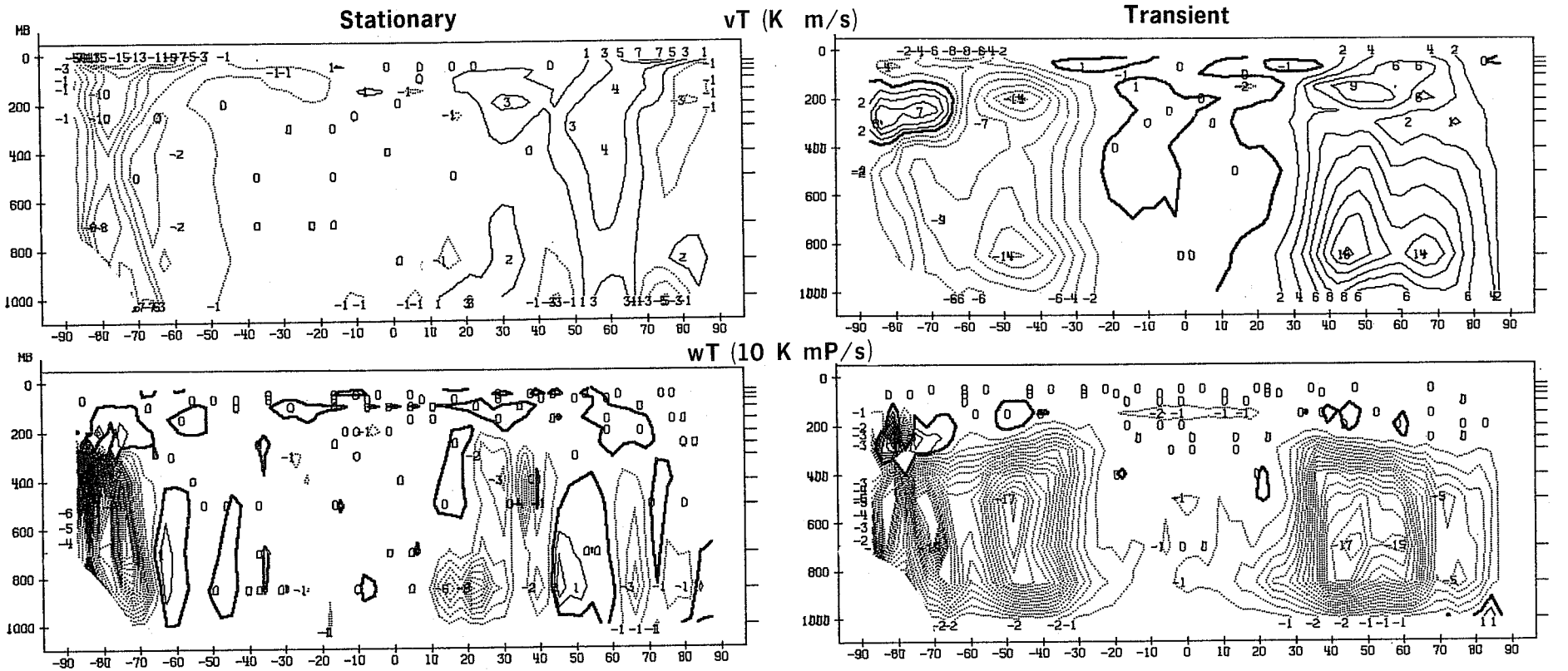

Fig. 15 Northward and upward transport of temperature resulting from stationary (left) and transient (right) eddies for mean April 1981. Units as shown.

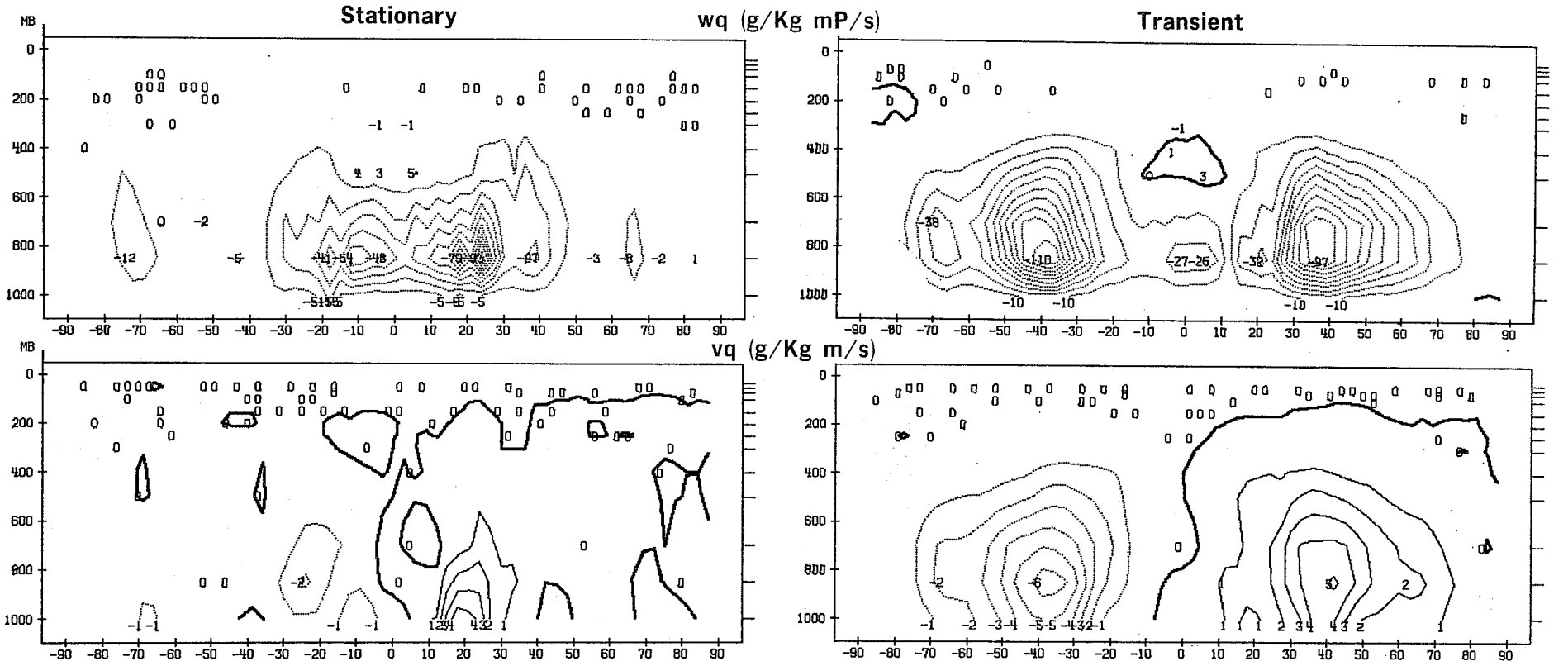

Fig. 16 Northward and upward transport of humidity resulting from stationary (left) and transient (right) eddies for mean April 1981. Units as shown.

Results from Oort and Rasmusson (1971) (denoted by OR below) for 5 April means are presented in order to compare stationary parts (Fig.17). OR's values are defined as variance of the variable resulting from stationary eddies [A^{*2}] and transport of the variable by stationary eddies [x*A*], where

$$\bar{A} = \frac{1}{t_2 - t_1} \int_{t_1}^{t_2} A \, dt \qquad \text{time average of A}$$

$$A' = A - \bar{A} \qquad \text{departure from time average of A}$$

$$[A] = \frac{1}{2\pi} \int_{0}^{2\pi} A \, d\lambda \qquad \text{zonal average of A}$$

$$A^* = A - [A] \qquad \text{departure from zonal average of A}$$

x meaning any of the wind components

The fact that the values presented here have been calculated using a different method: averaging first in space and after in time, could lead to some discrepancies, as pointed out in Reiter (1969) and also in Lau and Oort (1981).

The variances of the components of the wind resulting from stationary eddies in Northern Hemisphere are much stronger in April 81 for u and v (Fig. 12) than in the five year average . The results suggest that the stationary wave amplitudes were twice the long term average, due perhaps to the finer resolution data used here. As for the other fields there is good agreement in magnitude and distribution.

The poleward and upward stationary eddy fluxes of westerly momentum for April 81 (Fig. 14) and the 5 year average (Fig. 18) have similar distributions of positive and negative values but the April 81 fluxes have larger amplitudes. There is good agreement regarding the fluxes of sensible heat by stationary eddies and northward eddy transport of specific humidity (latent heat) but

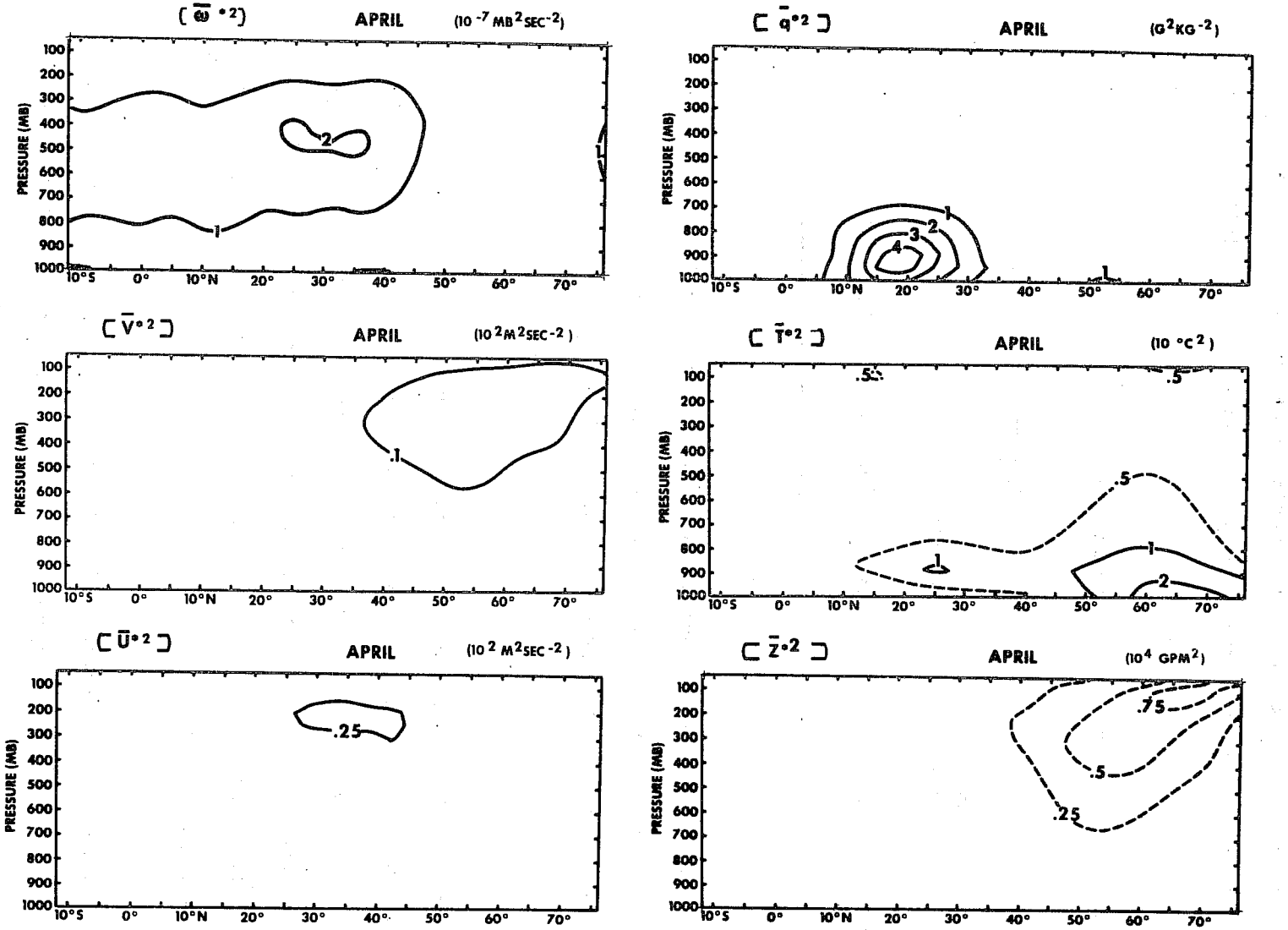

Fig. 17 Variance of the three wind components, humidity, temperature and geopotential resulting from stationary eddies for mean April. After Oort and Rasmusson (1971).

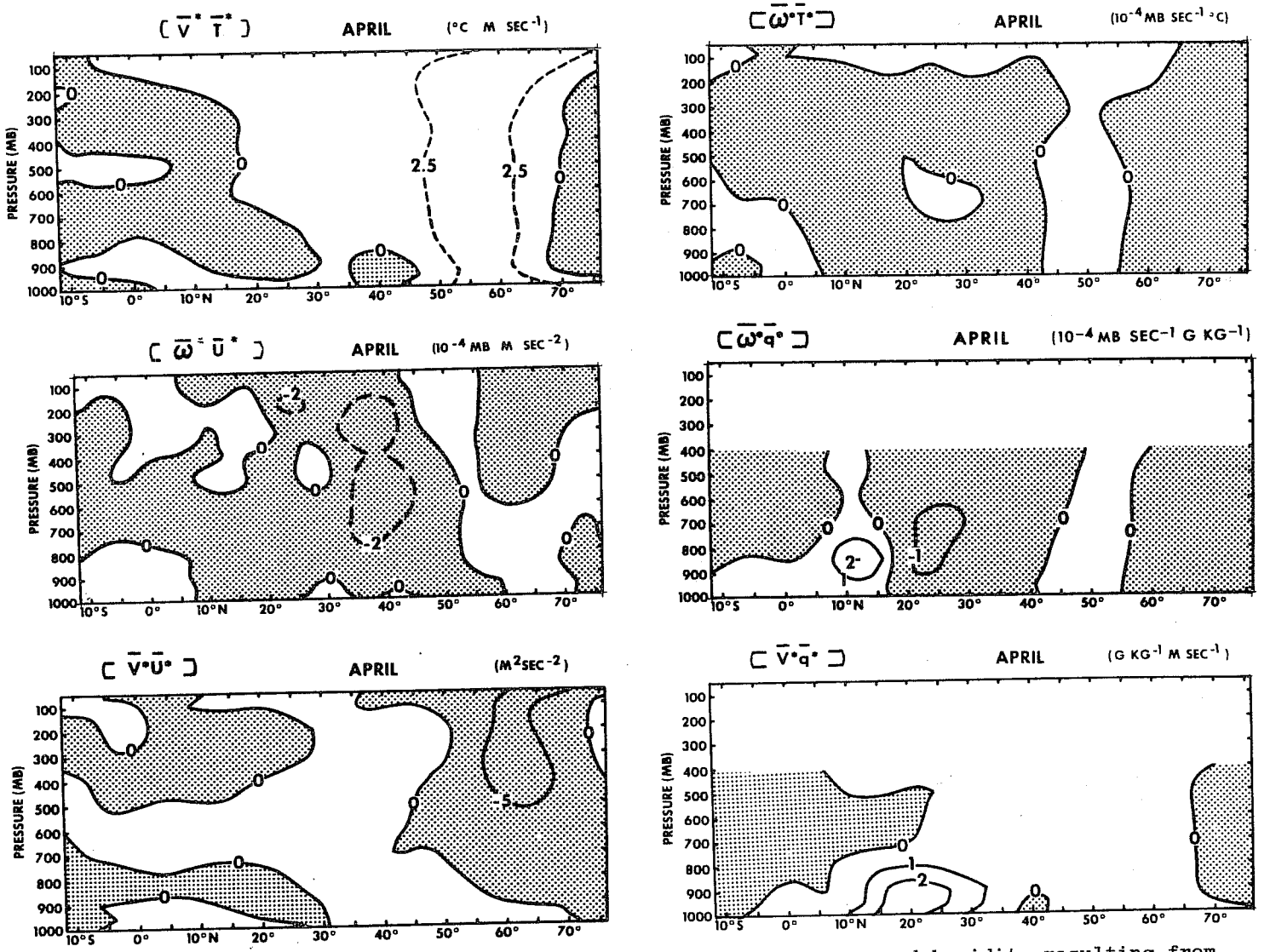

Fig. 18 Northward and upward transports of momentum, temperature and humidity resulting from stationary eddies for mean April. After Oort and Rasmusson (1971).

its downwards transport is almost absent in the ECMWF case, which looks much more realistic.

4.3 Comparison of zonal mean energetics and fluxes with those by other authors

In Fig. 1 the values found by Oort and Rasmusson (1971) for KZ for mean January and July from 10°S to 75°N were also shown. Note that OR's values should be divided by g to compare both sets. There is a good agreement between the two sets of data regarding the position of the jets in both months (even the subtropical jet in July). The polar night jet in January is not found in OR's figure because their data ended at 100 mb. As regards the intensity, the jet in January is much stronger in the ECMWF data. In Fig. 4 the eddy kinetic energy is compared with results presented by Peixoto and Oort (1974). Again the distribution is very similar in both sets although their results are smoother, possibly due to the resolution and the longer series of data used. The present calculations show higher values, especially in January at 30°N. The local maximum at 200 mb, 10°N was not found by Peixoto probably due to lack of data in the area.

AZ and AE can be compared with results from the same paper (Figs. 2 and 5) for the Northern Hemisphere; isolines labelled in 10^5 J/m^2/bar, are equivalent to J/m^2/P. AZ for January has the same spatial distribution in both sets. Best agreement is found in high latitudes, while in the tropical belt present values are lower, especially in the boundary layer. In July the AZ distributions are again similar but values are smaller at high latitudes and higher in the tropics, being quite the same in the stratosphere. This can be explained by the fact that the calculations presented involve the use of a volume-mean temperature (see Appendix A1) which will be lower when including the Southern Hemisphere area, therefore increasing $(\bar{T}-\bar{T}_G)^2$ in the tropics and decreasing it in polar areas, where T_G is the global mean temperature.

Regarding AE, the January values agree remarkably well (the choice of area is

irrelevant in this presentation), except for the lowest level where values are lower in the ECMWF calculations. The stability seems to be a good candidate for explaining the boundary layer differences since it shows up in AZ as well; a combination of less stable stratification and larger variances of temperature could explain the higher values found by Peixoto and Oort.The contourlines with values 5 and 15 are practically in same position and the isoline 25 is situated similarly except that it covers the belt between 40 and 55°N in the ECMWF case and goes up to 65°N in their figure. In July AE is slightly lower in the upper troposphere in these calculations but higher at the boundary layer. The differences in mid latitudes and mid troposphere can be accounted for by the use of 400 mb data in the ECMWF results as will be seen later. There is good agreement in general in the structure but globally integrated values are lower in the data considered.

Comparisons for CA, to be seen in Fig. 7, are taken from Oort and Peixoto (1974). Note that the units used differ by a factor of 10. The main differences between both sets of January values for CA are in the vertical structure, and there is an overall increased conversion in the present study. The first feature might be connected with the previously-mentioned less-stable stratification in Oort and Peixoto's calculation. Larger values of CA may be related to larger values of AE exhibited in Fig. 5. The origin of the boundary layer maxima shown by Oort and Peixoto is obscure because they correspond to levels where no data were available. In July, ECMWF values are also slightly higher too but there is a good similarity in the pattern.

The definition of CK in the Oort and Peixoto paper has opposite sign to the one used here so that signs should be changed and a factor of 10 should be applied for the comparison on Fig. 9. The positions of the extrema are similar but in general the present calculations are much stronger than Oort's values being almost double, perhaps due to higher variances of u and v as

shown before.

Only an indirect comparison of CK can be made; this is accomplished by using the horizontal eddy heat flux $\overline{v'T'}$ and comparing it with Oort and Rasmusson (1971) results for July, as found in Stone et al (1977). It can be seen in Fig. 19 that there is a good agreement regarding position and intensity of the maxima, the only difference being in the polar region in the upper troposphere. A direct comparison is made in Fig. 6 using seasonal means from Tomatsu (1979) for one year of data; the only disagreement is that maxima are found at higher levels in January (it might be due to the choice of levels, which is different in both studies) but the actual amounts are very much the same (there is again a factor of 10 due to the units used). The use of the virtual temperature in the CE calculations makes results slightly different, (see Appendix A4).

CZ is compared with Tomatsu's results in Fig. 3. The location of negative conversions of CZ between 50-70°N and up to 250 mb in January agree well and also the stratospheric structure at high latitudes, but values are higher in the data presented for January compared to the winter mean. Conclusions regarding this disagreement in magnitude are difficult because both calculations are only for one particular year and therefore may not be representative. The lower resolution and large smoothing in Tomatsu's calculations make a comparison difficult.

The most complete study including the Southern Hemisphere was published by Newell et al in 1974. Their results are not presented here because they contained large spatial gaps in the data; global values will be compared later in Sect. 8.3.

As a summary of the above considerations it can be said that similarities between present calculations and those by other authors can be found. The

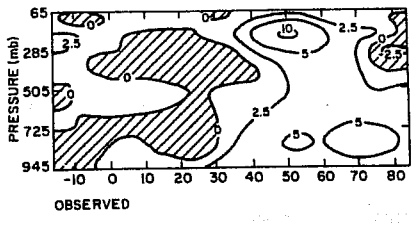

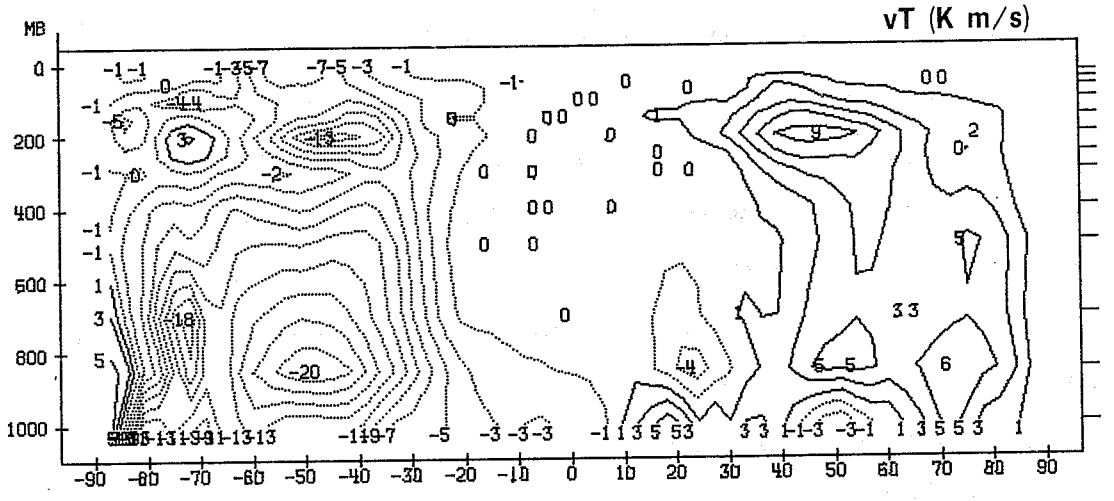

Fig. 19 Meridional eddy transport of temperature for July 1981.
Unit ^{o}K m/s.
Top panel: means found by Oort and Rasmusson (1971). Unit ^{o}C m/s.

variances of wind components are larger and the vertical structure in the static stability seems to be less pronounced in the ECMWF data analyses, (that will become more evident in the next Section).

Both factors lead to differences in all the energy parameters, with the stability affecting mainly the boundary layer. Other differences can be attributed to the small amount of smoothing used in this study.

4.4 Calculations of eddy available potential energy

When a comparison of AE was made in Fig. 5, there was on the whole a good agreement, with lower values in the data considered in this study. This tendency for these results to show lower values becomes more obvious when averages over the whole Northern Hemispheric atmosphere are compared (see Sect. 8.1). Speth (1978) showed that there is quite a large interannual variability of AE, which could have caused these differences, but it was found that ECMWF's values were consistently lower than the ones from other sources for all months.

The eddy available potential energy is dependent on temperature variances and a factor involving the static stability. In the present work this latter value is calculated at each latitude and each level for every day while other authors use monthly means for each level or even climatological values. In order to see the impact of such differences in technique, a comparison was made between the globally integrated values found for monthly means calculated either from daily values using actual stabilities or using a mean monthly stability for each level; results are shown in the last three columns of Table 3. In August, September and October 1980 the differences were very significant as between the methods (of the order of 20%) but after November values are very similar and even slightly higher using the actual stabilities. The change points out to the analysis scheme used until November 1980 as an explanation for the very low values found during the first months. The next section will look to this point in more detail.

In the same Table 3, mean values for the stability-dependent factor $\gamma = -\frac{R}{C_p}\frac{1}{\frac{\partial \bar{T}}{\partial p} - K\frac{\bar{T}}{p}}$ are presented for each level and month. As was already pointed out by Speth (1975), the values are not very different from month to month. Speth found the maximum for a mean January at 500 mb, while here it is found at 400 mb (a level not used by Speth). On the other hand the values considered when compared with Speth's, are smaller for the lower troposphere and slightly bigger at the levels above 400 mb. That implies that given the same variances of temperature, which are decreasing with height (see Fig.20c), the overall values for AE would be somewhat smaller in the ECMWF case.

Fig.20 presents the cross-sections of AE for a particular day, calculated using the operational method (b) or a mean stability at each level (a). It can be seen that the change of calculations for γ does not make much difference, at least for a single day. In the same figure, the variances of temperature (c) and the distribution of the γ factor (d) are shown for the same case. It becomes clear that the actual distribution of the values of AE depends very much on that of the temperature variances. Without detailed information about the values of the temperature variances used by Speth, it is not possible to describe the larger values of AE found by him as being predominantly due to either the variance term or the stability term.

4.5 Impact of the analysis of increments method

The change found in the last section in the values of AE after the introduction of this new analysis scheme is also present in the other fields, and should be taken into consideration especially when looking at the time changes of the parameters later on (Section 8 below).

Some FGGE analyses are available using both schemes and a comparison of the basic fields for one particular case was made. The most affected part was the variance, which experienced an increase of 10% in some areas, especially

Table 3 Monthly mean global stability factor at each level. Units: J/Kg. Comparison of AE values using two different calculation methods. Units: KJ/m^2.

Year	Level / Month	1000	850	700	500	400	300	250	200	150	100	70	50	30	AE using $\bar{\gamma}$	AE operational	%
80	Au	5.5	6.6	9.8	9.9	14.2	12.8	10.8	9.0	6.6	5.0	4.3	4.2	4.3	353	299	18
	S	5.7	6.7	9.9	9.9	14.3	12.6	10.6	8.9	6.5	5.0	4.3	4.2	4.3	402	323	24
	O	5.7	6.6	9.7	9.9	14.1	12.2	10.1	8.7	6.5	5.0	4.3	4.2	4.2	443	384	15
	N	5.5	6.3	9.3	9.8	13.8	11.8	9.9	8.6	6.5	5.0	4.3	4.1	4.2	422	389	8
	D	6.1	6.6	9.0	9.7	13.8	11.6	9.5	8.1	6.6	5.2	4.2	3.8	3.8	518	521	-0
81	Ja	6.6	6.7	8.8	9.5	13.5	11.5	9.3	8.2	6.9	5.2	4.1	3.6	3.7	548	557	-2
	F	6.5	6.7	8.8	9.5	13.1	11.1	9.3	8.3	6.9	5.3	4.2	3.7	3.7	546	554	-1
	Mr	6.7	6.9	9.1	9.8	13.5	11.5	9.2	7.9	6.8	5.3	4.2	3.6	3.7	470	483	-3
	Ap	6.8	7.1	9.4	9.9	13.7	11.7	9.5	7.9	6.7	5.3	4.2	3.6	3.7	441	448	-1
	My	6.6	7.0	9.5	10.0	13.9	12.1	9.7	8.0	6.7	5.3	4.2	3.6	3.7	407	419	-3
	Jn	7.3	7.3	9.6	9.9	14.1	12.4	10.1	8.3	6.7	5.2	4.3	3.8	3.9	457	475	-4
	Jl	8.4	7.8	9.3	9.7	14.1	12.6	10.7	8.9	6.7	5.1	4.3	4.0	4.1	438	441	-0
	Au	8.4	8.0	9.4	9.6	14.1	12.4	10.3	8.9	6.8	5.1	4.3	4.0	4.1	418	421	-0
	S	8.7	8.0	9.4	9.7	14.3	12.5	10.2	8.7	6.6	5.0	4.3	4.0	4.1	427	429	-0
	O	8.8	7.8	9.3	9.7	14.0	12.3	9.9	8.4	6.6	5.1	4.3	4.0	4.1	474	480	-1
	N	8.2	7.5	9.3	9.8	13.5	11.9	9.6	8.3	6.7	5.2	4.3	4.0	4.1	515	511	0
	D	7.7	7.3	9.2	9.6	13.2	11.6	9.4	8.1	6.7	5.3	4.4	4.0	4.0	542	549	-1

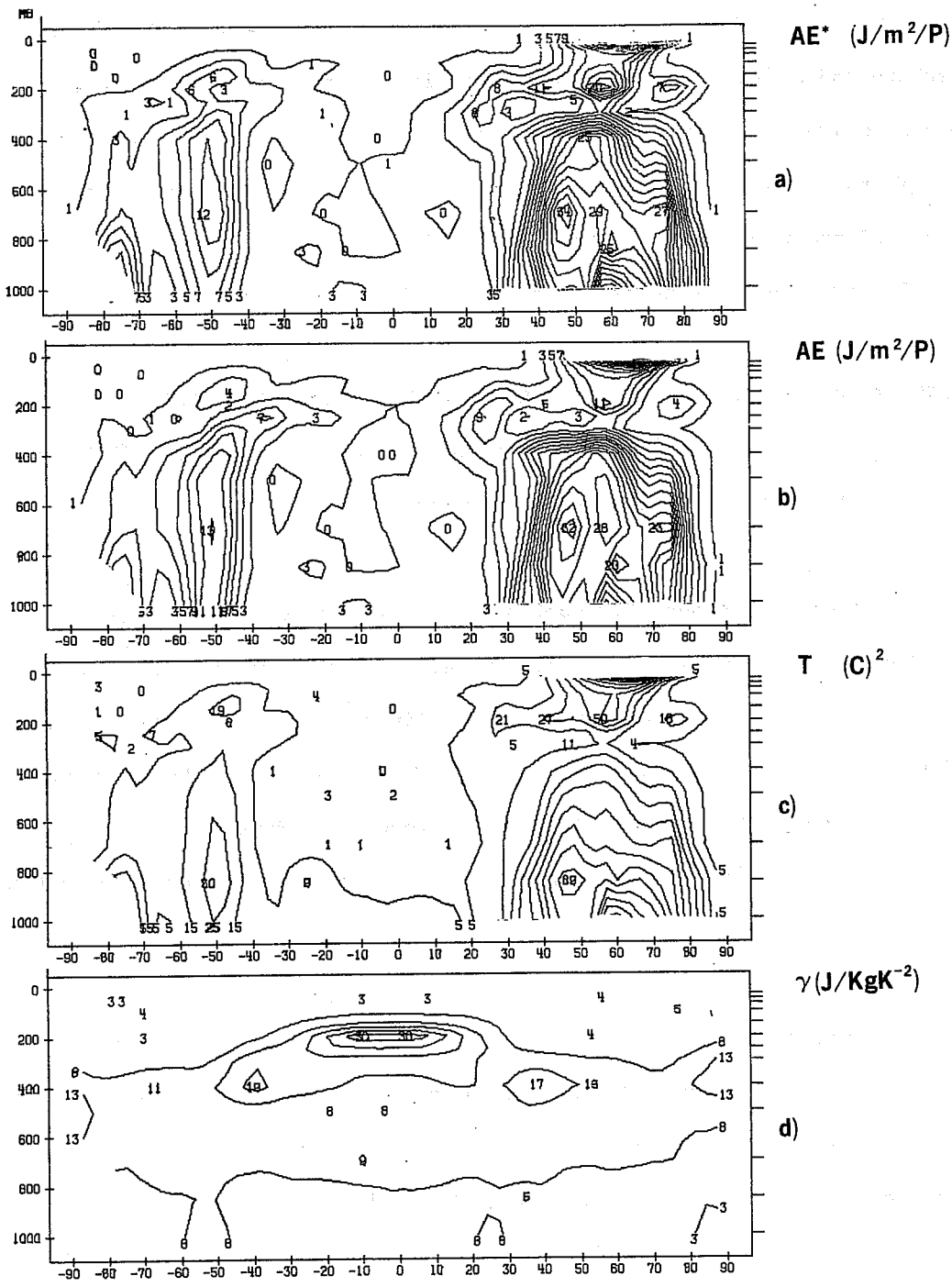

Fig. 20 Eddy available potential energy found for one single day using mean stability (a) and operational stability (b). Units: $J/m^2/P$. Variance of temperature (c) and γ at each point for the same day (d).

in the lower troposphere for the temperature (not shown), and the upper troposphere and stratosphere for the three wind components (Fig. 21).There was some increase in the mean temperature of the boundary layer and stratosphere and changes in the vertical structure of the meridional component of the wind. For this particular day, the whole energy cycle was increased, the changes being of the order of 10% or even more.

5. VERTICAL AND HORIZONTAL MEANS OF THE TERMS IN THE ENERGY BUDGET

A useful summary of the results given by the cross-sections of the fields can be found by studying their vertical or horizontal averages.

5.1 Contribution to the energy budget by wavenumber groups

The following zonal wave groups are investigated in what follows: long planetary waves (1 to 3), medium mostly baroclinic waves (4 to 9) and short waves(10 to 15) for January and July 1981. Values over the Antarctic are disregarded because they include data below ground. The main body of the pictures shows the vertical integral whilst the horizontal integral is on the right.

5.1.1 Eddy kinetic energy

In the eddy kinetic energy (bottom panel Fig. 22 and 23) one finds on the whole similar contributions from the long and medium waves except near the poles and at the latitude of the northern subtropical jet stream. The strong variability with latitude found in Fig. 5 for the Northern Hemisphere winters can be clearly attributed to the long waves.

5.1.2 Eddy available potential energy

The long waves contribute most to the eddy available potential energy in both months (Fig. 22 and 23, middle panel), but they are especially noticeable in January in the regions north of 40°N. The medium waves are almost as important as the long waves in most of the Southern Hemisphere; in both months there is a region where the AE due to cyclonic waves is slightly

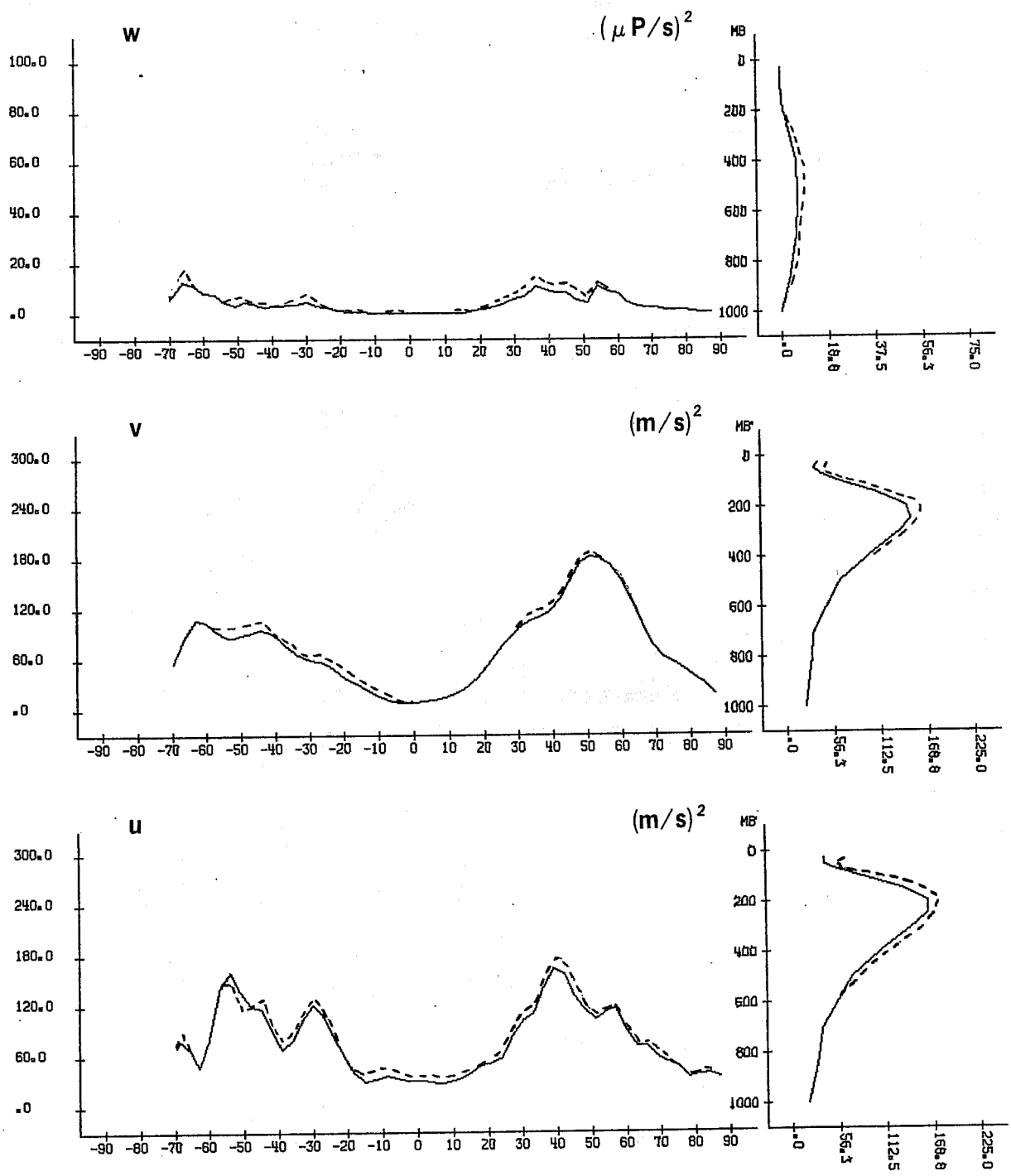

Fig: 21 Variance of the three wind components for a single day (———) without analysis of increments (----) with analysis of increments. Units as shown.

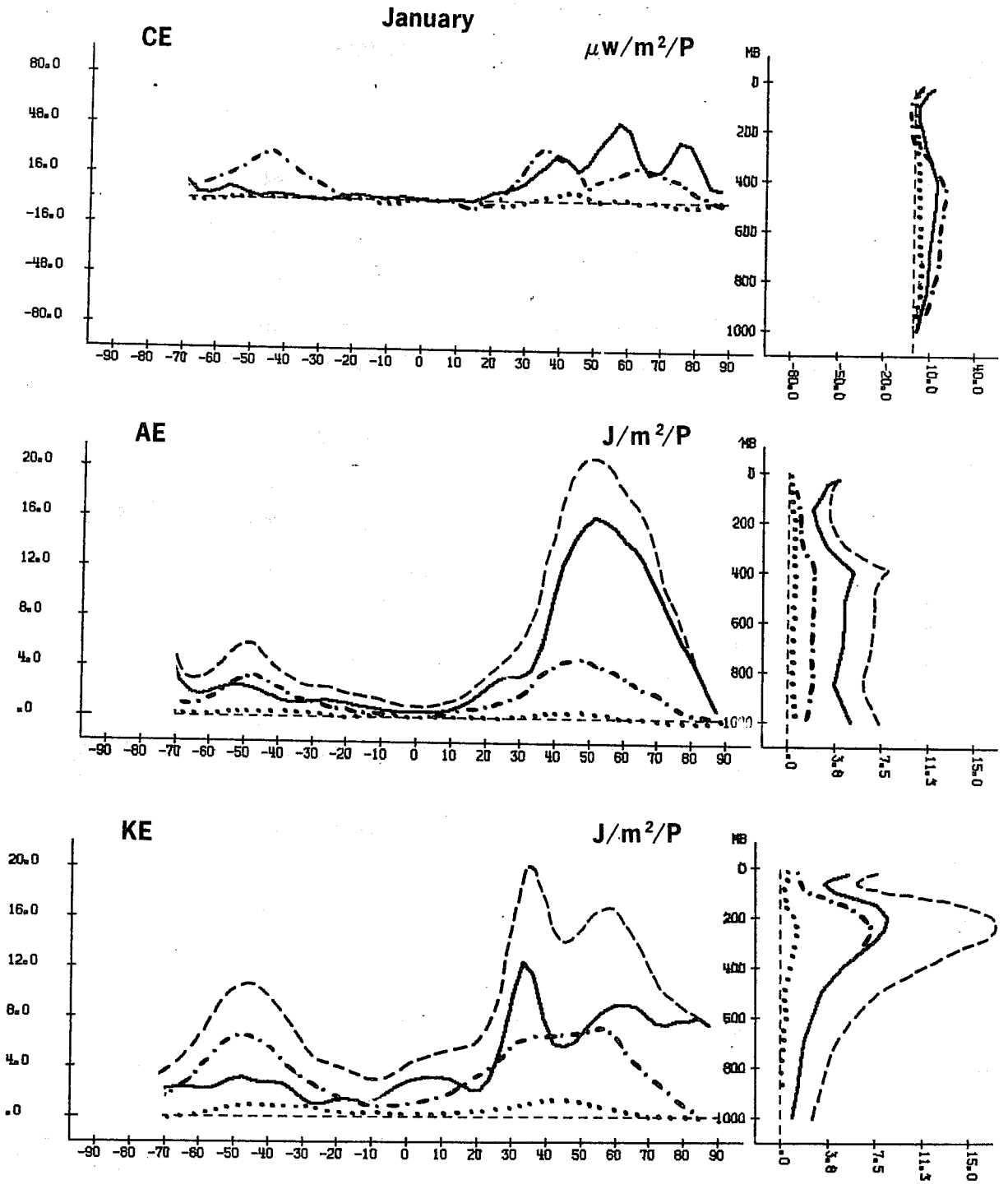

Fig. 22 Vertical and horizontal means of eddy components of available and kinetic energies and their conversions for January 1981. (——) long waves (.-.-.-) medium waves (....) short waves (----) all waves. Units as shown.

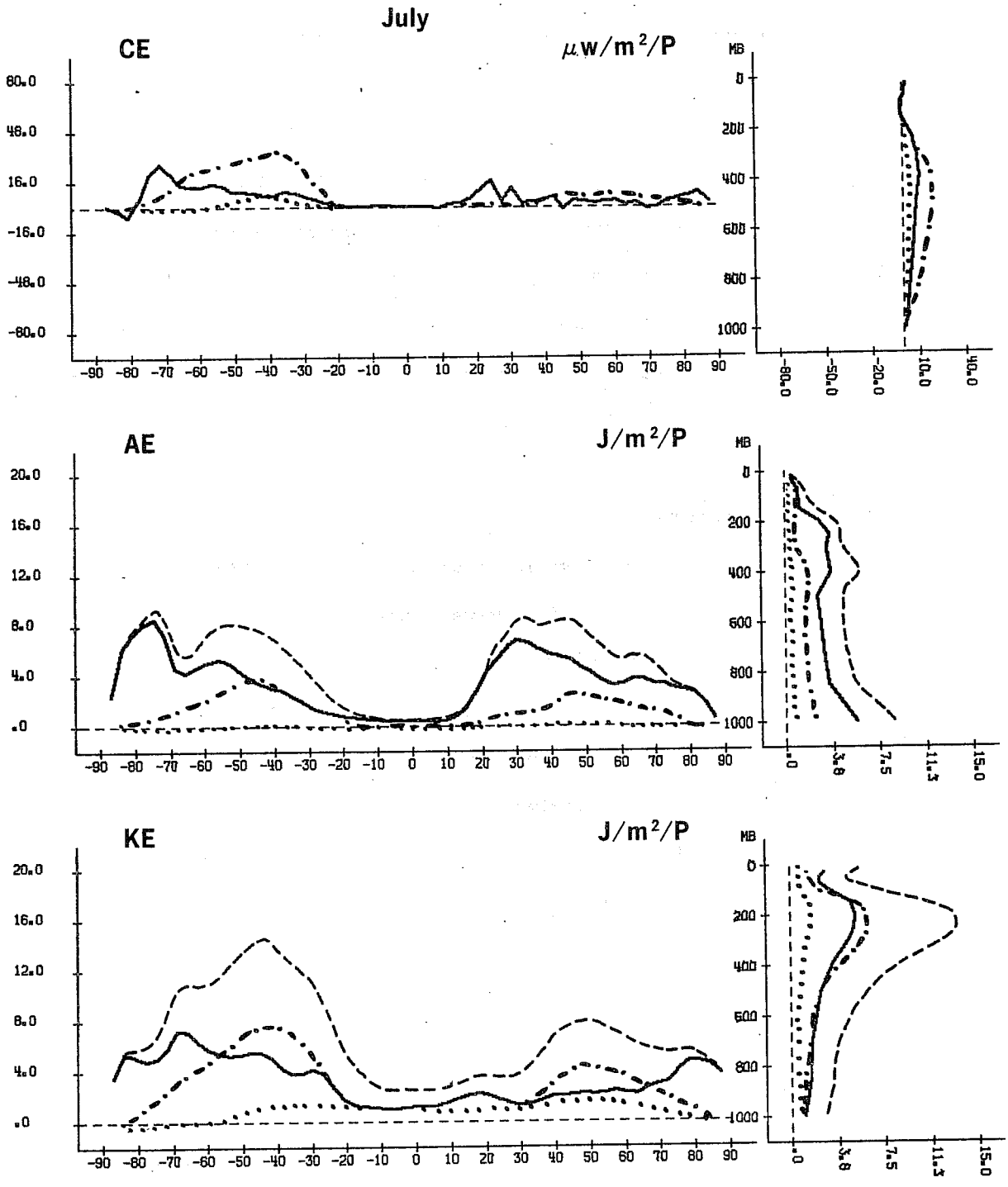

Fig. 23 Vertical and horizontal means of eddy components of available and kinetic energies and their conversions for July 1981. (———) long waves, (.-.-.-)medium waves (....) short waves (----) all waves. Units as shown.

higher than the AE due to long waves. Minor maxima occur at 400 mb due to a minimum of stability at this level for all scales (see Table 3).

5.1.3 The conversion term CE

The conversion between both forms of eddy energy (Fig. 22 and 23, top panel, only the three groups of waves are shown) is due mainly to the medium waves, with maxima between 400 and 500 mb. In many respects the seasonal change of CE reflects the corresponding behaviour of KE. The much stronger annual cycle of the Northern compared to the Southern Hemisphere is shown here to have contributions from both medium and long waves.

5.1.4 The conversion term CA

The conversion from zonal to eddy available potential energy (Fig. 24 and 25, medium panel) is dominated by the medium waves except for the stratosphere and north of 40°N in January, where long waves are predominant. The distribution and magnitudes are very similar to those of CE but with more marked latitudinal variability. In the Southern Hemisphere the conversion is done mainly be medium waves. The maximum at 45°S is higher in July (winter) than in January. In July there is a negative conversion by long waves in Northern Hemisphere which is compensated by a positive one due to medium waves.

5.1.5 The conversion terms CK,LK

A dominant feature in Fig. 9 was the dipole of CK near the subtropical jet in Northern Hemisphere winter. From Fig. 24 one can see that this is mainly due to long waves while medium waves give mostly negative values, that is, conversion from eddy to zonal kinetic energy. From this difference in the behaviour in each of the wavegroups and the fact that the Southern Hemisphere energy budget is dominated by medium waves it can be understood why the dipole shape is not so strong there. The CK of the long waves contributes very little to the total (as one can see in the vertical profile) therefore the forcing of the zonal flow is done mainly by the medium waves.

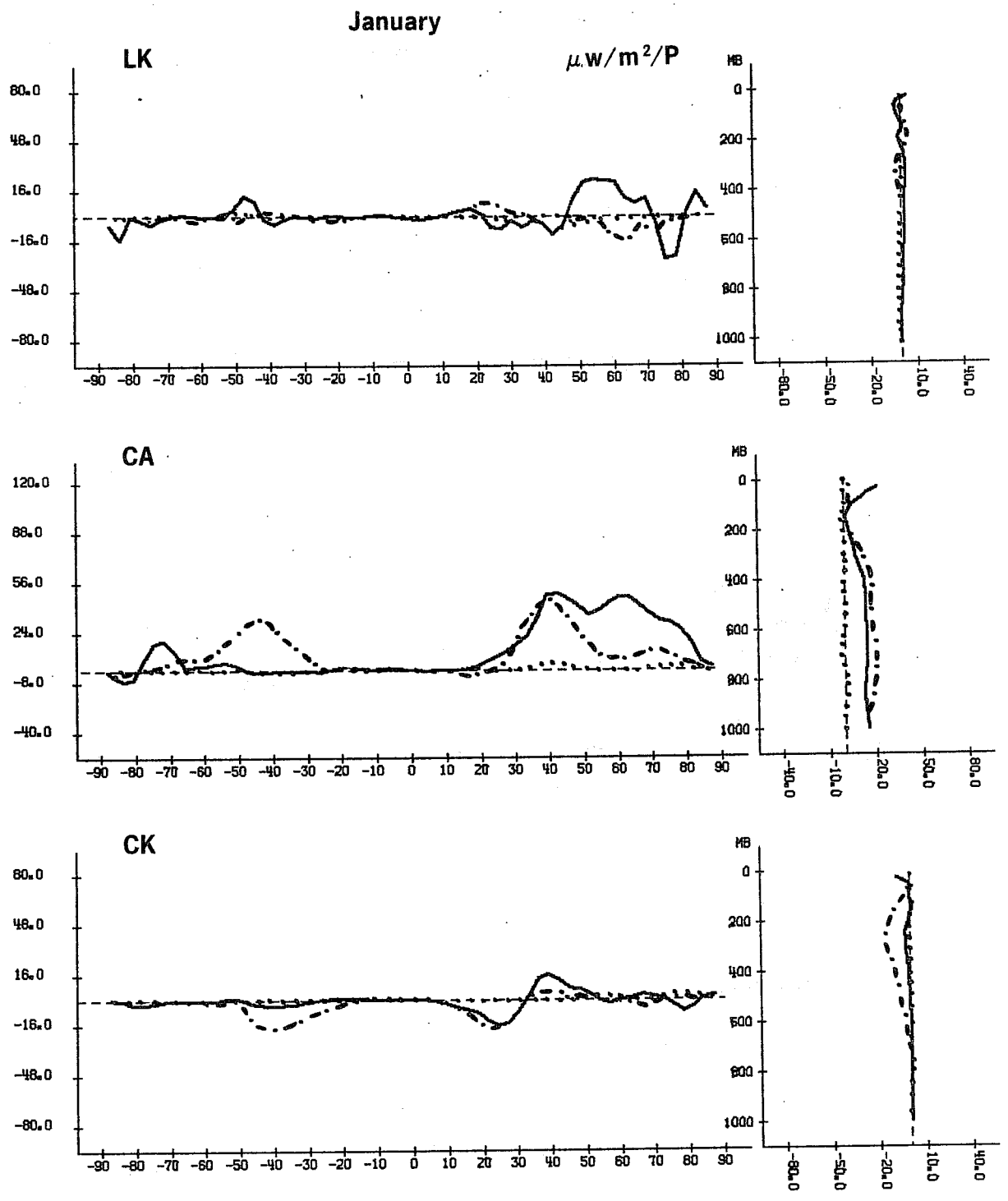

Fig. 24 Vertical and horizontal means of the conversions between eddy and zonal kinetic energy, eddy and zonal available potential energy and non-linear redistribution of eddy kinetic energy for January 1981. Units: $\mu w/m^2/P$.
(——) long waves, (.-.-.-) medium waves (....) short waves

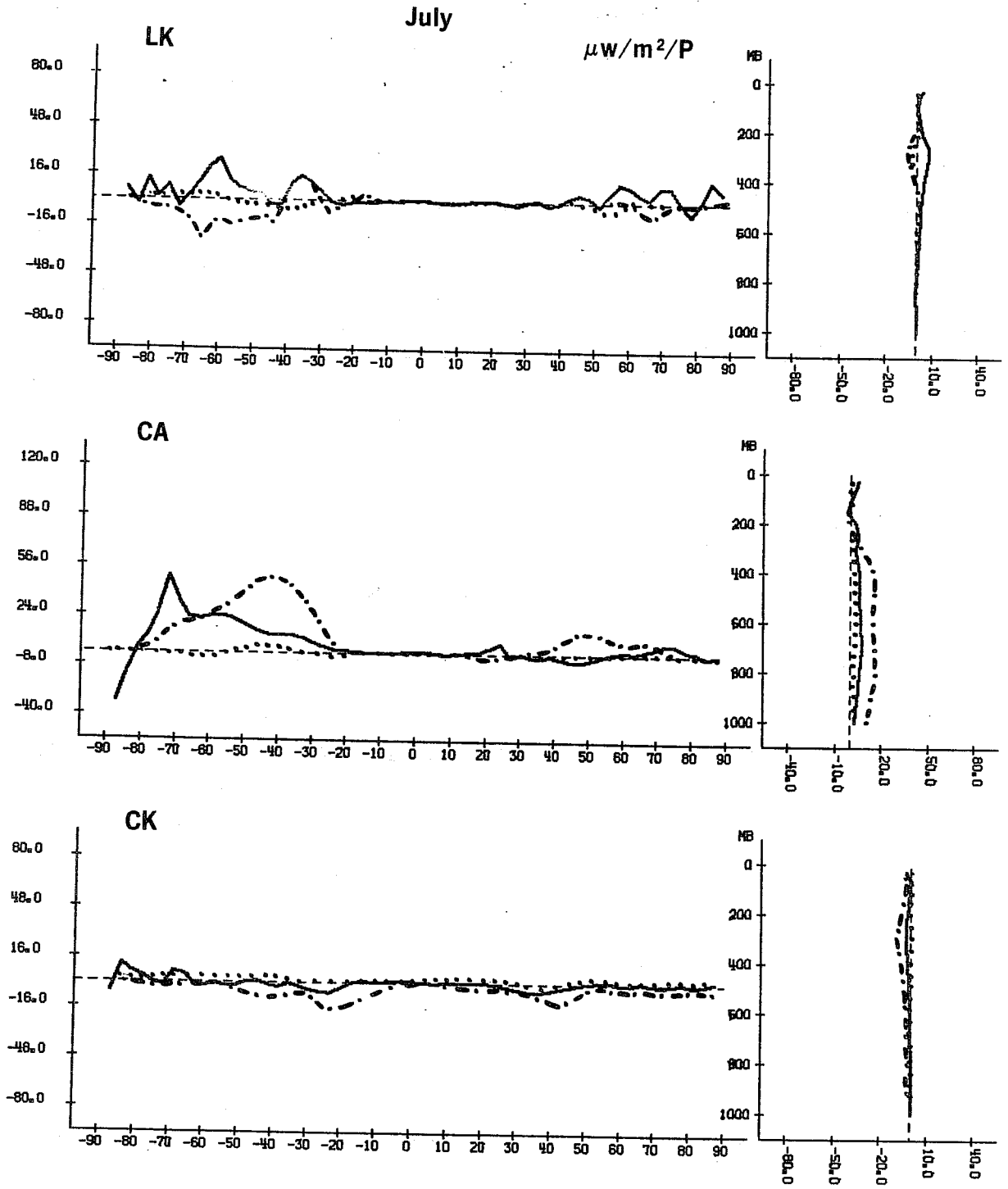

Fig. 25 Vertical and horizontal means of the conversions between eddy and zonal kinetic energy, eddy and zonal available potential energy and non-linear redistribution of eddy kinetic energy for July 1981. Units: $\mu w/m^2 P$.
(——) long waves, (.-.-.-) medium waves (....) short waves

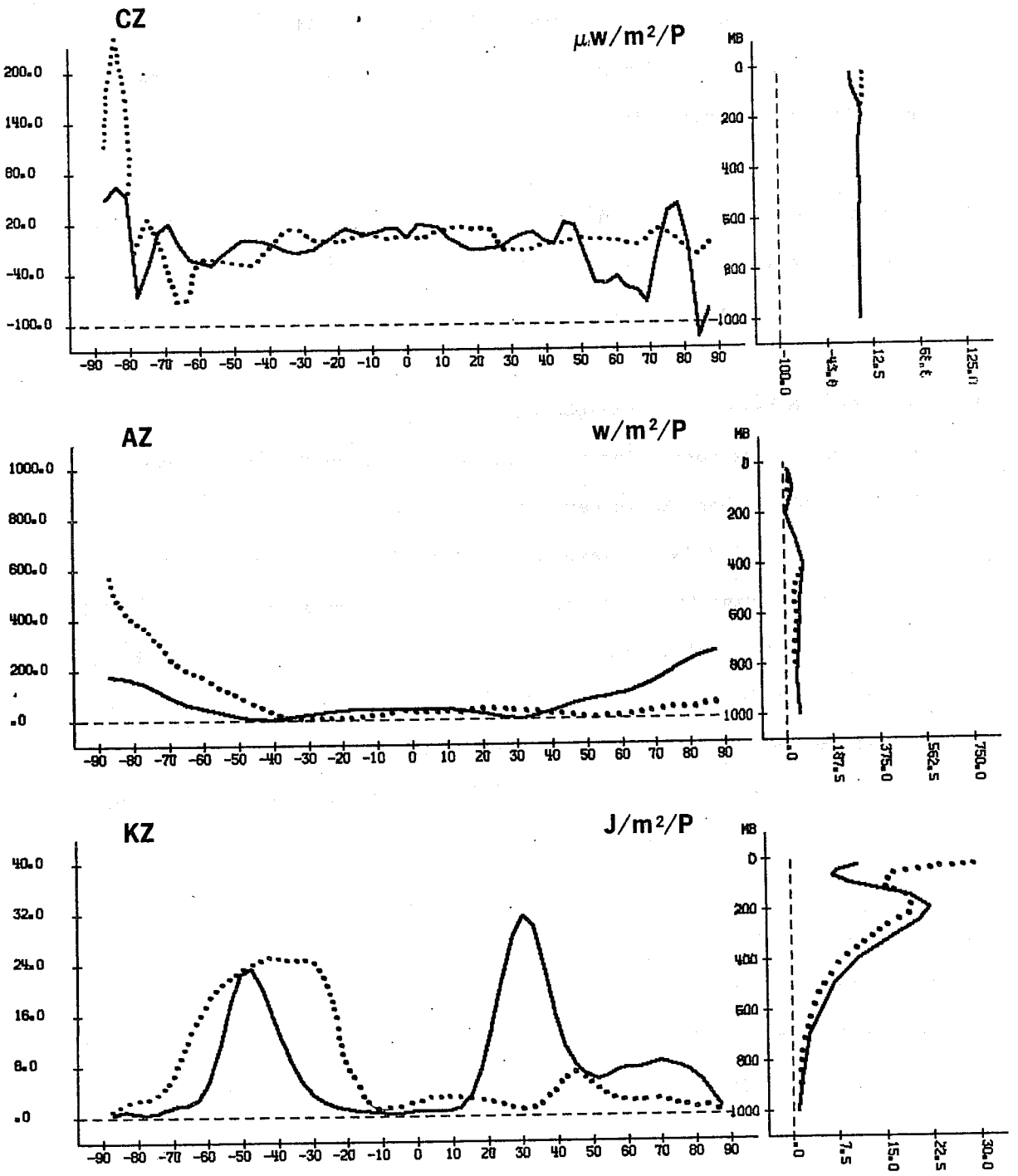

Fig. 26 Vertical and horizontal means of zonal components of available and kinetic energy and their conversions.
(——) January 1981 (....) July 1981. Units: as shown.

Regarding LK, the horizontal means are only significantly different from zero at the upper troposphere where the medium waves are feeding the long waves, particularly in July. An examination of the left panel shows that this forcing effect is strongest in the winter hemisphere.

For completeness, vertical and horizontal averages of KZ, AZ and CZ are presented in Fig.26 for both months. No comments further to what was already said when showing their cross-sections are necessary.

5.2 Comparison between both hemispheres

In Fig. 27 and 28 horizontal integrals corresponding to Northern Hemisphere (solid line) and Southern Hemisphere (broken line) are shown for all modes of energy in January and July. These are useful for comparing the vertical structure corresponding to the winter and summer hemispheres. It should be pointed out that the total horizontal average of the conversions have a non-zero annual cycle because the Northern Hemisphere cycle is larger than the Southern Hemisphere's. It is also interesting to mention that there is a small variation of the height of maximum KE and CK between summer and winter, and that they are situated at higher levels in summer in both hemispheres.

6. DAILY VARIABILITY OF THE ENERGETICS

6.1 Integrated daily values

The daily values of the integrated energetics are shown for two complete months to see their fluctuations; this enables one to see sudden changes and is consequently more informative than a knowledge of standard deviations.

In Fig.29 the four energy components for the whole winter hemisphere (1000-30 mb) are presented. Note that there is a different scale for AZ. Variations within the month are quite large, especially in the Southern Hemisphere winter, where AE and KE have a good temporal correlation, as also has AZ with KZ. Of particular interest is the increase of the zonal components which

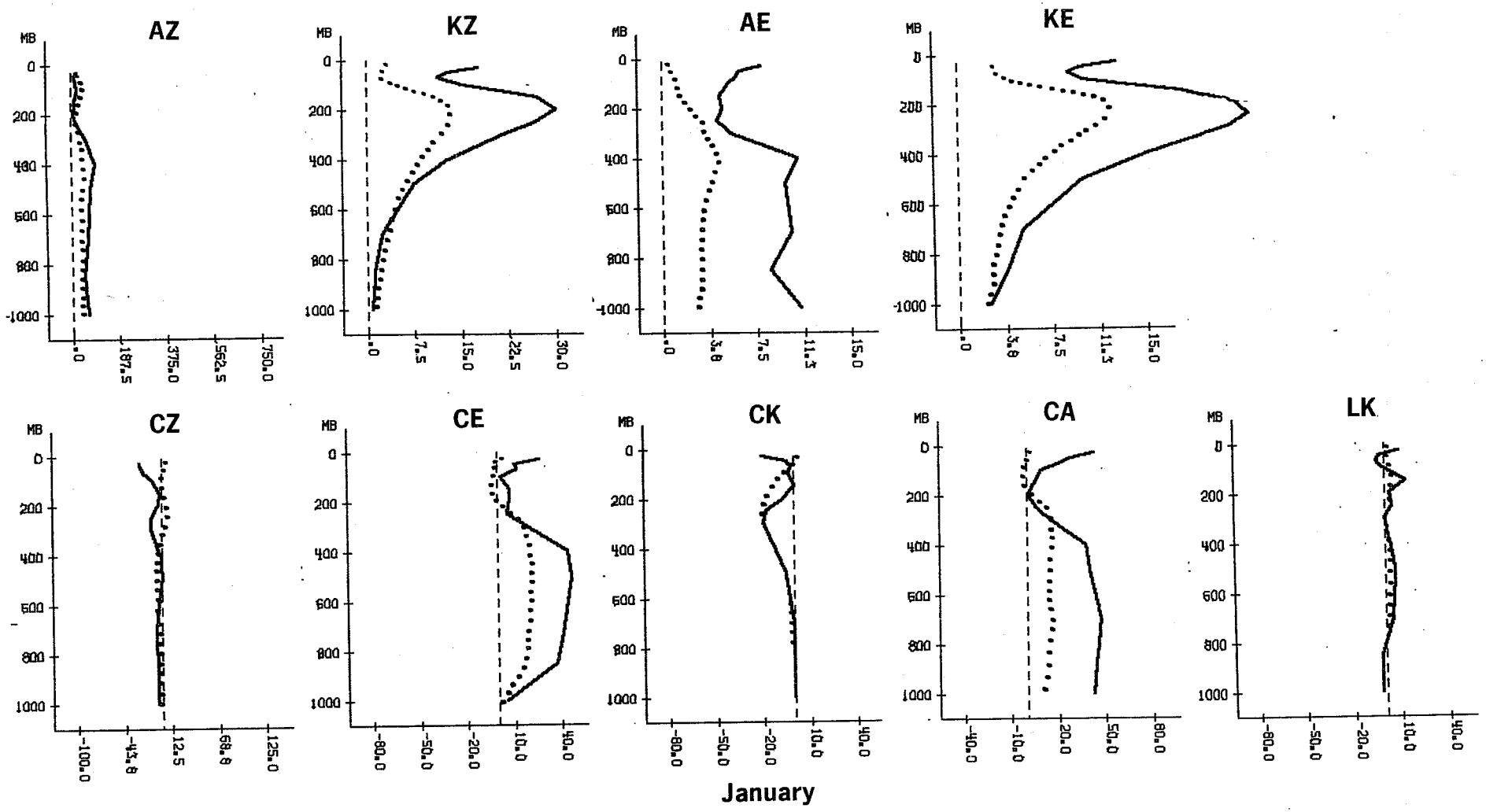

Fig. 27 Horizontal means all energy modes and conversions for January 1981 Northern (——) and Southern (....) Hemispheres. Units $J/m^2/P$ (energies) and $\mu w/m^2/P$ (conversions).

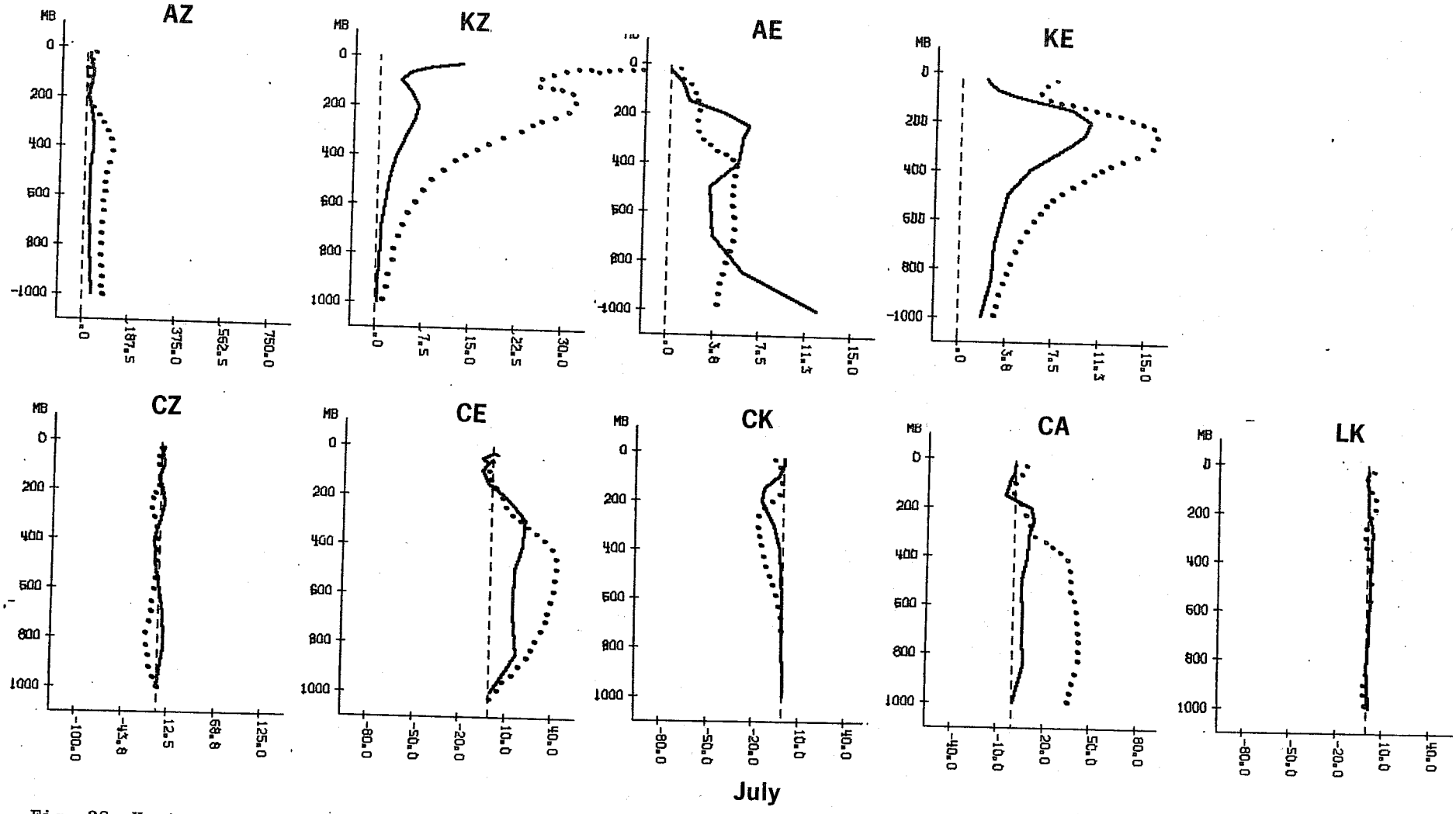

Fig. 28 Horizontal means all energy modes and conversions for July 1981 Northern (——) and Southern (....) Hemispheres. Units $J/m^2/P$ (energies) and $\mu w/m^2/P$ (conversions).

begins on the 11 July coinciding with a sharp decrease of both eddy components. In the Northern Hemisphere in January, AZ and KZ do not change significantly but AE starts increasing around the 9th of January and this continues steadily until the 24th; KE also increases, albeit less quickly than AE, but stops increasing a few days before AE.

In Fig.30 the conversions for the same hemispheres are presented. Two different time scales can be discerned. One is of the order of a few days with all conversions highly correlated with each other. This corresponds to the lifetime of individual cyclones. The other ones, which seems to be more than 10 days are difficult to find with only thirty days of data and will be studied in a future paper. In this frequency band only CZ with CK and CE with CA are correlated. The shorter frequencies have larger amplitudes in the Southern Hemisphere.

Maps of 500 and 1000 mb for selected days of January 1981 for the Northern Hemisphere are shown (Fig. 31) and a description of the synoptic events during that month is done.

The first day of the month was a typical example of winter circulation. At 1000 mb the Azores high was dominating much of the Atlantic and the Siberian high was also present; Scandinavia and Northern Europe were under the influence of a very deep cyclone as were Alaska and New Foundland. These features were also reflected at 500 mb showing a wave 3 pattern, but at 100 mb (not shown) the circulation was almost zonal. From that day onwards the situation remained very much the same, with stationary highs over the oceans and a new high developing over the Rockies being well established on the 6th (CA maximum), while cyclones were slowly filling and moving westwards to be again rather active on the 9th (maximum of negative CK on the 7th); cyclonic activity occurred in the Mediterranean, North Sea, New Foundland, Pacific.

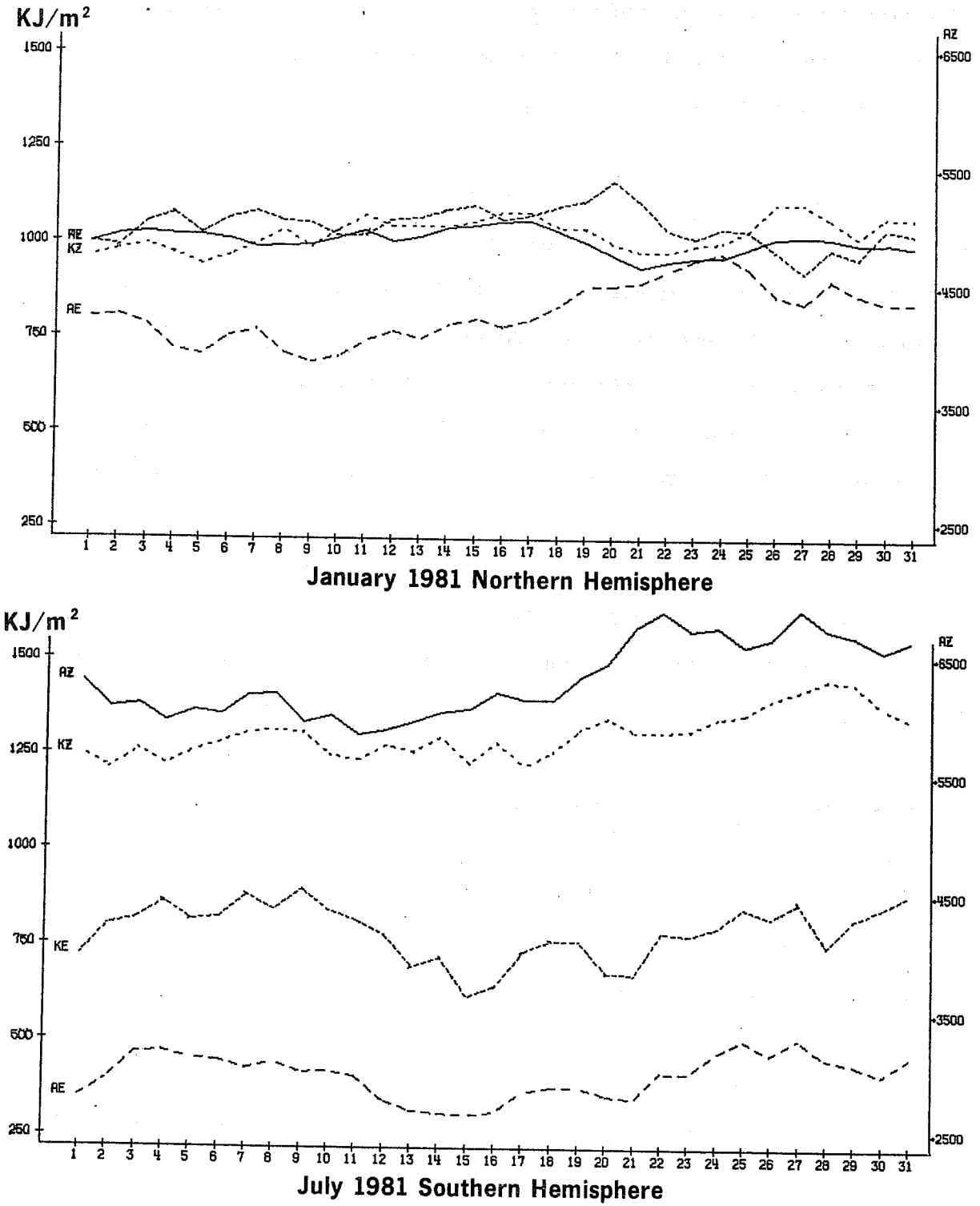

Fig. 29 Daily integrated values of energy modes for winter hemispheres: January NH (above) and July SH (below). Units KJ/m^2 (AZ scale on the right) AZ (——) KZ (....) KE (----) AE (— — —)

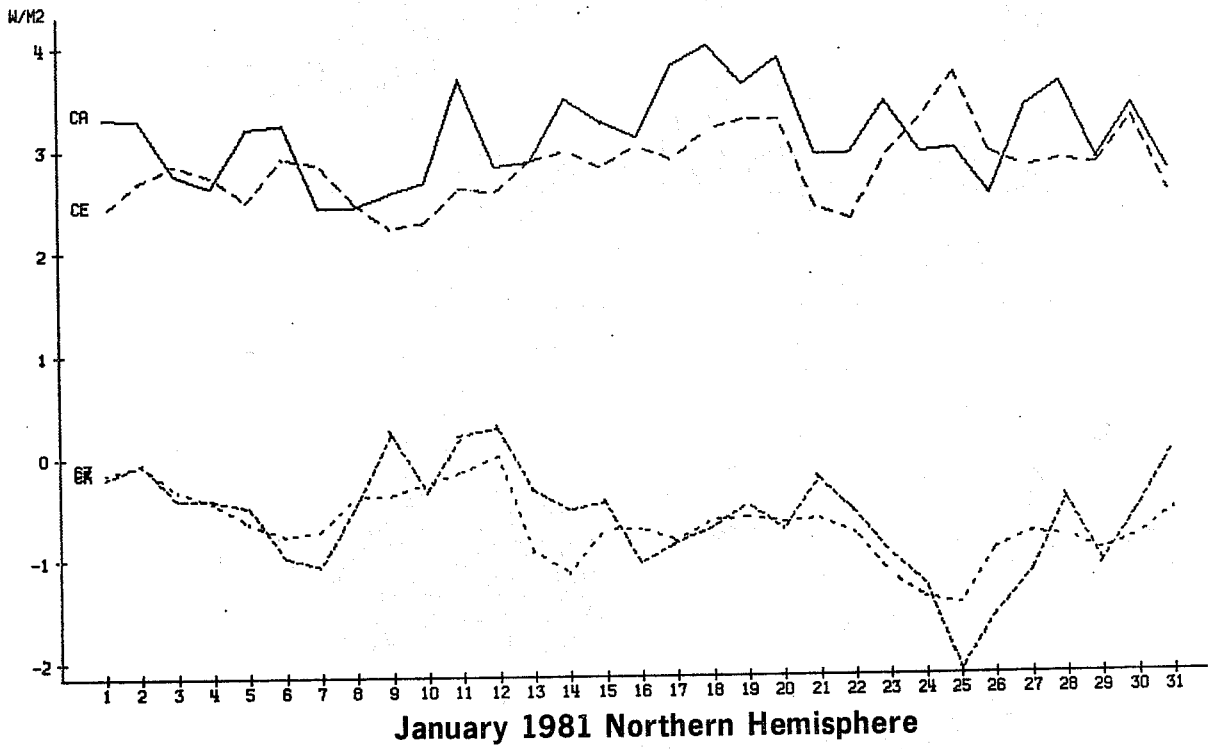

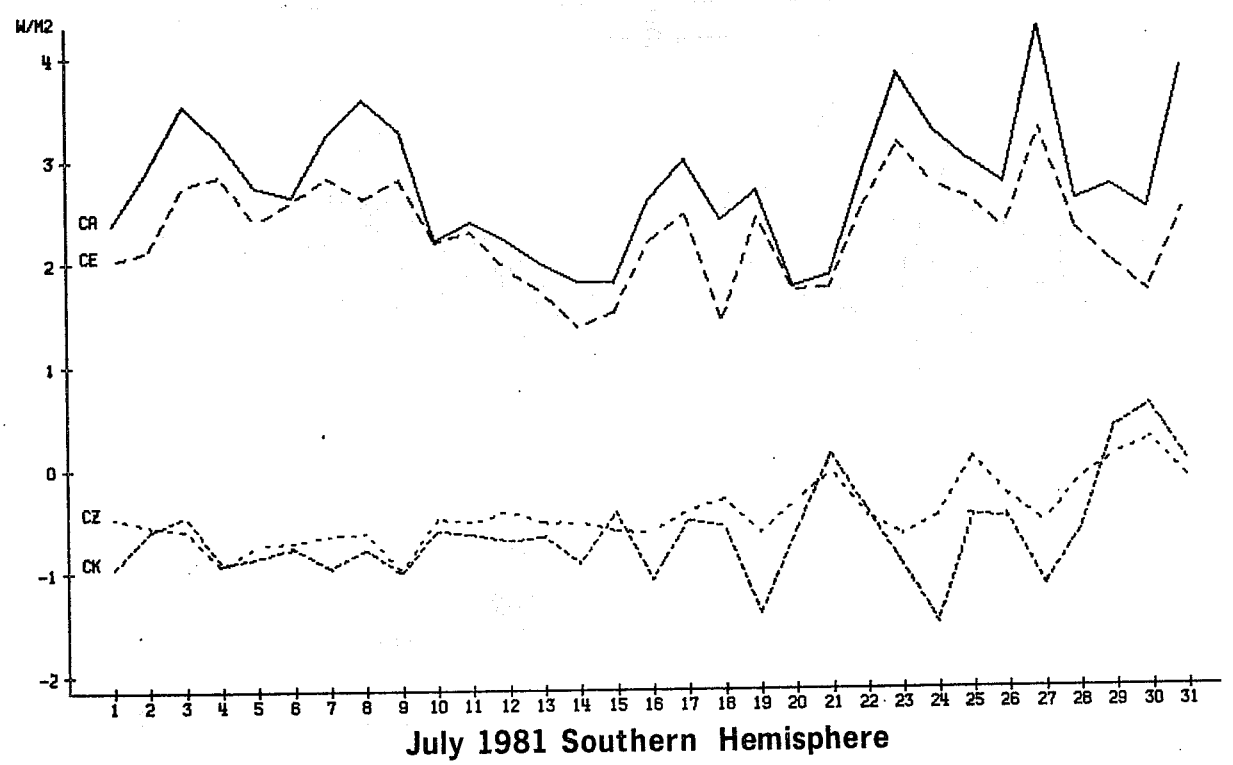

Fig. 30 Daily integrated values of conversions for winter hemispheres: January NH (above) and July SH (below). Units w/m^2.
CA (———) CZ (....) CK (----) CE (— — — —)

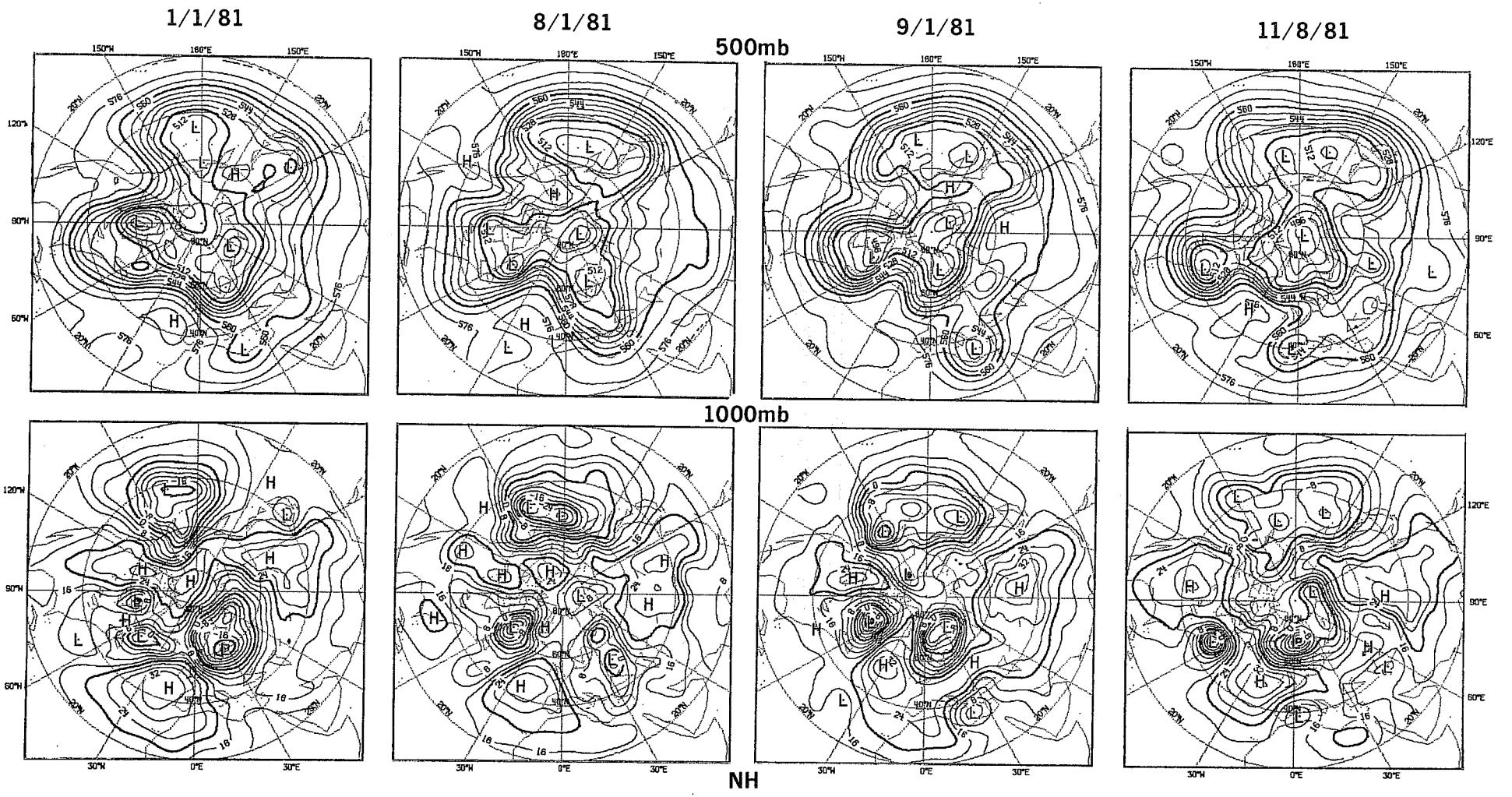

Fig. 31 Hemispheric 500 and 1000 mb maps for selected January 1981 days.

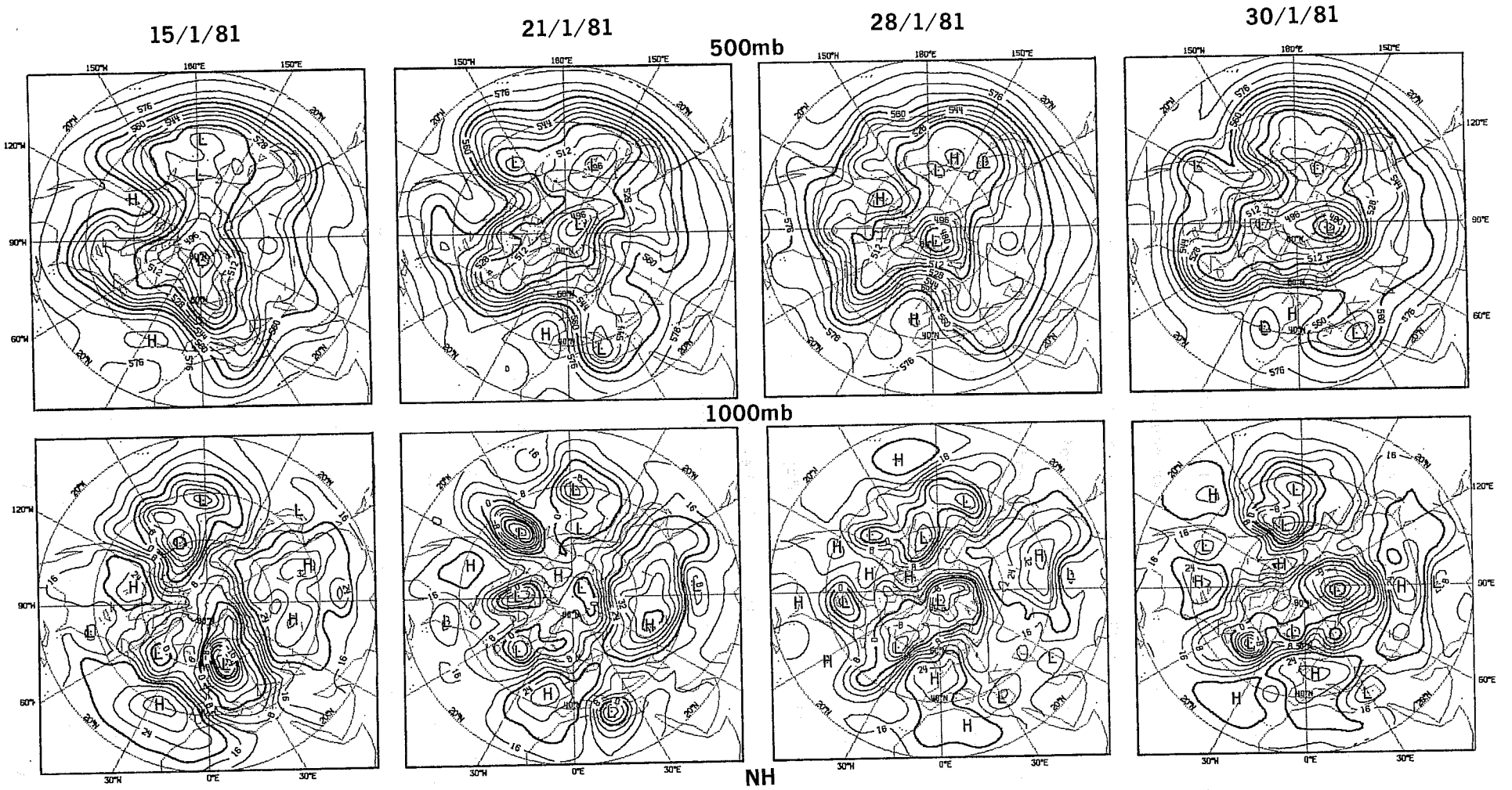

Fig. 32 Continuation of Fig. 31.

At 100 mb the circulation was mostly meridional. Two days later high pressure dominated the American continent, Asia and the Atlantic and two areas of intense cyclonic activity were located over New Foundland and North Cape. Four waves started to show by the 13th (positive CK maximum) when a deep trough penetrated Europe and a ridge formed over the Rockies; the circulation at 100 mb became zonal by the 15th (Fig.32) when another intense cyclone dominated Europe (increasing values of CE). Over the next few days cyclonic activity increased almost everywhere (high CE) when the Atlantic high moved north and the Rocky ridge persisted. By the 21st there were deep cyclones west of Alaska, over America and the Mediterranean, and on the 23rd the Atlantic high started to break down. One day later deep cyclones moving and deepening rather quickly were dominant (CE at its absolute maximum) and a high index circulation was established on the 26th, with CK negative and maximum at 300 mb, and wave number 8 or 9 was present. Fast moving fronts dominated the weather the following day and thereafter large depressions appeared again and gradually established the pattern of highs separating areas of deepening cylones which lead to a more meridional circulation by the end of the month.

Although it is difficult to relate local synoptic events with the energy parameters, which are averaged for a latitude row, some of the most dramatic changes reflected in their value. In particular the index cycle can clearly be seen in the peak reached by CK around the 26 of the month. It has already been mentioned that large values of CA, especially for long waves, have been related with blocking situations and this seems to be also confirmed here for January 1981.

6.2 Rate of change of energy parameters

An interesting aspect concerning the daily variations of the different energy modes is their rate of change. In Fig. 33 to 36 they are presented against the relevant conversions for the whole globe for January 1981. These values which oscillate a lot in the case of $\partial AZ/\partial t$, would although be rather small

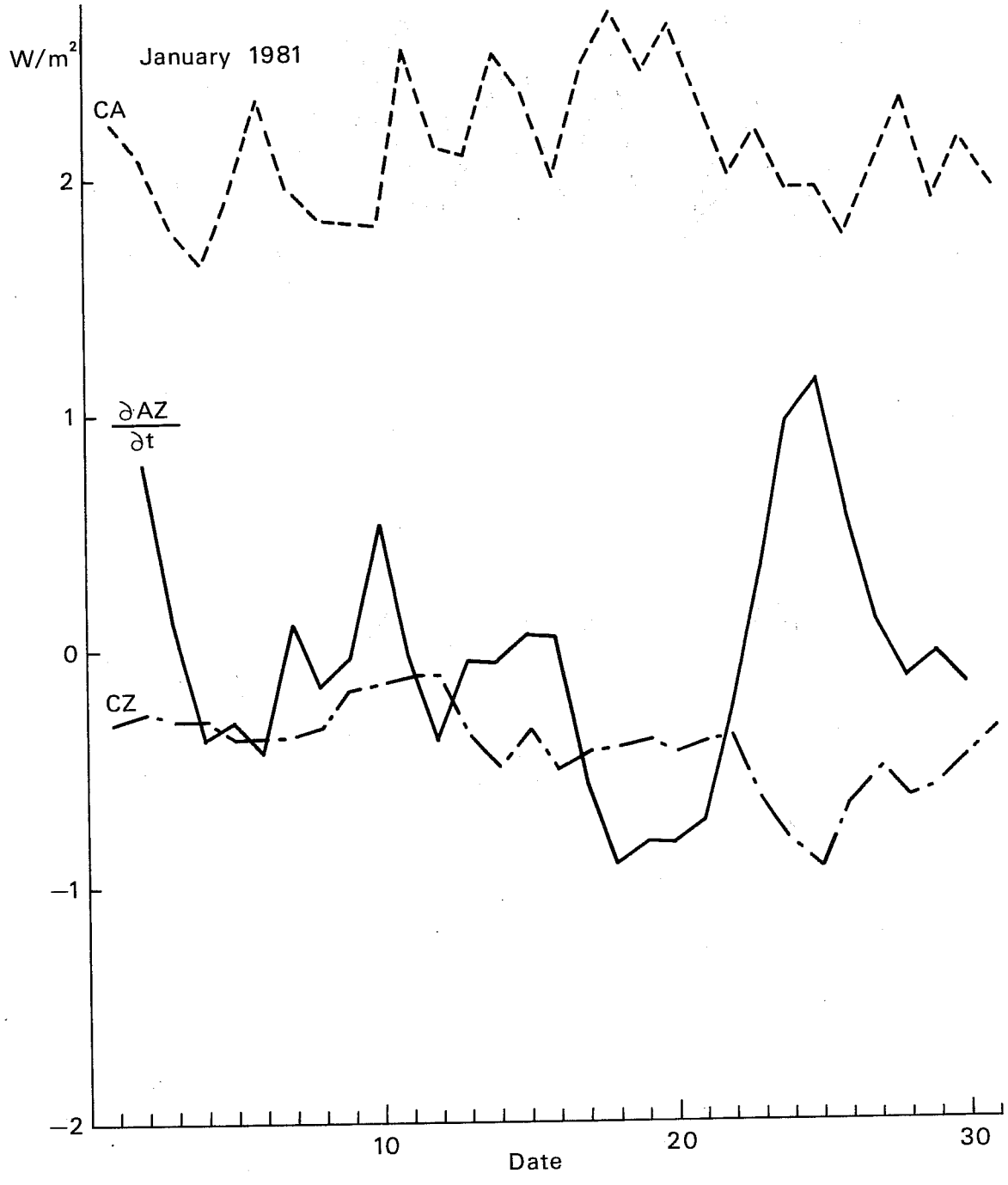

Fig. 33 Daily globally integrated values of CA and CZ and time variation of AZ for January 81. Units w/m^2.

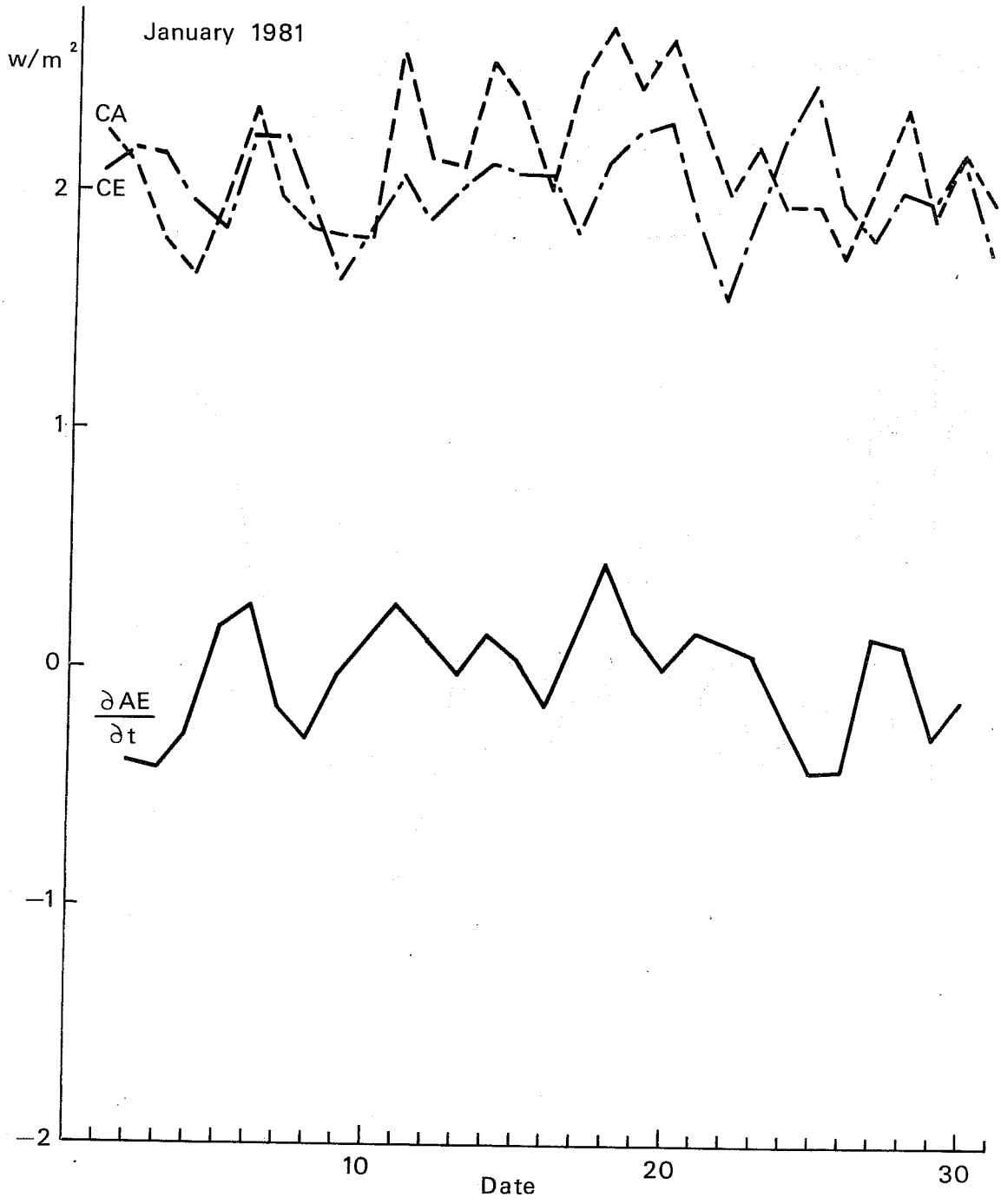

Fig. 34 Daily globally integrated value of CE, CA and time variation of AE for January 81. Units:w/m^2.

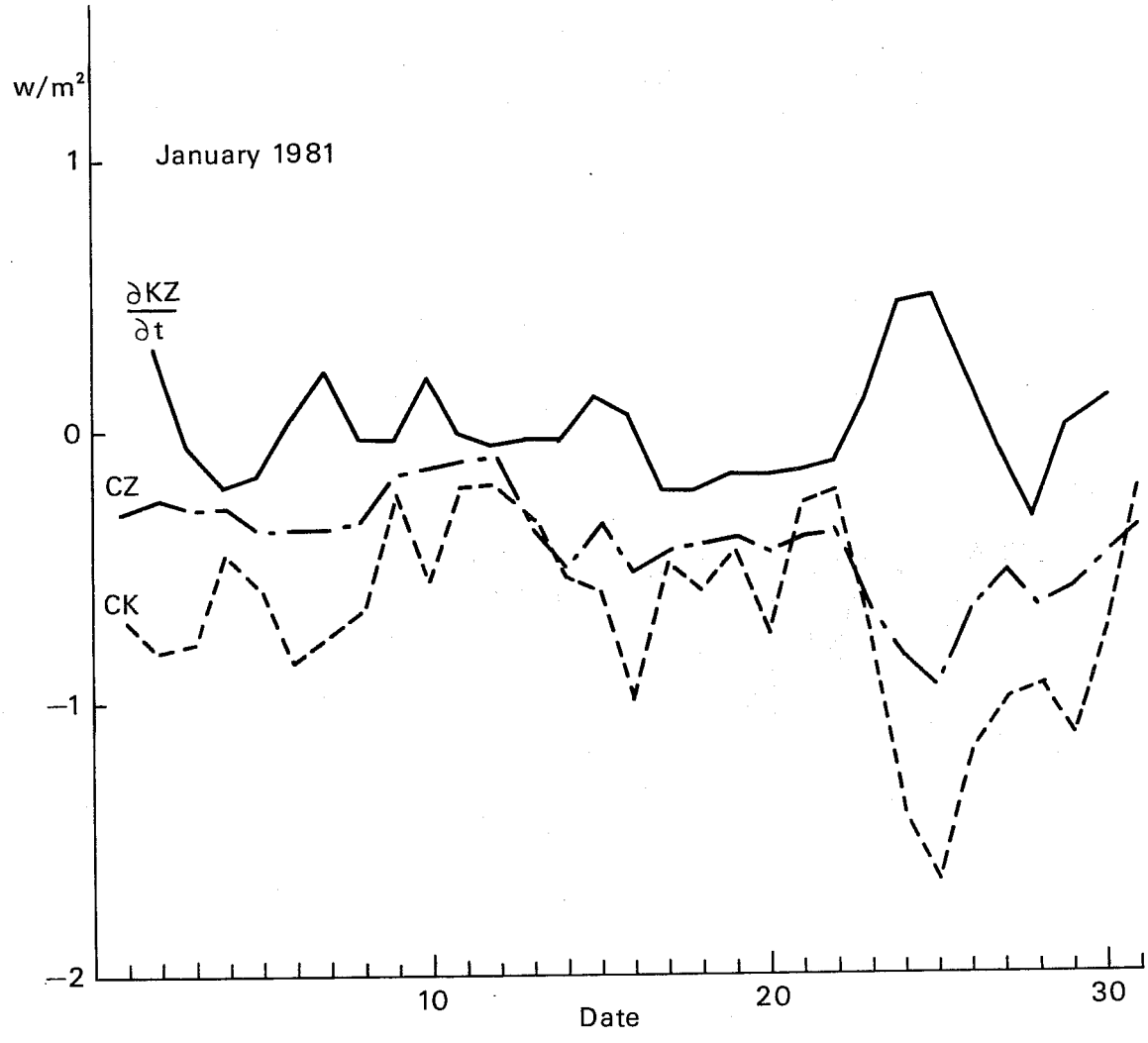

Fig. 35 Daily globally integrated value of CZ, CK and time variation of KZ for January 81. Units: w/m^2.

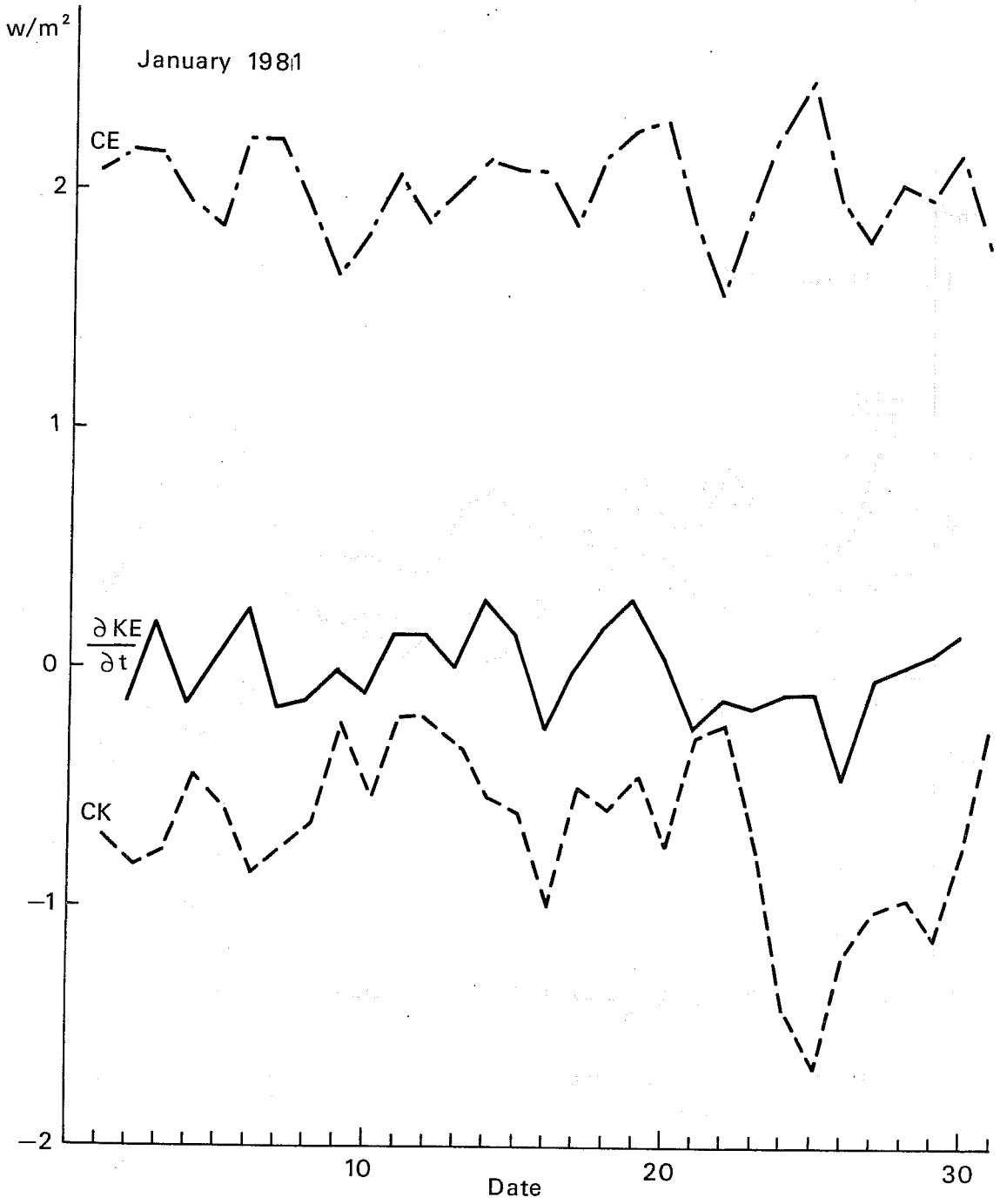

Fig. 36 Daily globally integrated value of CE, CK and time variation of KE for January 81. Units: w/m^2.

after averaging for the month. On a daily basis the time changes of the zonal energies are of comparable magnitude with the conversion terms and should be taken into account when calculating generation and dissipation terms as residuals. The time changes for the eddy energies look rather noisy and it seems doubtful that their inclusion in the calculation of generation and dissipation would improve the accuracy of the latest.

In Fig. 37 results including the tendencies are shown. The dissipation of eddy kinetic energy has a tendency to decrease throughout most of the month having a period of maximum values between the 10th and 13th of January and a high peak on the 20th, with minimum dissipation on the 26th; dissipation of zonal kinetic energy is rather variable but increases very sharply on the 22nd reaching the absolute maximum on the 25th; negative values are unrealistic but rather small.

Generation of eddy available potential energy decreases steadily in the early part of the month being at its lowest value on the 18th when it starts increasing very quickly to reach its maximum on the 25th. Although GE is for most of the time negative, there is positive generation due to diabatic processes for a few days in the beginning of the month and especially on the 24, 25 and 26th; the negative values are mostly found in the Northern Hemisphere and are attributed, in part, to cold air outbreaks over the warm oceans. The generation of zonal available potential energy is always positive (except for the 25th) indicating a high correlation between the zonal mean of diabatic heating and temperature; values are very high for the first two weeks reaching a maximum on the 19th, decreasing dramatically over a few days, and recovering to the previous values towards the end of the month. It is interesting to point out that the period from the 18th to the 26th includes all absolute maxima and minima for the four parameters; also from the 24th to 26th DZ > DE and GE > GZ unlike the rest of the month. Although events in the Northern Hemisphere are principally responsible for

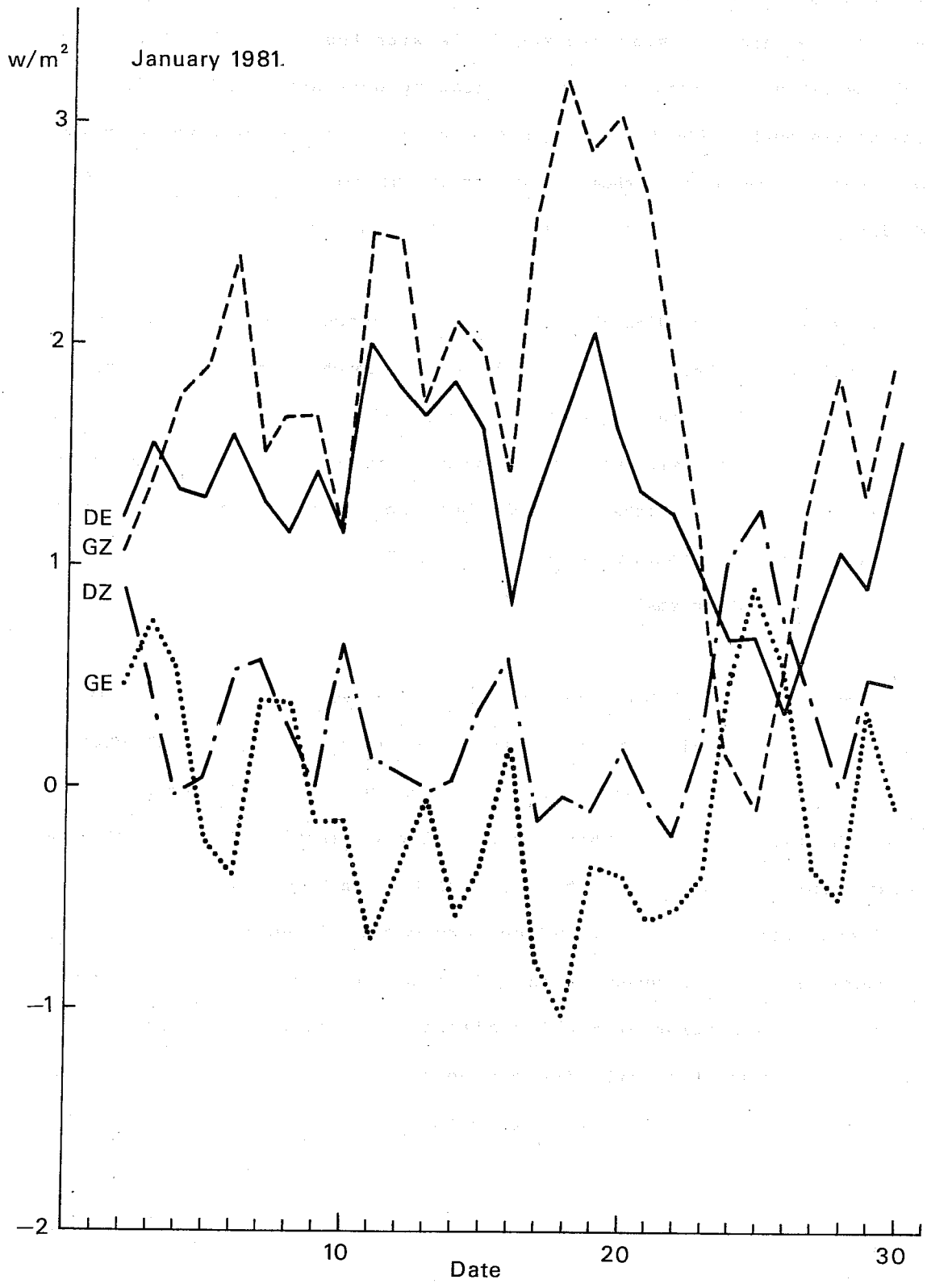

Fig. 37 Daily globally integrated generation and dissipation of energy including the time variations, for January 1981. Units w/m^2.

the overall behaviour - there is more activity in the winter hemisphere - there was also an unusual increase of CK in the areas around 26°N and 45°S at 300 mb which resulted in a conversion from KE to KZ in the Southern Hemisphere. The decrease in KE in Northern Hemisphere affected the strength of the zonal mean flow, as was discussed above.

7. POTENTIAL ENERGY GENERATION AND KINETIC ENERGY DISSIPATION

The generation and dissipation of energy are important measures of the intensity of the general circulation, so it is interesting to study them in detail. In what follows their values for the monthly means are calculated neglecting fluxes and also the time rate of change (as suggested in 6.2 above). Residuals are calculated from the conversions only. Results are presented in Table 4.

Table 4 Generation and dissipation of energy at each level for winter and summer hemispheres. Units: $\mu w/m^2/P$.

	GZ				GE				DZ			
level	Jn NH	Jl SH	JL NH	Jn SH	Jn NH	Jl SH	Jl NH	Jn SH	Jn NH	Jl SH	Jl NH	Jn SH
1000	36.4	34.5	- .1	6.9	-36.9	-33.9	.6	-7.5	-4.4	-1.9	- .8	-2.0
850	38.4	30.6	12.4	14.3	- 6.8	-14.3	10.2	2.8	-4.3	-8.8	6.4	.1
700	38.7	36.3	10.8	15.7	- 4.5	- 6.9	9.1	4.1	-6.5	-2.8	6.1	2.2
500	39.0	39.3	- .3	8.1	7.3	6.4	10.1	8.7	5.6	9.1	-3.8	1.4
400	35.1	34.6	1.6	9.1	7.1	4.3	12.1	7.9	10.9	13.4	-4.0	6.6
300	1.9	1.1	11.5	17.9	3.9	4.0	11.9	2.2	7.3	7.9	8.7	23.7
250	-8.4	-2.0	17.9	20.9	.5	-1.8	2.5	-3.1	4.6	5.3	16.4	30.1
200	-4.3	3.4	12.0	4.9	6.3	2.1	-2.9	-1.5	2.4	3.7	16.8	24.2
150	1.9	.5	-9.4	-10.7	2.8	- .1	3.2	1.0	-2.1	2.8	9.8	9.1
100	-2.8	-3.0	- .2	- 4.8	-7.1	-4.5	-3.2	-1.6	-7.7	- .9	6.9	3.1
70	.1	.5	.7	- .1	-9.4	-4.8	-1.6	1.4	-19.2	-1.8	3.6	1.7
50	2.9	4.0	.3	- .9	-17.2	-6.4	-6.5	-3.4	-19.9	2.1	1.1	- .6
30	15.6	.5	3.1	2.1	-16.0	-5.3	.4	4.4	-5.5	1.8	3.6	1.9

Generation of zonal available potential energy due to the north-south heating gradient produced mainly by the radiation balance and precipitation has in winter very large positive values up to 250 mb with maximum of 39 $\mu w/m^2/P$ at 500 mb; in summer smaller positive values are found in both hemispheres up to 150 mb. At 100 mb GZ is always negative while at upper levels it is again mostly positive.

There is a significant destruction of AE in winter in the lower troposphere with a maximum value of 37 $\mu w/m^2/P$ in the boundary layer, probably caused by surface fluxes of sensible heat or convective precipitation within cold air outbreaks. GE is positive and rather small in summer for levels up to 300 mb, being mainly negative in the stratosphere. There is a source of AE in the middle and upper troposphere, where frontal precipitation is produced, and a sink again at stratospheric levels, due to radiation.

In winter several levels have unrealistic negative values of DZ which could perhaps be cancelled by vertical fluxes which have not been calculated $\left(\frac{\partial \bar{\omega}\ \overline{KZ}}{\partial p}, \frac{\partial \bar{\omega}\ \bar{\phi}}{\partial p}\right)$. This could also account for the absence of a maximum in the boundary layer. On the other hand, these values are derived as residuals and involve therefore the values of CZ which are unreliable due to the already mentioned initialization problem, however CZ is likely to be small anyway. Dissipation of zonal kinetic energy is higher in summer and maximum values are situated there around 250 mb level.

The only available geopotential fluxes are those required for the eddy kinetic energy calculations; a more comprehensive study of all terms involved in the calculations of DE, including also the contribution due to non-linear redistribution of energy, could be carried out for example. In Table 5 there is a list of the conversions taking place at each layer and the upward geopotential flux for (different) layers, all expressed in 10^{-3} w/m^2.

The conversion from eddy available to eddy kinetic energy minus the conversion from the latest to zonal kinetic energy (column CE+CK) is quite large in the lower and middle troposphere with a maximum at around 700 mb in all cases. It is positive up to 400 mb except for the July Northern Hemisphere where there is a positive contribution at 200 mb; in stratospheric layers values are negative except for the January Northern Hemisphere.

Redistribution of eddy kinetic energy (LK) is of the order of 10% of the other terms in each tropospheric layer becoming significant in the winter stratosphere.

From the last four columns in Table 5 it can be shown that there is divergence of kinetic energy in layers between 850 and 400 mb and up to 250 mb in the July Northern Hemisphere; maximum divergence occurs usually in the layer 700-500 mb while maximum convergence is found at 300-250 mb in winter and around 150 mb in summer. Convergence in upper levels is higher in summer and divergence in lower ones in winter.

Adding up the values in the relevant columns it is found that there is small negative dissipation of KE between 800 and 500 mb in winter while in summer there is dissipation practically everywhere. Total eddy dissipation between 1000 and 30 mb is 2.0 w/m^2 in January Northern Hemisphere, 1.4 w/m^2 in July Southern Hemisphere, .8 in July Northern Hemisphere and .7 in January Southern Hemisphere. These latest values are in agreement with results found by Savijärvi (1980) for FGGE data. It was shown there that total dissipation was almost halved when using initialized data and this fact suggests again a cautious interpretation of their physical meaning; this applies especially to negative numbers.

Table 5 Contributions to the dissipation of eddy kinetic energy in each layer for winter and summer hemispheres. Units: 10^{-3} W/m^2.

	Jan NH		Jul SH		Jul NH		Jan SH	
Layer (mb)	CE+CK	LK	CE+CK	LK	CE+CK	LK	CE+CK	LK
1000-925	29.2	-24.0	18.7	-11.2	9.7	3.0	10.5	-6.0
925-775	538.5	-43.5	361.5	-33.0	243.0	-7.5	255.0	-9.0
775-600	712.2	73.5	563.5	40.2	241.5	15.7	308.0	21.0
600-450	610.5	90.0	399.0	64.5	204.0	24.0	231.0	43.5
450-350	313.0	27.0	256.0	12.0	177.0	23.0	104.0	21.0
350-275	-11.2	-4.5	-13.5	-24.0	110.2	21.0	-27.0	-1.5
275-225	-62.5	20.5	-45.5	7.0	20.0	11.5	-61.5	6.5
225-175	-.5	13.0	9.0	7.5	-38.5	-1.5	-104.0	5.5
175-125	34.0	64.5	-12.0	33.0	-80.0	.5	-94.0	29.5
125-85	-8.8	-4.8	-26.4	.0	-41.2	.8	-38.0	4.4
85-60	24.7	-14.7	-6.2	-2.2	-11.2	-2.2	-1.0	-2.0
60-40	11.2	-7.8	-9.0	-.0	-14.6	-1.6	-7.4	-1.4
40-10	15.3	25.5	-19.8	10.5	-.3	.6	13.8	-1.8
Σ	2205.6	219.2	1475.3	104.3	819.6	87.3	589.4	109.7

	Jan NH	Jul SH	Jul NH	Jan SH
Layer (mb)	$-\frac{1}{g}w\phi\Big]_{p_1}^{p_2}$			
1000-850	820.4	575.2	342.5	274.4
850-700	-736.4	-540.5	-235.9	-339.8
700-500	-917.5	-750.7	-208.2	-390.7
500-400	-246.9	-204.6	-153.7	-111.3
400-300	190.4	205.7	-145.4	62.3
300-250	223.8	220.1	-31.7	87.6
250-200	140.2	145.2	59.9	131.3
200-150	23.7	33.9	98.2	132.2
150-100	3.6	12.2	134.7	61.0
100-70	13.5	25.0	16.5	5.2
70-50	11.8	26.4	10.9	10.1
50-30	56.6	22.9	2.9	39.0
Σ	-416.8	-229.3	-109.3	-38.7

Table 6 Mean generation and dissipation of eddy kinetic energy at each latitude for January and July 1981. Units: $\mu w/m^2/P$.
(*) Dissipation includes horizontal fluxes.

SOUTHERN HEMISPHERE					NORTHERN HEMISPHERE				
	JANUARY		JULY			JANUARY		JULY	
lat	GE	DE*	GE	DE*	lat	GE	DE*	GE	DE*
87°S	6.5	-35.8	-29.9	- 0.7	87°N	5.7	- 9.9	3.5	- 9.4
84	9.1	- 0.3	6.7	-95.1	84	5.2	- 3.2	10.8	1.0
81	15.2	-43.6	- 9.0	-118.1	81	6.3	21.6	6.4	7.8
78	-1.8	-33.7	- 6.2	-26.5	78	11.9	44.4	4.1	12.4
75	-7.1	7.2	-11.1	7.5	75	12.0	50.3	1.0	7.9
72	-1.1	38.5	-35.1	60.6	72	.1	38.8	-5.7	5.2
69	-1.5	40.2	-17.6	118.2	69	-11.1	31.2	-5.8	10.9
66	1.3	17.4	-9.4	67.9	66	-16.6	29.0	.3	17.6
63	3.0	8.7	-6.4	18.3	63	- 3.4	46.3	5.7	- 7.8
60	5.3	8.2	- 9.9	16.0	60	12.6	52.7	8.5	5.9
57	7.9	9.4	-12.0	32.0	57	21.7	44.4	8.5	8.4
54	.6	12.3	-16.3	36.3	54	16.1	34.7	5.6	12.2
51	-2.5	16.2	-20.6	41.4	51	3.3	40.5	5.8	15.1
48	- .8	5.3	-21.2	55.1	48	-23.4	47.9	7.8	14.9
45	3.3	4.1	-18.0	59.0	45	-32.2	64.6	2.8	4.6
42	5.3	9.3	-14.8	42.0	42	-27.1	82.9	12.3	14.8
39	3.0	10.6	- 9.5	17.8	39	-32.7	74.0	12.9	18.8
36	3.4	8.2	- 6.0	7.4	36	-12.9	59.2	9.7	- .2
33	4.9	7.3	- 4.0	8.6	33	- 1.6	42.9	11.3	- 6.6
30	5.0	6.1	.6	18.3	30	- 1.5	31.1	17.9	13.8
27	5.0	2.7	3.2	22.0	27	.6	20.3	11.2	6.8
24	6.4	3.1	3.4	11.4	24	1.0	4.1	17.3	16.7
21	4.3	2.8	1.7	0.3	21	2.8	- 6.5	11.3	6.5
18	2.8	3.5	.7	- 1.5	18	1.1	-10.2	8.0	9.6
15	1.4	.5	.6	.9	15	- .3	- 9.7	4.8	10.6
12	1.3	-0.1	1.8	2.2	12	.4	- 3.6	2.6	8.9
9	2.2	2.0	2.0	1.6	9	1.4	3.5	2.3	9.5
6	2.1	4.3	2.1	3.7	6	1.5	8.0	2.0	8.3
3	2.0	4.8	1.6	3.5	3	1.1	8.0	1.4	0.0
0	-.1	5.2	1.1	5.4					

In Table 6 the geographical distribution of GE and DE averaged for the 1000-30 mb layer for January and July (horizontal fluxes not included) is listed. For DE, convergence or divergence of $v'\phi'$ has been taken into account (see also Fig. 38). GE has small positive values in January in the Southern Hemisphere and from the equator to 30°N; then there are alternate bands of sources and sinks of energy (width 15°), with important losses at mid latitudes. The latter may be related to convective precipitation in cold air outbreaks, especially in the troughs to the lee of the Rocky Mountains and Himalayas. Warm air intrusions towards the north, which are subject to cooling will have the same effect on GE. In July behaviour is similar in the summer hemisphere, but with bigger positive values; on the other hand, there is sink of energy in all the extratropical Southern Hemisphere.

DE is positive everywhere except a very few areas in the Northern Hemisphere. The biggest dissipation occurs in the winter hemispheres with noticeable high values in January around 45°N. There is some evidence that the introduction of PAOBS in March reduced some of the noise found in the values of DE in the Southern Hemisphere. The values corresponding to mid latitude were found to be more regularly distributed and larger in April 81 than in February, and this would explain the more realistic behaviour corresponding to July.

A final comparison of the total generation for both months is made in Fig. 39. In July there is a source of available potential energy everywhere except for a small region in Southern Hemisphere near the Pole. in January there are some places with negative values. Larger values (apart from polar regions) are at mid-latitudes in the winter hemispheres and there is a remarkable symmetry regarding the maximum values in each season (horizontal fluxes are not taken into account).

8. ANNUAL CYCLE

The monthly mean integrated values of the energetics have been calculated for Northern and Southern Hemispheres and their seasonal evolution for the

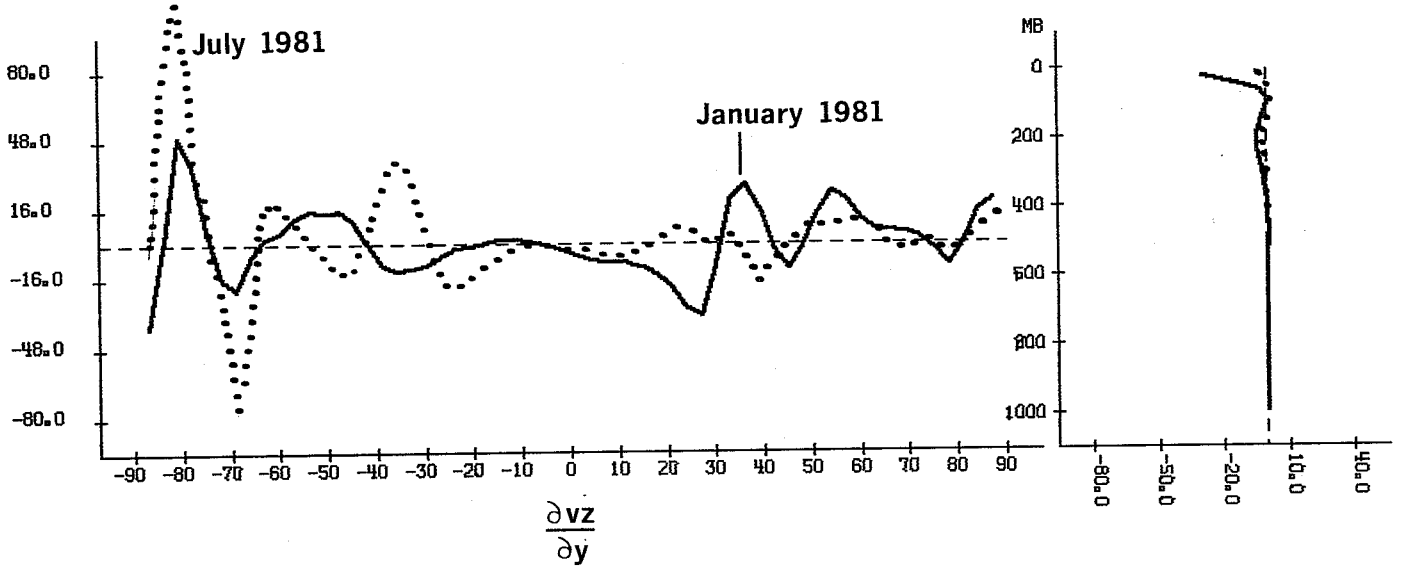

Fig. 38 Horizontal convergence of geopotential flux vertically integrated for January (——) and July (....). Units $\mu w/m^2/P$.

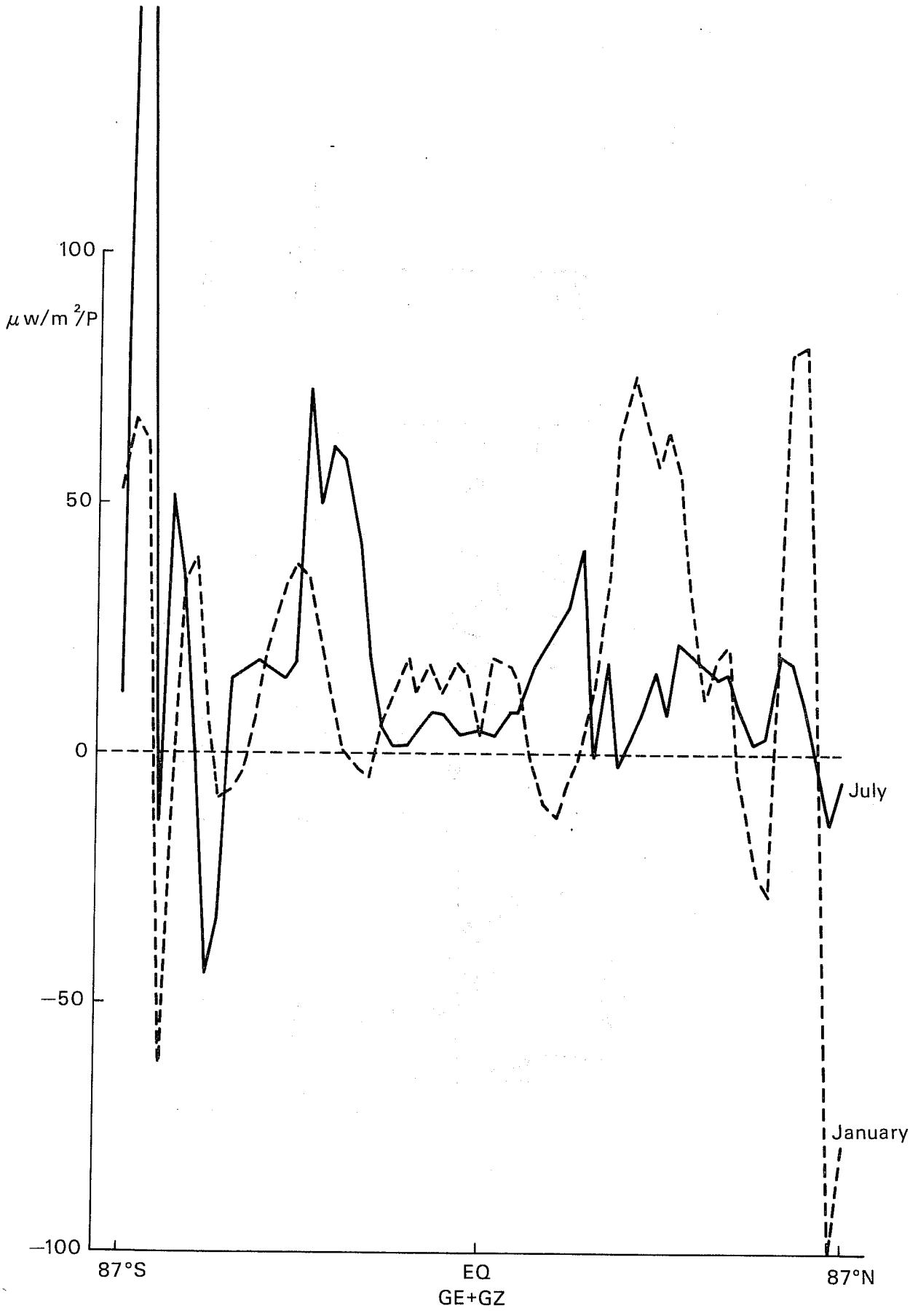

Fig. 39 Generation of eddy available potential energy for January (----) and July (——) 1981. Units $\mu w/m^2/P$.

complete year August 80-July 81 is discussed below.

8.1 Hemispheric integrals of energetics terms

In Fig. 40 it can be seen that the zonal components of both forms of energy are much higher in the Southern than in the Northern Hemisphere, having in both hemispheres a clear annual cycle. (Note the different scale for AZ). The eddy components are more important in the Northern Hemisphere where there is a dramatic change from winter to summer, while AE in particular does not change much in the Southern Hemisphere. Maximum values are found in January for all modes of energy in the Northern Hemisphere except for AZ which has its maximum in February; the minima in the Southern Hemisphere all occur in January. Both AE and KE have noticeably higher values in July 81 than in August 80 but a longer time series of data would be needed to know whether this can be attributed only to changes in the analyses or can be included in the interannual variability.

The corresponding annual curves for the conversions terms are shown in Fig. 41. The Northern Hemisphere shows a quite regular annual cycle for CE and CA, both having their maxima in January; CZ has a minimum (negative) in the same month and is positive in summer. CK is strongest in November and March. For the Southern Hemisphere, patterns are not very symmetric with respect to the solstice: the minima are found in January for CE and CA but the maxima occur in September. CZ has a sharp decrease (in absolute values) in November and remains roughly the same until March, while CK does not appear to have an annual cycle and if there is any trend it would be to decrease slightly during the period in consideration; both remain negative.

Generation and dissipation rates calculated only as residuals from the conversion terms (thereby ignoring tendency terms, which are small for a monthly mean) are compared in Fig. 42 for both hemispheres. The only one that becomes negative is GE during the winter periods: March to December in

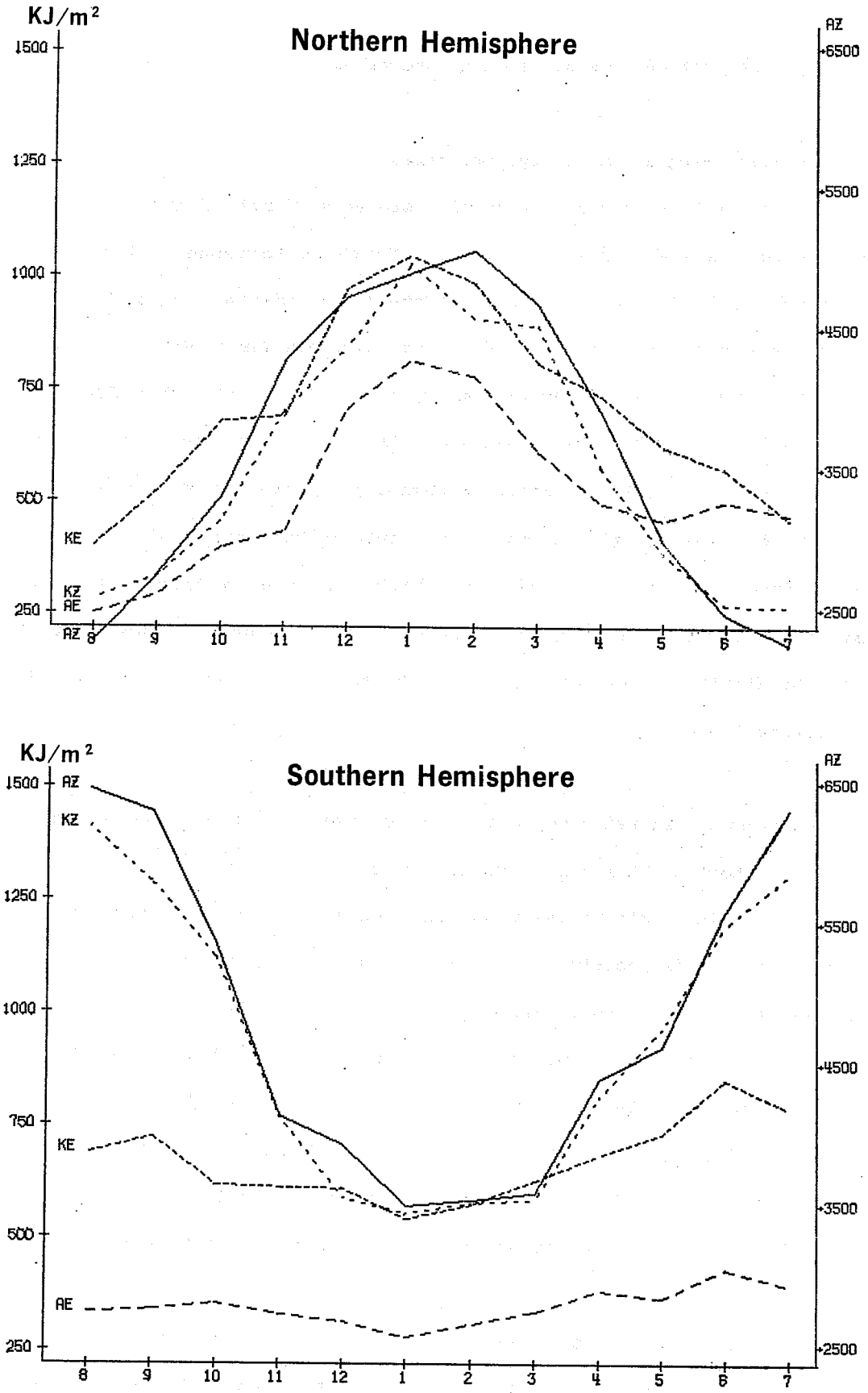

Fig. 40 Monthly means energy modes for Northern (top) and Southern (bottom) Hemispheres from August 1980 to July 1981. Units MJ/m^2. Scale for AZ on the right hand side.

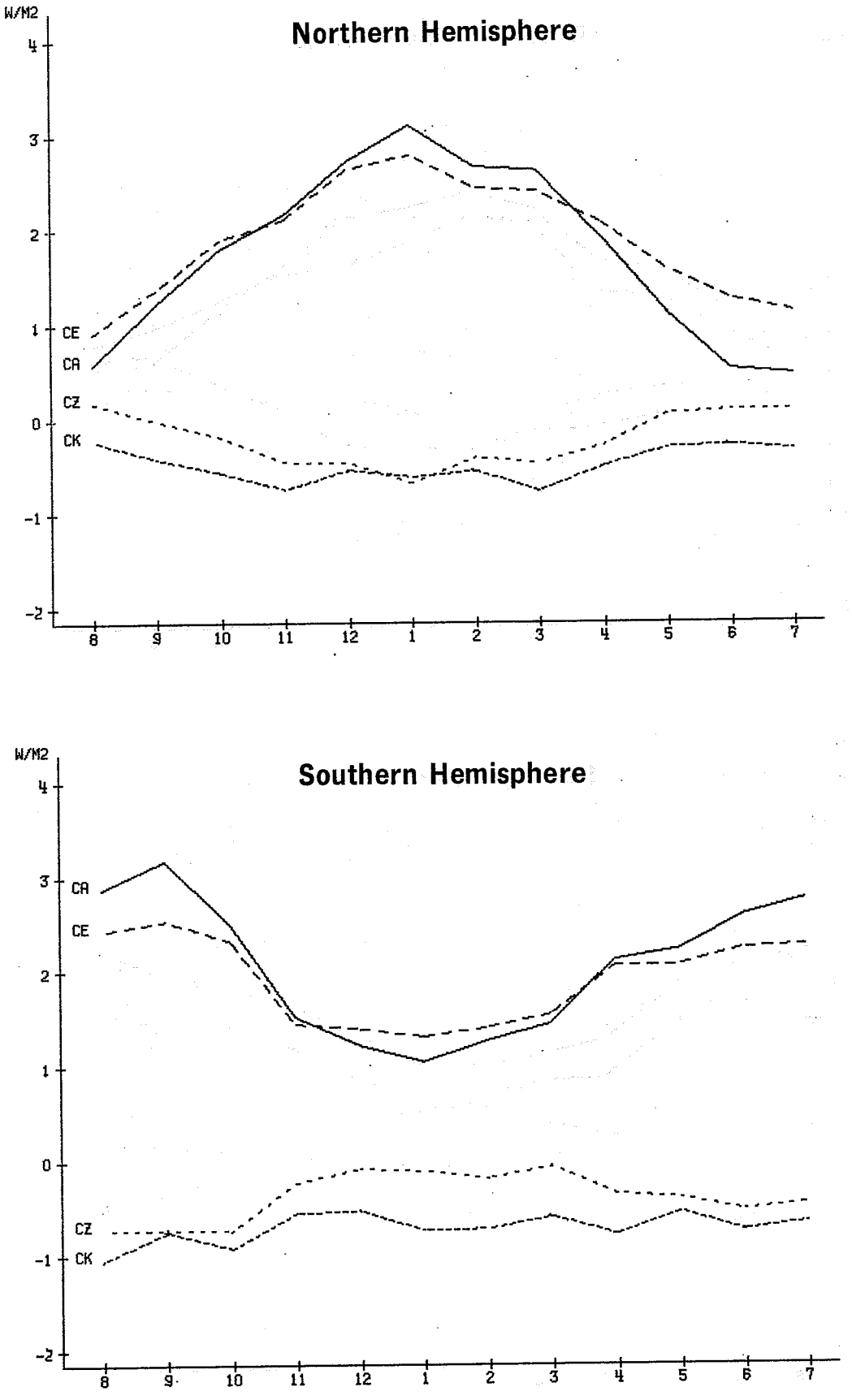

Fig. 41 Monthly means energy conversions for Northern (top) and Southern (bottom) Hemispheres from August 1980 to July 1981. Units:w/m^2.

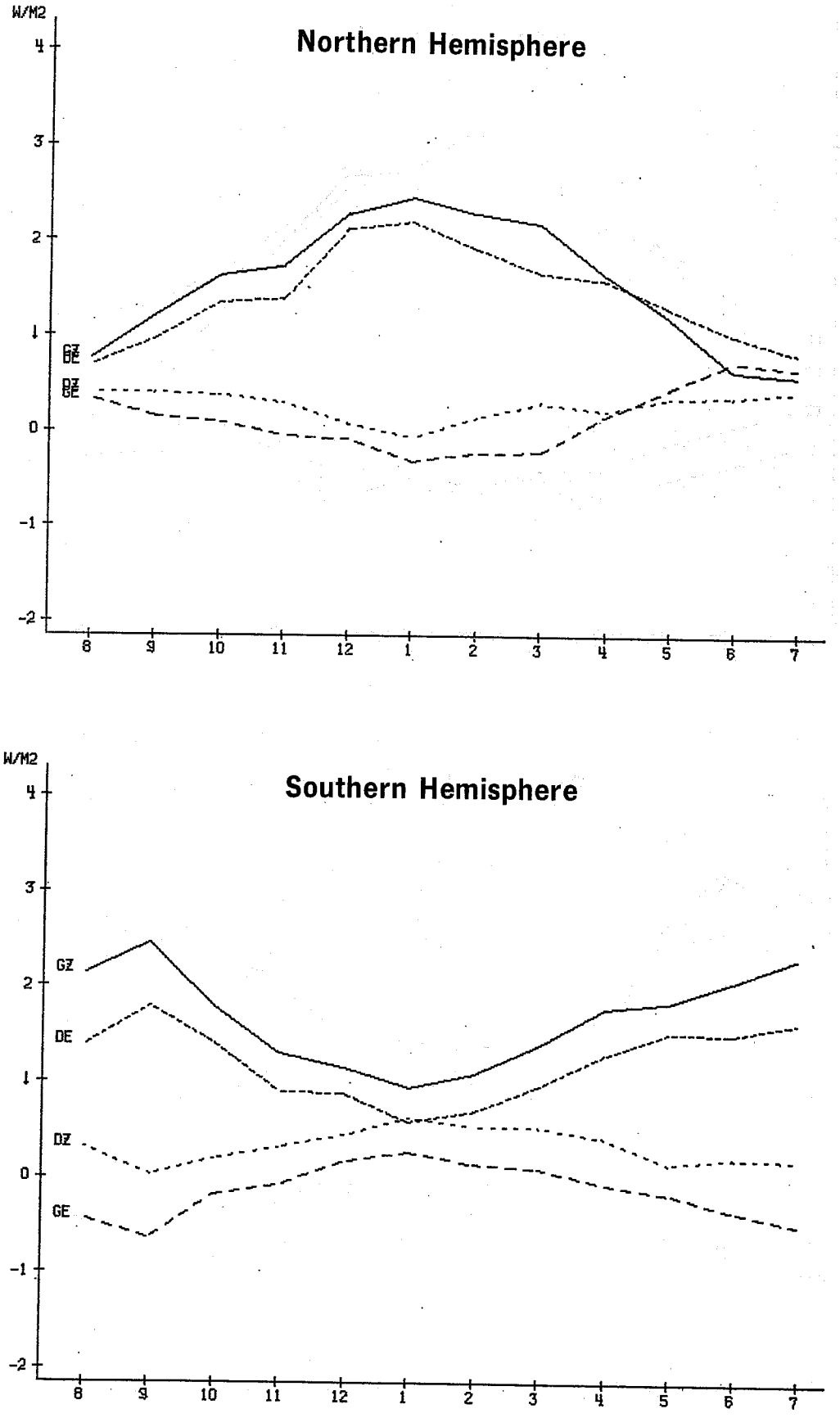

Fig. 42 Monthly means residuals for Northern (top) and Southern (bottom) Hemispheres from August 1980 to July 1981. Units: w/m^2.

Southern Hemisphere and November to April in Northern Hemisphere; this pattern was also found by Winston (1969) as quoted in Oort (1974). Brown (1964) reported a source of GE only in July. The extreme values for all the conversions in the Southern Hemisphere are found in September (rather than July) and January; and they occur in January and June in Northern Hemisphere; again there appears to be a secular trend towards larger values (especially for GE) in Northern Hemisphere that could either be explained by changes introduced in the analysis system, or interannual oscillations in the values of GE of the order of 100%. A noteworthy point in relation to the above remark occurs in the Northern Hemisphere in June, in the sense that GE > GZ; this might imply that the diabatic effects arising from eddy processes are for these two months slightly larger than the contributions from zonally averaged terms in the Northern Hemisphere.

The introduction of a new (more realistic) orography in April 81 coincides with two 'events' that occurred in the same month in the Northern Hemisphere, GE "overtook" DZ and, more importantly, DE became larger than GZ. It remains to be seen from more recent data if the change in the sign and magnitude of GE is a true seasonal effect or is due to a change in the orography. Very limited tests (on a single day) indicate some sensitivity to the precise orography used; it is not known if such sensitivity would be found in monthly mean values.

8.2 Vertical profiles of the time-evolution of the energetics

Following Wiin Nielsen (1967) the vertical structure of the energetics over the year, is shown separately for each hemisphere in Fig. 43 to 46 (the Southern Hemisphere does not include antarctic latitudes in the case of AZ and CZ). Comparisons can be made with results for Northern Hemisphere found by Tomatsu (1979) and Wiin Nielsen (1967) in Fig. 47.

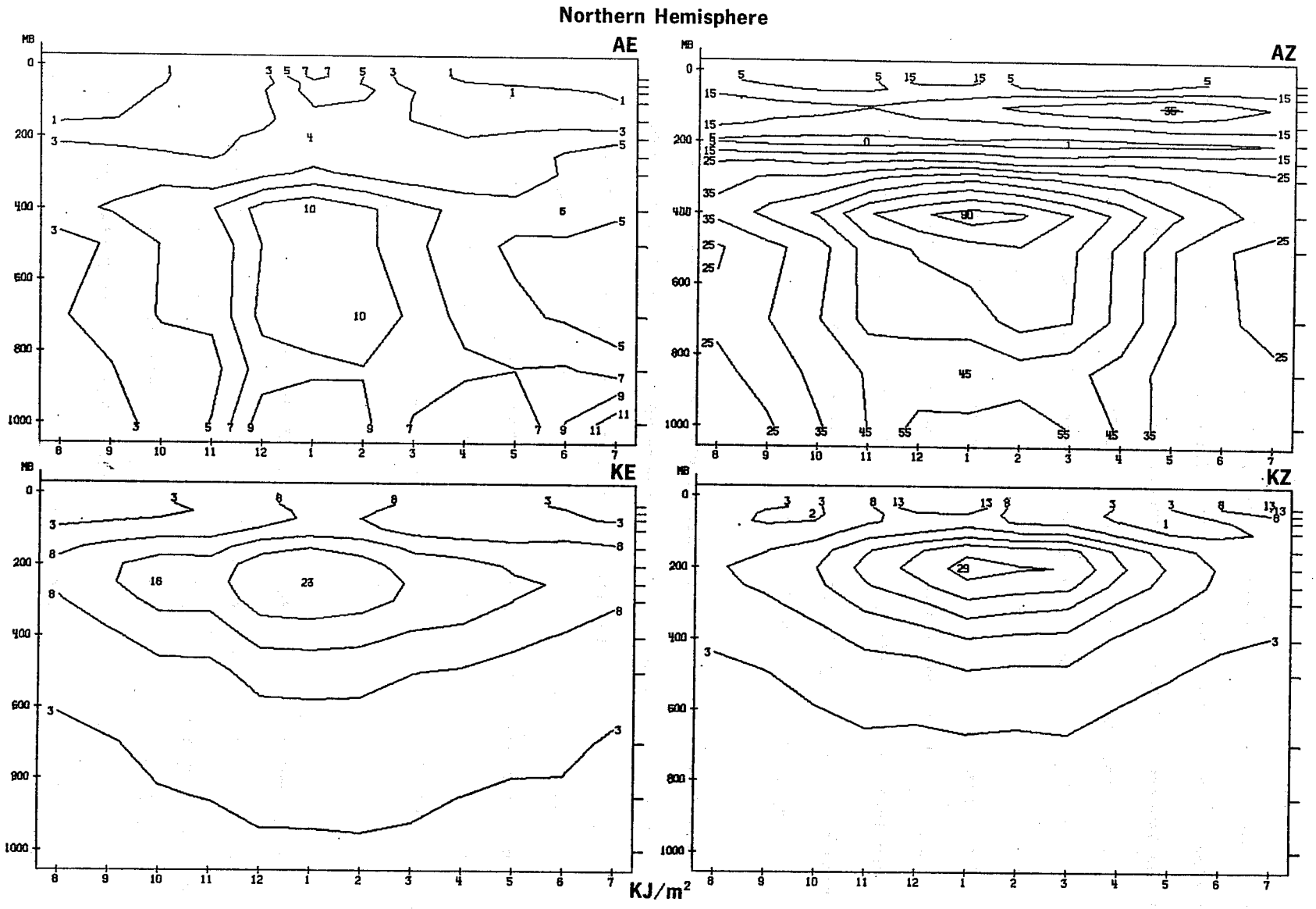

Fig. 43 Pressure-time cross-sections of the monthly means energy integrands from August 1980 to July 1981, for the Northern Hemisphere. Units: KJ/m^2.

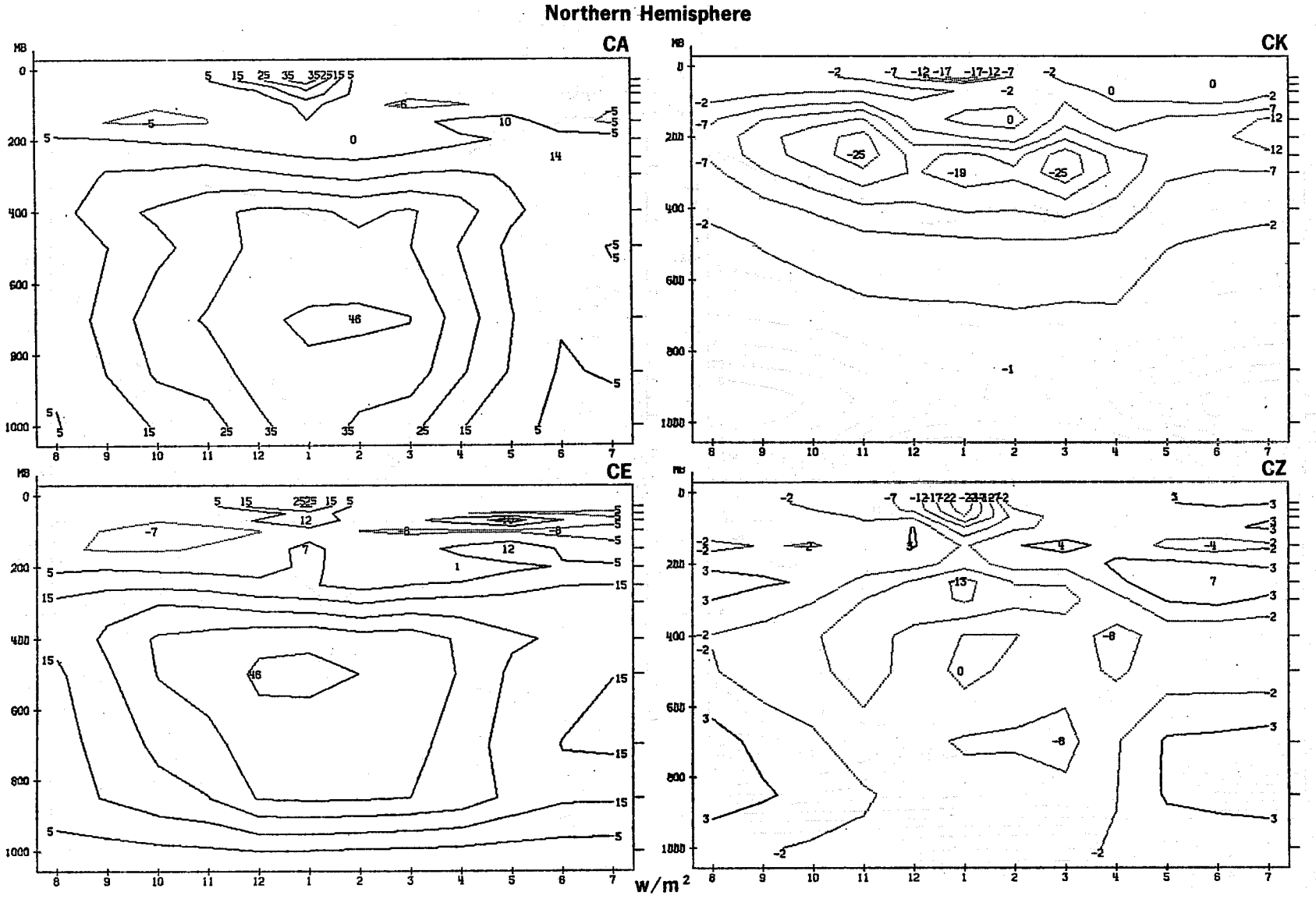

Fig. 44 Pressure-time cross-sections of the monthly means conversion integrands from August 1980 to July 1981, for the Northern Hemisphere. Units w/m^2.

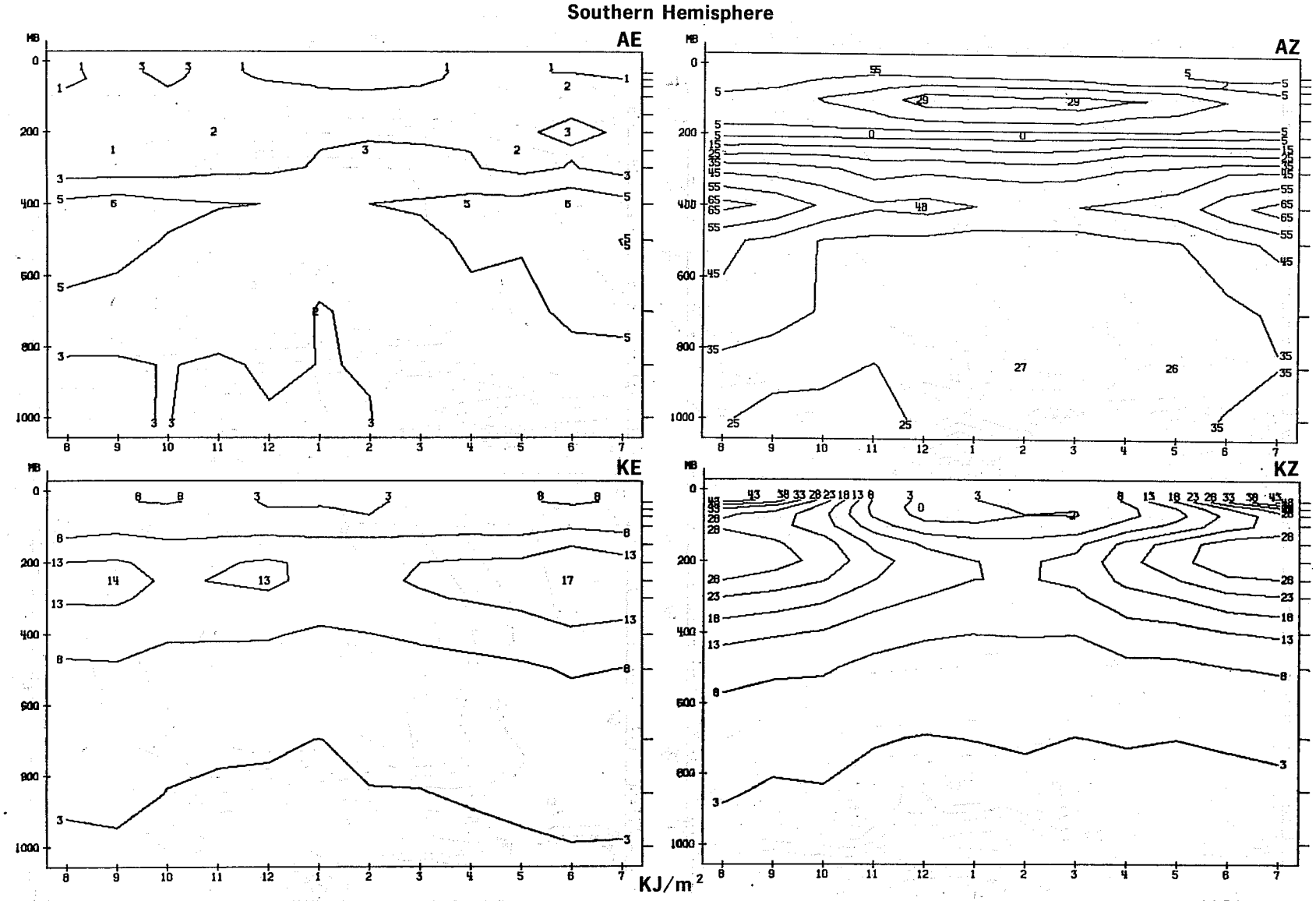

Fig. 45 Pressure-time cross sections of the monthly means energy integrands from August 1980 to July 1981, for the Southern Hemisphere. Units KJ/m^2.

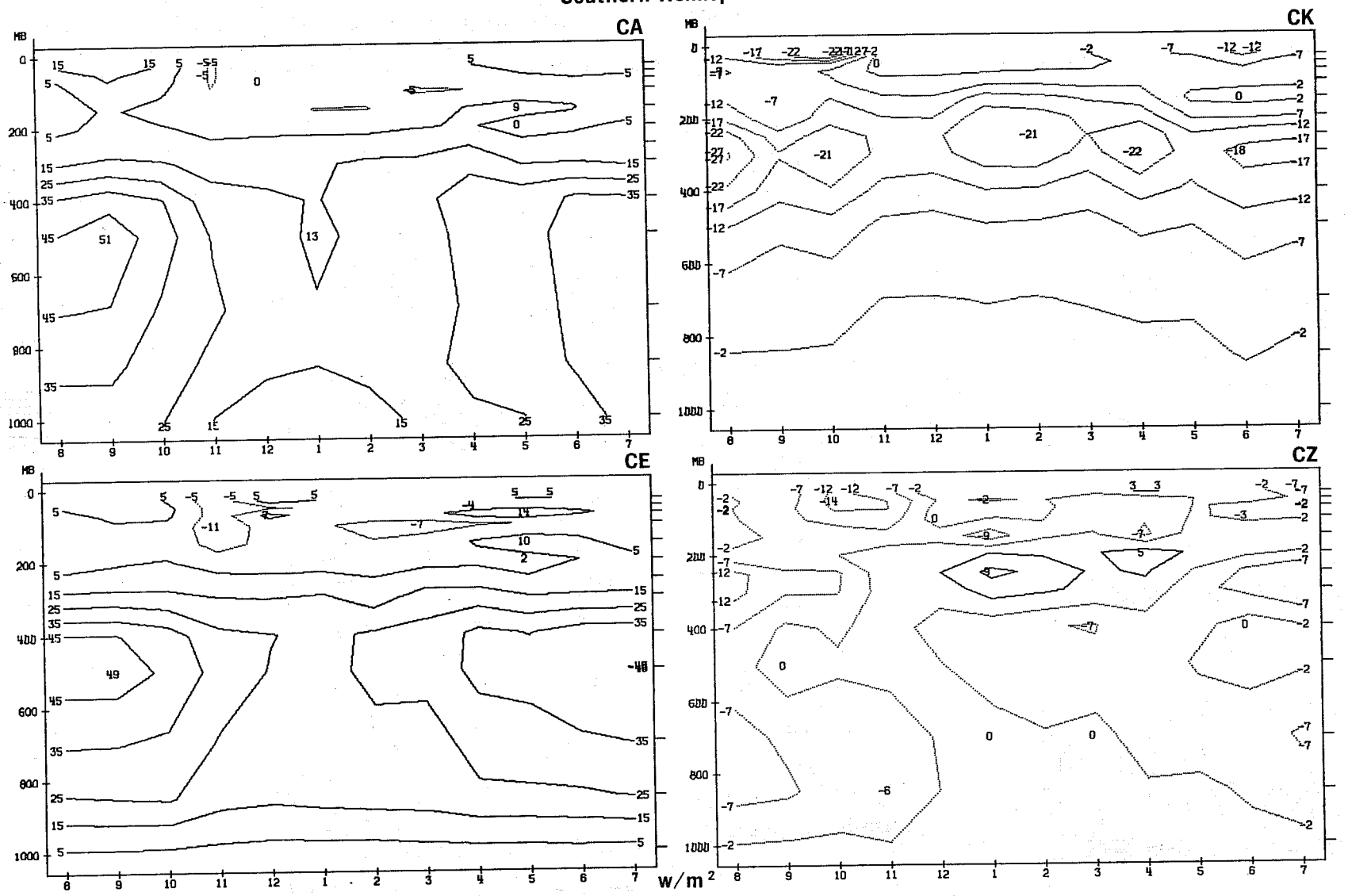

Fig. 46 Pressure-time cross-sections of the monthly means conversion integrands from August 1980 to July 1981, for the Southern Hemisphere. Units w/m^2.

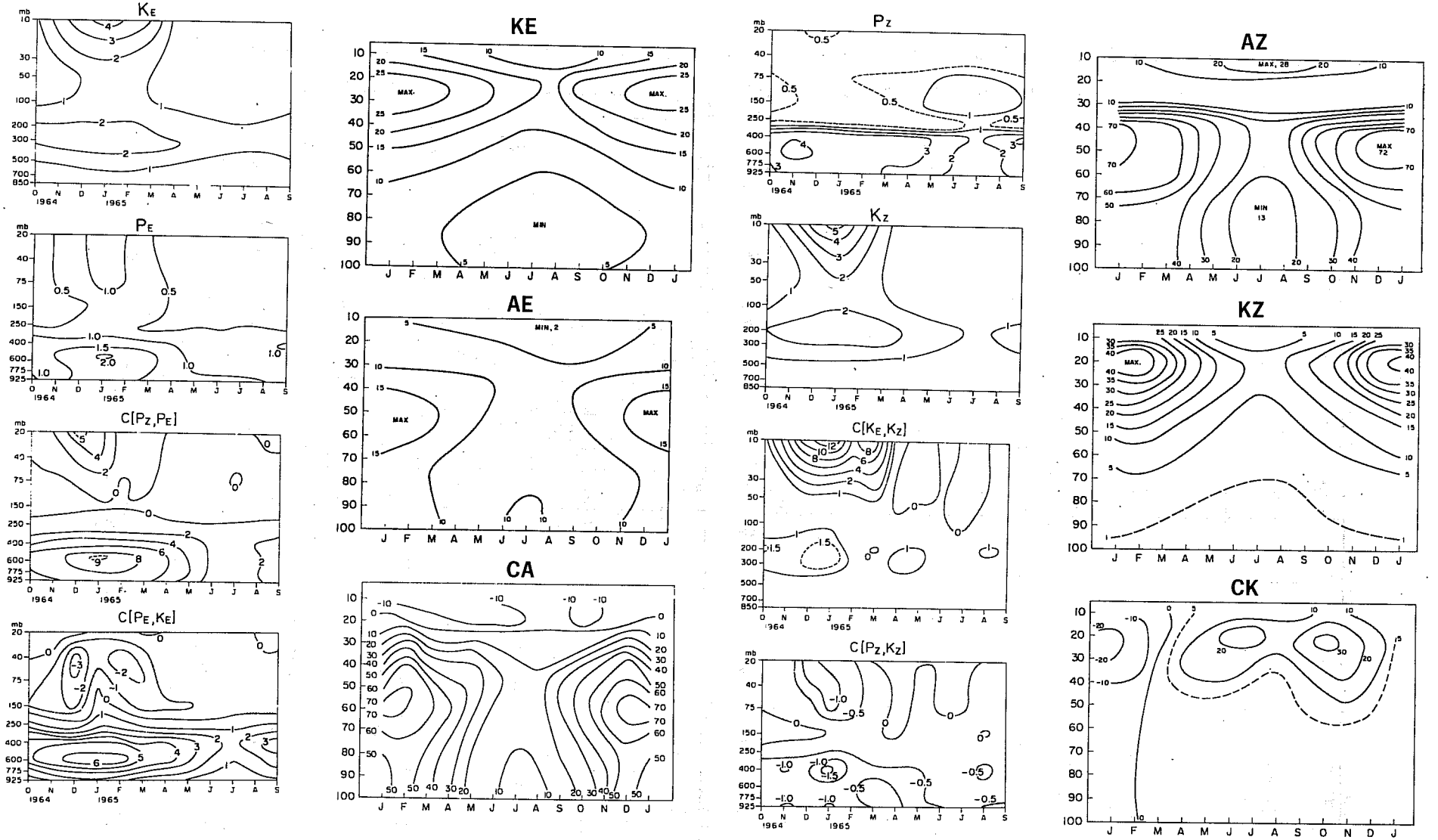

Fig. 47 Pressure-time cross-sections of the monthly mean energy and conversion integrands as found by Tomatsu (1979,small pictures) and Wiin-Nielsen (1967,large pictures).
Units: $J/m^2/mb \simeq 10^{-2} J/m^2/P$ and $mW/m^2/mb \simeq 10\ \mu w/m^2/P$ (Tomatsu)
$KJ/m^2/cb \simeq J/m^2/P$ and $10^{-6} KJ/m^2/s/cb \simeq \mu w/m^2/P$ (Wiin-Nielsen)

In the case of AZ it is interesting to note the contribution from the 400 mb level where there is a maximum of 90 $J/m^2/P$ in the Northern Hemisphere and of 65 $J/m^2/P$ in Southern Hemisphere; the structure of the isolines and even the values, agree more with Wiin-Nielsen's results than Tomatsu's: this may be due to the fact that the coverage both in latitude and levels are different. Another point is a weak maximum at 100 mb in late spring in the Northern Hemisphere and in the Southern Hemisphere throughout their summer. This different behaviour might be due to the exclusion of antarctic temperatures in this calculation, which include only 60°S to equator whilst the Northern Hemisphere is complete.

The time evolution for AE, KZ, KE agrees quite well with Tomatsu and Wiin-Nielsen in both magnitude and distribution, although the discussed values for AE are lower, as mentioned before. There is a good deal of similarity between KZ and KE in the Northern Hemisphere as found by Wiin-Nielsen. It is interesting to note the weak annual cycles for AE and KE in the Southern Hemisphere for this particular year. Wiin-Nielsen's results for CK suggested a negative maximum in summer and autumn while Tomatsu's larger values were in winter and autumn. The ECMWF values for CK are always negative and maxima are found from October to March at around 300 mb; positive conversions (KZ to KE) are only found at 150 mb in February and they are very small. The pattern is very similar for the Southern Hemisphere with Nov-Dec being less active in the upper troposphere.

The baroclinic conversion term CE has a broad maximum at 500 mb in January in the Northern Hemisphere while Tomatsu finds it at 600 mb. This disagreement is probably due to a different selection of levels for the calculations. Both conversions show a minimum activity at all levels in July; lower values in the present case can be due to the inclusion of the tropics. A similarity in the stratospheric structure of CE and CA in this study is not found in Tomatsu's. For the Southern Hemisphere there is a good agreement for both

conversions above 850 mb. The stratosphere is more active for CE conversions than for CA, except in September.

The Northern Hemisphere integral of CZ shows a minimum at 300 mb in January and also in the stratosphere, the general picture being quite similar to Tomatsu's except for the positive values in summer.

To finish this section and for the sake of completeness, a list of all monthly mean values for the entire atmosphere is presented in Table 7.

Table 7 Integrated monthly mean energies and conversions for all the globe. Units: KJ/m^2 and w/m^2.

Year	Month	AZ	AE	KZ	KE	CA	CK	CZ	CE
80	Au	4444	299	663	554	1.77	-.65	-.30	1.71
	S	4584	323	635	627	2.26	-.60	-.38	2.01
	O	4368	384	806	658	2.21	-.76	-.48	2.17
	N	4233	389	751	662	1.90	-.66	-.37	1.83
	D	4356	521	732	801	2.03	-.54	-.30	2.08
81	Ja	4226	557	807	802	2.14	-.69	-.41	2.11
	F	4331	554	759	790	2.03	-.64	-.31	1.99
	Mr	4156	483	754	728	2.10	-.69	-.29	2.03
	Ap	4175	448	709	720	2.06	-.65	-.36	2.11
	My	3830	419	689	687	1.73	-.43	-.20	1.87
	Jn	4082	475	747	721	1.60	-.51	-.24	1.80
	Jl	4363	441	800	632	1.66	-.50	-.19	1.75
	Au	4587	421	835	679	1.69	-.39	-.21	1.70
	S	4631	429	865	657	2.10	-.68	-.39	1.97
	O	4543	480	820	726	2.24	-.84	-.45	2.17
	N	4433	511	761	746	2.10	-.71	-.41	2.12
	D	4387	549	779	767	1.89	-.83	-.37	1.96

9. THE ENERGY CYCLE

Having given an extensive discussion of the individual terms the energy cycle will be considered as a whole.

9.1 Hemispheric energy cycles

Assuming that the monthly mean fluxes across the equator are negligible, the energy cycles for both hemispheres can be compared for January and July, and the cycles are shown in Fig. 48 and 49.

As expected, the mean cycle is much more intense in the winter hemisphere for both months, the northern being more active in its conversions, although the overall behaviour is the same. It is worthwhile to note that CZ in winter always implies a conversion from zonal kinetic to zonal available potential energy.

The only differences worthy of comment are the much higher values of the zonal parts of both forms of energy in the Southern Hemisphere winter, which was already noted before, and a 10% higher total dissipation in the Northern Hemisphere. The very low negative value of DZ for January in the Northern Hemisphere might be regarded as an exceptional case, since it has not been observed since.

In summer there are some differences between both hemispheres in behaviour and intensity. CZ, the most unrealiable conversion is small in both summers and has opposite signs for the two hemispheres. Notice that the generation of eddy available potential energy GE, is larger in the Northern than in the Southern Hemisphere summer.

In the upper parts of the figures the partitions and exchanges between different scales are shown. The AE in both seasons and both hemispheres is largest in the long waves; in the Northern Hemisphere its long wave values

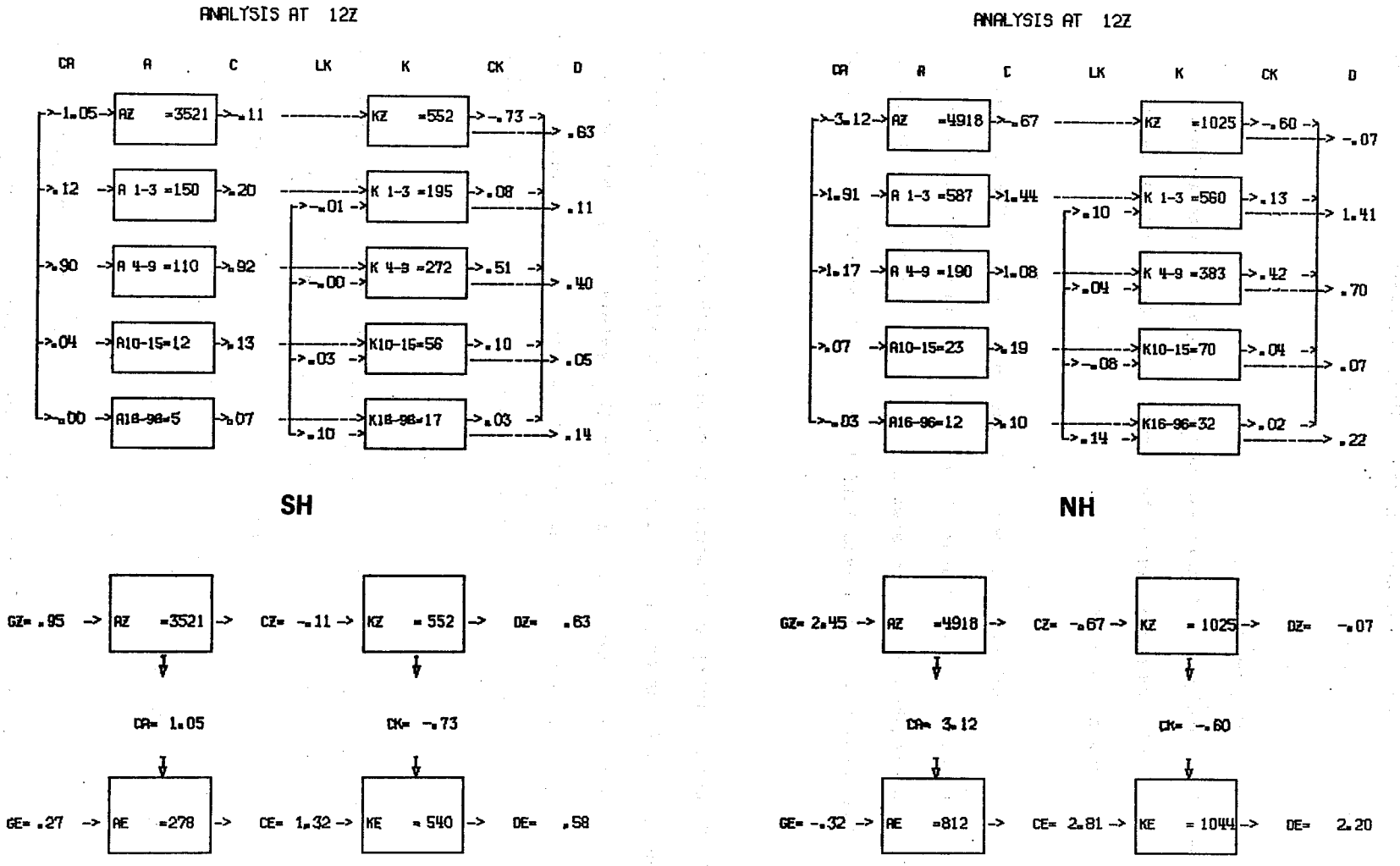

Fig. 48 Energy cycles for January 81, Southern Hemisphere (left) and Northern Hemisphere (right). Units: KJ/m^2 and w/m^2.

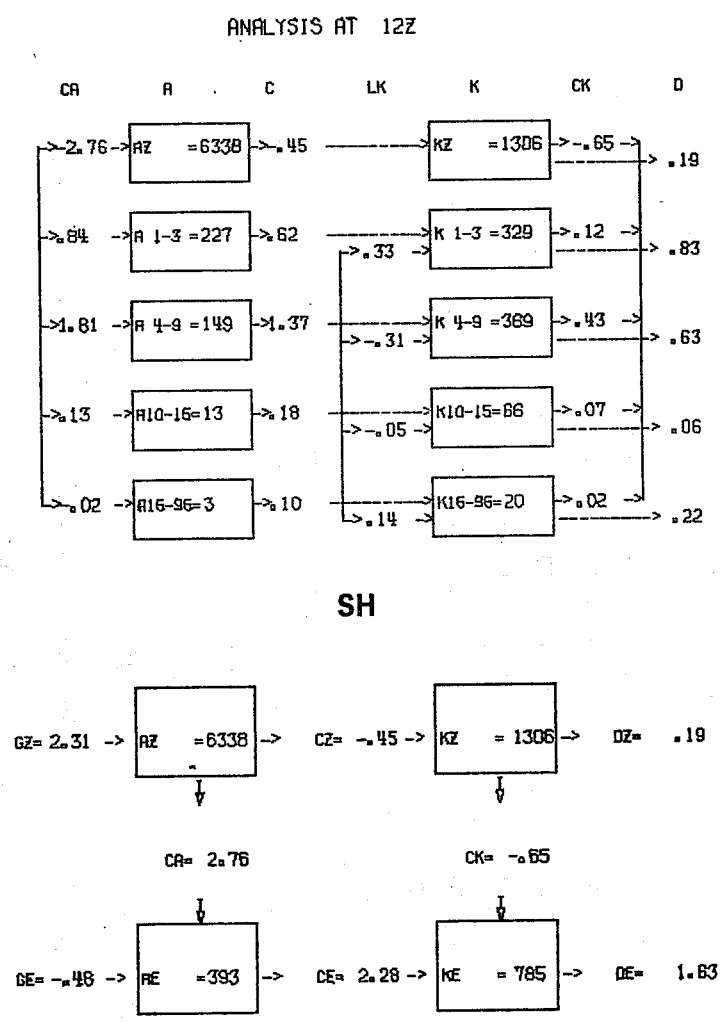

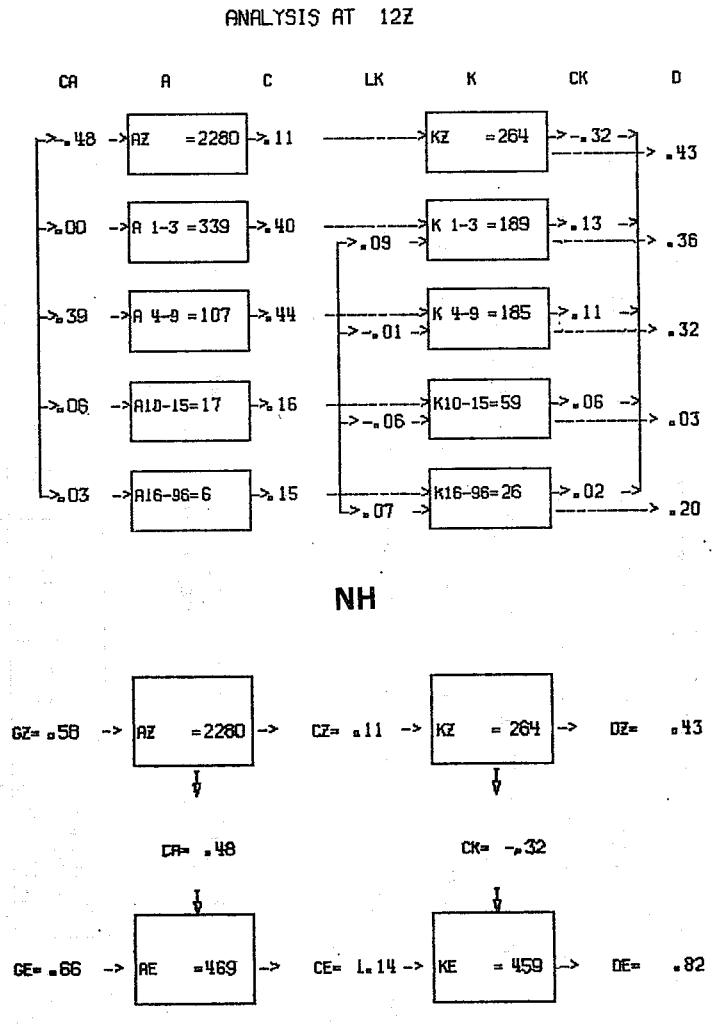

Fig. 49 Energy cycles for July 1981, Southern Hemisphere (left) and Northern Hemisphere (right). Units: KJ/m^2 and w/m^2.

are much higher than the medium wave values. In July in both hemispheres, KE is equally divided between long and medium waves. But in January cyclonic waves are more important in Southern Hemisphere and long waves in Northern Hemisphere. The conversion term CE is dominated by the medium waves in both months in Southern Hemisphere. In January the long waves are more active than the medium waves in Northern Hemisphere. In July in the Northern Hemisphere the long and medium waves are equally important. It is interesting to notice that the very short waves are not negligible in some cases (for example, CE).

Table 8 Non linear redistribution of eddy kinetic energy for all the globe and different wavegroups. Units: w/m^2.

Year	Waves / Month	1-3	4-9	10-15	16-96	1-15
80	N	.13	-.19	.02	.10	-.04
	D	.21	-.14	-.07	.12	.00
81	Ja	.05	.02	-.03	.12	.04
	F	.14	-.09	-.02	.12	.03
	Mr	.25	-.28	-.01	.13	-.04
	Ap	.23	-.14	-.06	.14	-.03
	My	.24	-.21	-.05	.12	-.02
	Jn	.17	-.13	-.01	.11	.03
	Jl	.21	-.17	-.06	.11	-.02
	Au	.12	-.08	-.05	.07	-.01
	S	.23	-.19	-.01	.12	.03
	O	.18	-.11	-.02	.16	.05
	N	.20	-.10	-.05	.14	.05
	D	.20	-.18	-.03	.11	.05

Some comments should be made regarding the global integral of the non-linear redistribution of eddy kinetic energy. In Table 8 there is a list of the contributions to the eddy kinetic energy due to each scale, for 16 months. It has already been said that this term is not expected to sum up to its

theoretical value of zero because of the interpolation at the extreme levels and the difference scheme used for calculations. From the table it becomes apparent that these inaccuracies always result in a positive, non-zero, residual when the contributions by all waves are summed. Nevertheless a clear picture is obtained with the long and very short waves being fed by intermediate waves.

In Fig. 50 the global and annual mean energy cycle is shown.

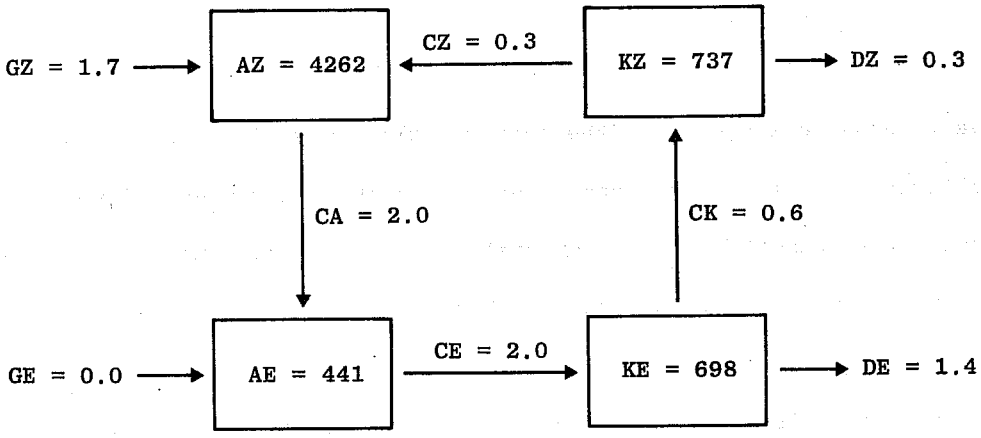

Fig. 50 Global mean energy cycle for the period August 1980 to July 1981. Units: KJ/m^2 and w/m^2.

Of the energy transferred from AZ via AE to KE, 60% is dissipated by friction and 30% converted to KZ; about half of the energy converted to KZ is then dissipated by friction. The total dissipation of 1.7 w/m^2 is somewhat smaller than values found by others (Newell et al 1970); those authors have shown that values could range from 1.5 to 5 w/m^2 depending on the method used: direct calculations, residual estimates etc. From these considerations one is lead to the conclusion that the results obtained might be acceptable. The zero value for GE comes from the fact that GE changes from sink to source along the seasons and cancel in a global integral.

9.2. The tropospheric and stratospheric energy cycles

To split the atmosphere horizontally, vertical fluxes of geopotential have to

be taken into account since they represent a major component to the KE budget (Miller, 1970). The monthly mean vertical flux convergence of eddy geopotential for the layer 150-30 mb are given in Table 9. There is always an upward flux through 150 mb, which is higher in the summer hemispheres.

Table 9

January Northern Hemisphere	=	.09 w/m^2
July Northern Hemisphere	=	.17 w/m^2
January Southern Hemisphere	=	.12 w/m^2
July Southern Hemisphere	=	.09 w/m^2

The above values are included in the energy cycles shown in Figs. 51 and 52, where following Tomatsu (1979), the lower stratosphere includes 150 to 30 mb. Contributions by these fluxes in the stratosphere are large enough to change the sign of the calculated residual DE. That might be the case also in DZ, which has unrealistic negative values in some winter cases (i.e. January 1981 in Northern Hemisphere). The results do not change much when the 30 mb level (which might have interpolation problems) is not included. The only possible way to overcome that difficulty would be to calculate all the vertical fluxes involved but this has not been done so far.

Tropospheric cycles are very much the same as those presented for the whole column and there is not much to add to what has already been said. The cycle in the lower stratosphere suggests a quite different behaviour; CE is normally negative, as found by other authors (Newell and Richards, 1969) and CA is on average negative (although positive in winter hemispheres). With some exceptions, the cycle suggested for the lower stratosphere would be

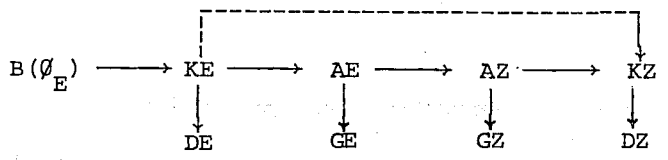

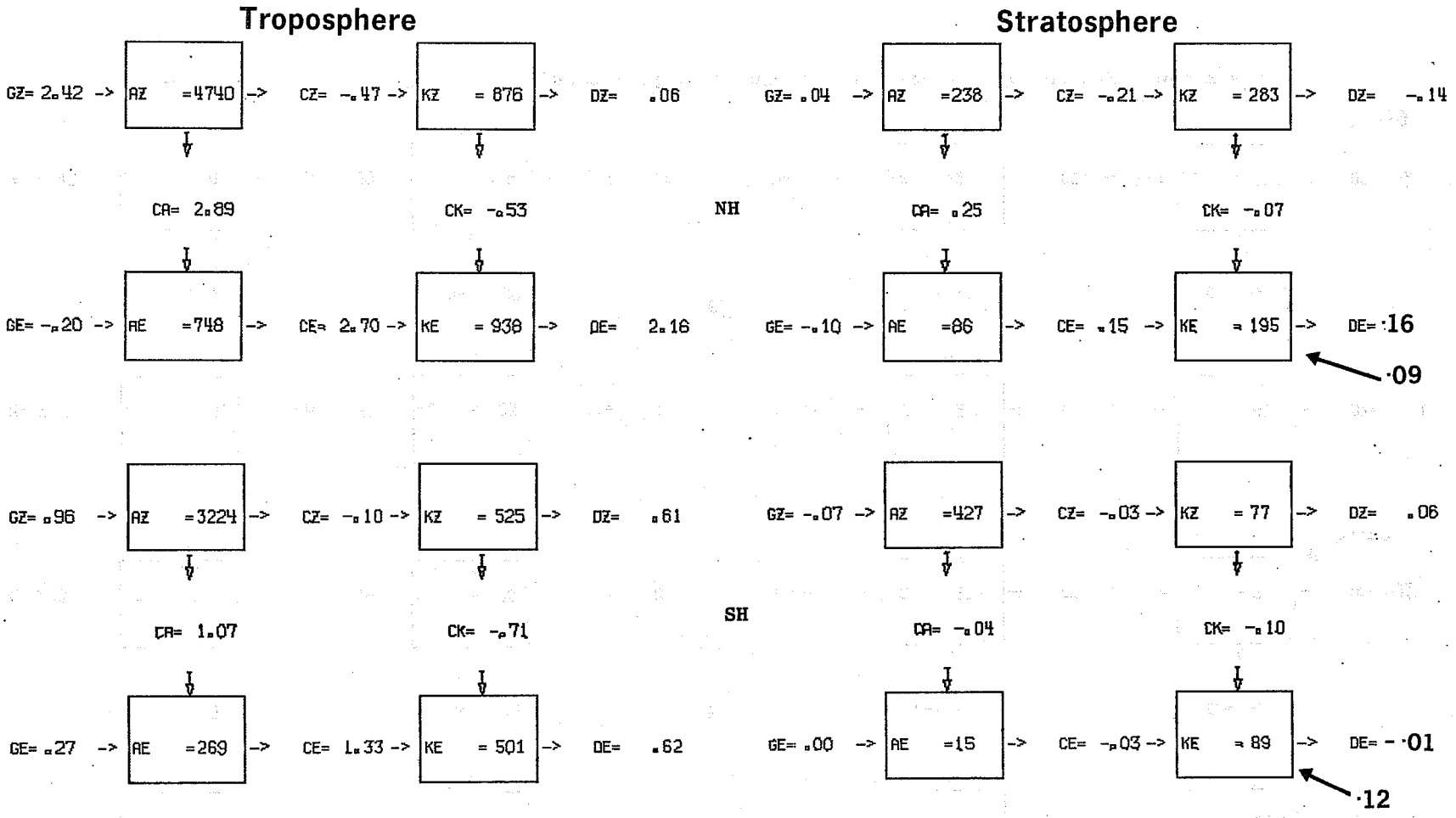

Fig. 51 Energy cycles for January 1981, troposphere (left), stratosphere (right). Units: KJ/m^2 and w/m^2.

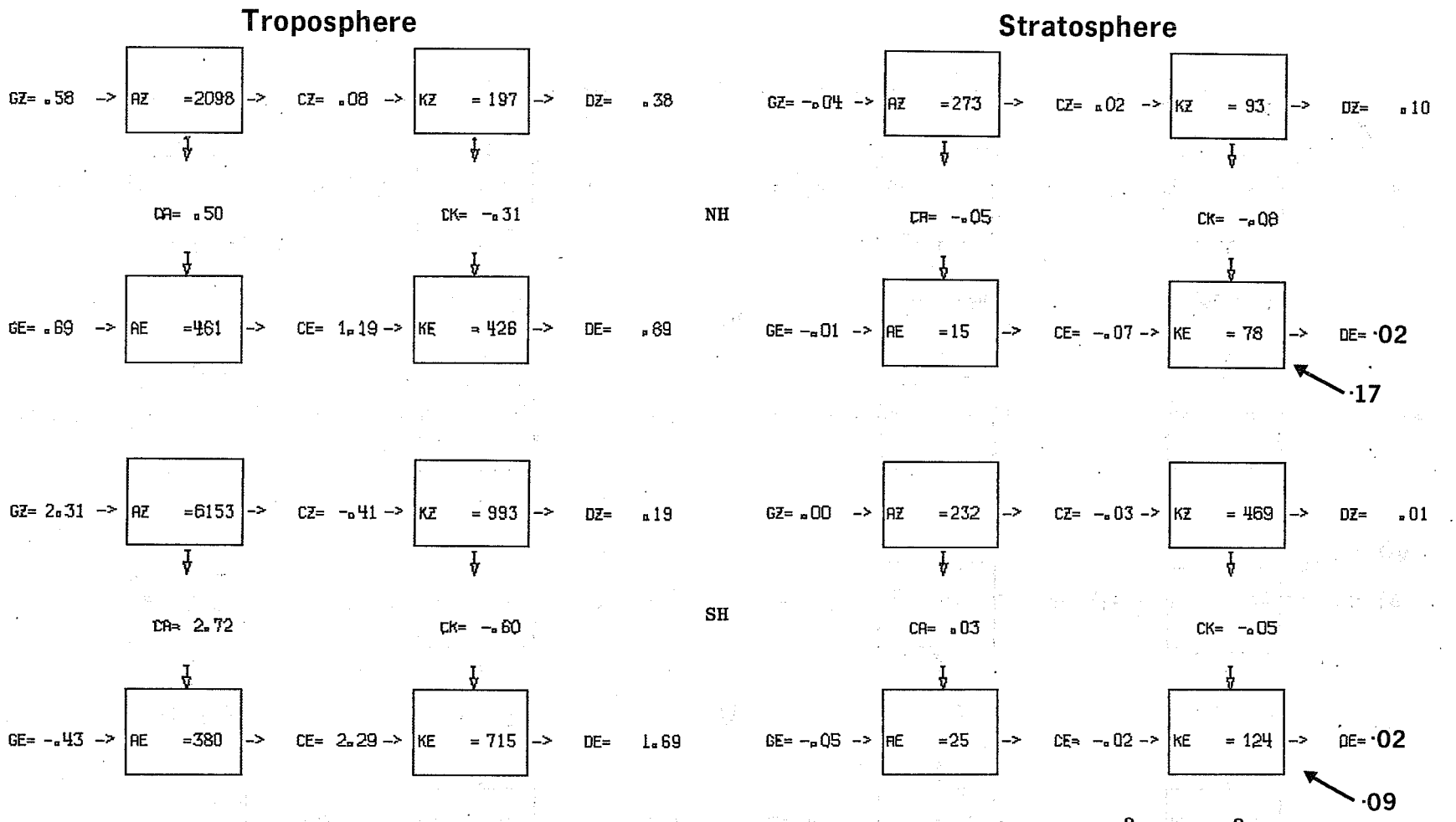

Fig. 52 Energy cycles for July 1981, troposphere (left), stratosphere (right). Units: KJ/m^2 and w/m^2.

9.3 Comparison of energy cycles with other authors

Since the introduction of the energy cycle by Lorenz in 1967, many studies describing the cycle for the Northern Hemisphere have been published. The different sources of data used, their coverage, length and methods employed make comparisons difficult and there are often disagreements between them. A selection of these publications is discussed; some of them have already been used.

The longest series of data with which to compare corresponds to the winter season for the Northern Hemisphere; they are presented in Table 10. Other values are also presented in the Appendix A5 for completeness.

The estimates of both forms of kinetic energy in the Northerm Hemisphere are in general agreement with other authors being higher than Newell's results and lower than the rest, especially for KE. The zonal available potential energy AZ is much higher in the present investigations except for values found in the Northern Hemisphere by Newell. By contrast values of AE are much lower, as discussed before, but similar to Newell's in the Southern Hemisphere. The fact that most authors do not include the tropics in their calculations must be a reason to account for some of the differences.

CZ is particularly sensitive to the above inclusion and could even explain the opposite signs found by different authors. Lau (1981) attributes higher values of CA to the use of the space domain; the present small values could be due to initialization, similarly for CE. As for CK, all authors find it to be negative and in general there is a good agreement for all values.

The most convenient calculations with which comparisons can be made are those obtained from NMC analyses (Miller, private com.). The NMC analysis scheme used is also an optimum interpolation method. The NMC calculations use a grid of 5°, and do not include the 30 mb level. For January 81 energies

Table 10 Comparison of results found by different authors for the winter period.

Author Year	Kruger 65	Saltzmann 70	Newell 74	Tomatsu 79	Rosen 80	Rosen 80	Lau 81	Lau 81	Oriol 82	Newell 74	Oriol 82
AZ		3550	5100	2288			3080	3020	4917	4700	6202
AE		1110	610 1010	1239			980	960	764	430 550	409
KZ		1000	690	1076			1120	1020	924	650	1287
KE		1430	870	1319			1140	1050	1001	780	829
CA	5.13	5.3	1.2 2.2	4.72	2.7	2.8	3.2	2.5	2.85	1.2 1.8	2.69
CK		-0.5	-0.23	-0.70	-0.7	-0.6	-0.2	-0.2	-0.56	-0.24	-0.65
CZ	-0.83	0.0	0.19	-0.64	0.2	0.0	0.4	-0.6	-0.51	0.14	-0.53
CE	3.71	3.0		3.0					2.64		2.38
		compiled different authors									
Length	Oct 58-July 63		5 yr	Oct 64-Sept 65	Dec-Feb 76-77	Dec-Feb 76-77	66-73	66-73	Dec 80-Feb 81	5 yr	Jul 81-Aug 81
Levels	850-200	all	1000-100	925-10	1000-50	1000-50	850-100	850-100	1000-30	1000-100	1000-30
Coverage	20-Pole	NH	NH	20-75	NH	NH	20-90	20-90	NH	SH	SH
Comments					station	grid	NMC	GFDL			
Period	←				Winter						→

discussed here are slightly lower in the Northern Hemisphere and higher in the Southern Hemisphere; the same being true for CA while CK is more active in both hemispheres. More detailed comparisons between both sets of analyses are planned.

10. EPILOGUE

Energy calculations have been used extensively in other Centres to diagnose numerical models by comparing the state of the atmosphere with the results obtained. There is a need to know how well the analyses produced by different techniques reproduce the real atmosphere.

The traditional method to study the general circulation consists of first compiling statistics for each single station and analyzing the final results; this method was good except for data-sparse areas. The method presented here makes use of daily objective analyses which incorporate data from satellites, buoys, etc. and have in some cases been smoothed by initialization procedures. It has also the advantage that the gaps have been "filled in" by a forecast model.

The results obtained agree well with the ones from earlier studies, particularly for mean fields. Energy calculations based on objective analyses are very much dependent on methods or formulae used, but comparisons between analyses and forecasts should not be affected by them (a report in this line is due to follow). It is expected that calculations based on forecasts will result in a more active "atmosphere".

As for the use of the analyses to study the general circulation of the atmosphere there is a need for longer periods of data which should make the results less sample dependent.

Acknowledgements

I wish to thank K.Arpe for his help during the implementation of the operational package and his suggestions during the preparation of this report. I am also very grateful to D.Burridge, A.Hollingsworth and A.Simmons for their comments on the final draft.

A P P E N D I C E S

$$KE = \frac{1}{2g} (\Phi_{uu} + \Phi_{vv})$$

$$KZ = \frac{1}{2g} (\bar{u}\bar{u} + \bar{v}\bar{v})$$

$$AE = - \frac{R}{2gp} \frac{1}{\frac{\partial \bar{T}}{\partial p} - K \frac{\bar{T}}{p}} \Phi_{TT}$$

$$AZ = - \frac{R}{2gp} \frac{1}{\frac{\partial \bar{T}}{\partial p} - K \frac{\bar{T}}{p}} (\bar{T} - \bar{T}_G)^2$$

$$CE = - \frac{R}{gp} \Phi_{\omega T}$$

$$CZ = - \frac{R}{gp} (\bar{\omega} - \bar{\omega}_G) (\bar{T} - \bar{T}_G)$$

$$CK = - \frac{1}{g} \left\{ \Phi_{uv} \left(\frac{1}{a} \frac{\partial \bar{u}}{\partial \phi} + \frac{\bar{u}}{a} tg\ \phi \right) + \Phi_{vv} \frac{1}{a} \frac{\partial \bar{v}}{\partial \phi} - \Phi_{uu} \frac{tg\ \phi}{a} \bar{v} + \Phi_{\omega u} \frac{\partial \bar{u}}{\partial p} + \Phi_{\omega v} \frac{\partial \bar{v}}{\partial p} \right\}$$

$$CA = \frac{R}{gp} \frac{1}{\frac{\partial \bar{T}}{\partial p} - K \frac{\bar{T}}{p}} \left\{ \frac{1}{a} \frac{\partial \bar{T}}{\partial \phi} \Phi_{vT} + \left(\left(\frac{\partial \bar{T}}{\partial p} - \frac{\partial \bar{T}_G}{\partial p} \right) - \frac{K}{p} (\bar{T} - \bar{T}_G) \right) \Phi_{\omega T} \right\}$$

$$LK = - \left(\frac{1}{g} \Phi_{uA} + \frac{1}{g} \Phi_{vB} + CK \right) \quad \text{where}$$

$$A = u \frac{\partial u}{\partial x} + v \frac{\partial u}{\partial y} + \omega \frac{\partial u}{\partial p}$$

$$B = u \frac{\partial v}{\partial x} + v \frac{\partial v}{\partial y} + \omega \frac{\partial v}{\partial p}$$

$R = 287.04\ J/Kg\ {}^{o}K^{-1}$

$g = 9.806\ m/s^2$

$a = 6.37122 \times 10^6 m$

$k = 287.04/1004.6$

A1. Formulae used for the calculation of the energy budget parameters. A bar indicates zonal mean. The subscript G indicates a global mean for the particular leve. Φ refers to the variances and covariances of the field.

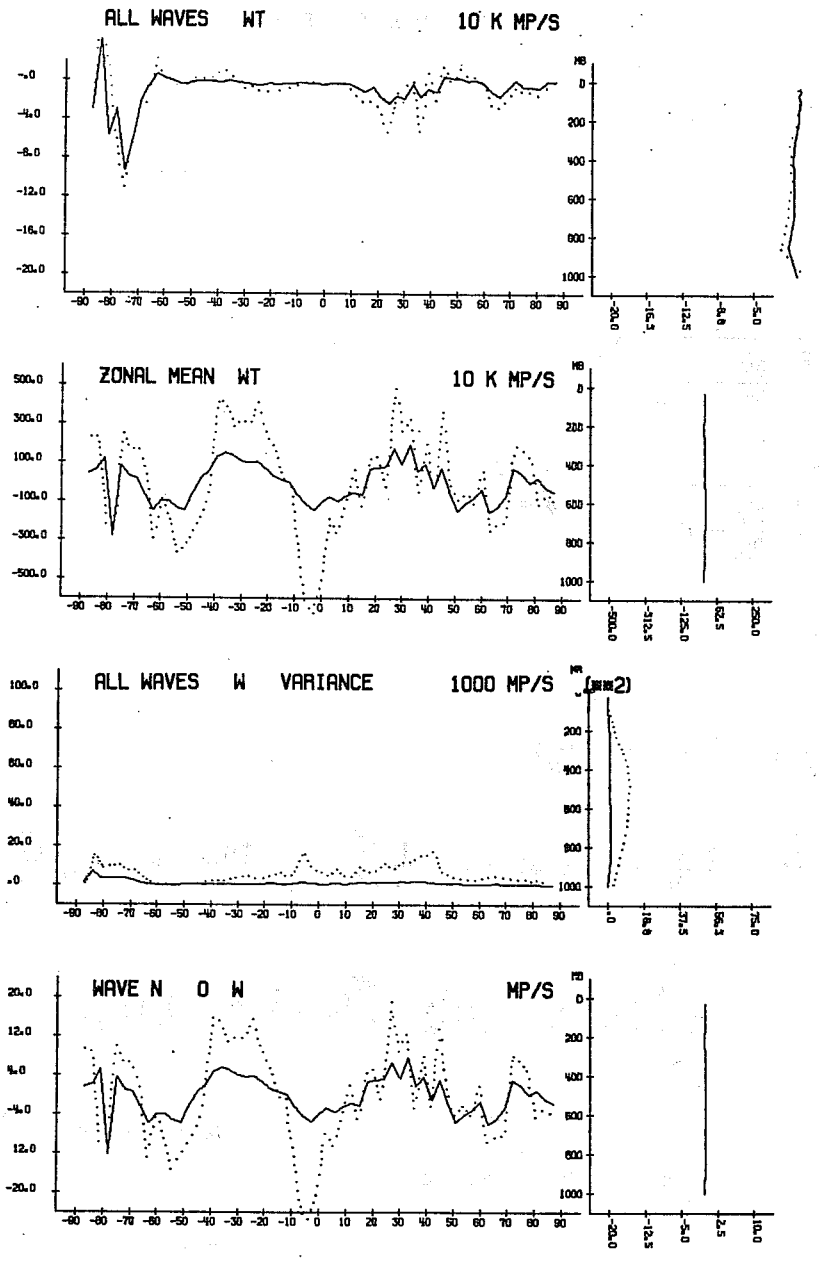

A2. Comparisons between initialized (full line) and uninitialized (dotted line) analyses for the monthly mean vertical velocity and the standing component of the vertical transport of temperature for April 1981 are shown in the Figure. The reduction of the values can be fully appreciated, although the uninitialized data in northern mid-latitudes are very noisy.

The integrated values of the conversion rates over the whole globe went for the standing component of CA from 0.41 to 0.32w/m^2; from 0.50 to 0.33 w/m^2 for CE and from 0.19 to -0.33 w/m^2 in the case of CZ.

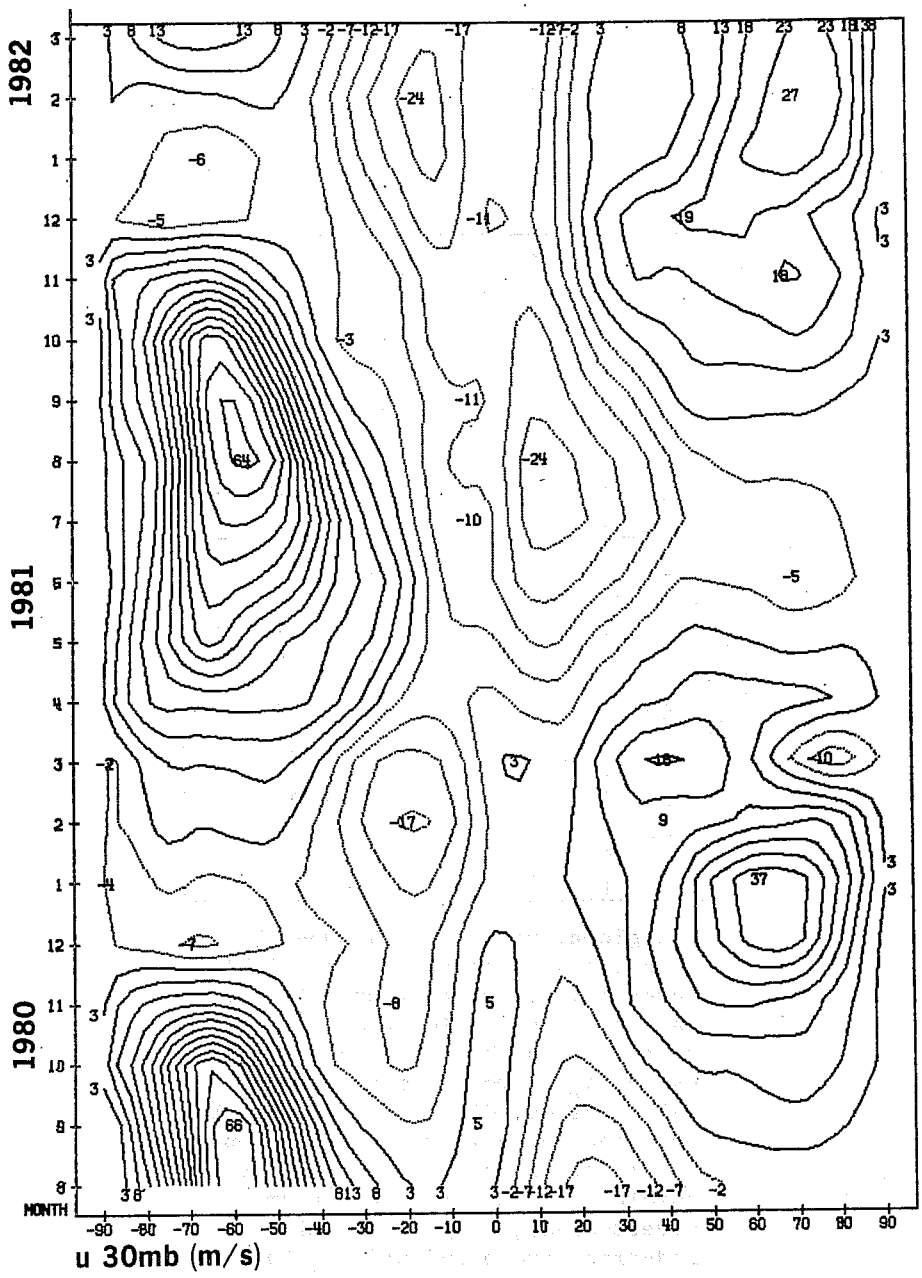

A3. The cross-sections of the zonal mean of the meridional component of the wind at 30 mb indicate an easterly flow over the tropical area from April 81 onwards. Maximum easterlies in that region amount to 24m/s and are found at 10°N in August 81 and 10°S in February 81. It seems that the transition from westerlies to easterlies was taking place during winter 80-81 (the period here studied) and that explains the values of KZ found before; this period agrees quite well with what would be expected according to the QBO (Klinker, private comm.), but some care should be taken when looking at analyses at stratospheric levels before May 81 (see Sect.2.1).

		CE (Tv)	CE (T)	%
80	Au	1.71	1.59	7
	S	2.01	1.87	7
	O	2.17	2.03	7
	N	1.83	1.70	8
	D	2.08	1.93	8
81	Jn	2.11	1.96	8
	F	1.99	1.83	9
	M	2.03	1.87	9
	Ap	2.11	1.93	9
	My	1.87	1.69	11
	Jn	1.80	1.62	11
	Jl	1.75	1.58	11

A4. The global values of the monthly mean covariances between eddy available potential energy and eddy kinetic energy are shown for two sets of calculations in the table below. The use of T_v increases slightly the values of CE; differences should be expected to be larger in the tropics and lower troposphere but as the absolute values are small there nevertheless, they occur mainly in mid-troposphere and mid-latitudes. The increase corresponding to an integration for the whole atmosphere is of the order of 10%.

	NH											SH			
Author	Wiin-Nielsen	Manabe	Manabe	Peixoto	Tenenbaum	Tenenbaum	Baker	Baker	Miller	Oriol	Oriol	Stone	Miller	Oriol	Oriol
Year	67	70	70	74	76	76	77	77		82	82	77		82	82
AZ	4077	4990	4990	5580	5710	6080	6400	6100	5059	4671	4918	2790	3038	3289	3521
AE	1191	410	430	1049	822	779	670	390	850	774	812	380	246	272	278
KZ	1442	1300	1330	803	1030	1050	1400	830	976	942	1025	480	492	543	552
KE	1365	380	550	931	680	545	410	130	1003	981	1044	330	531	522	540
CA	3.7	1.8	2.1	2.8	2.07	1.84	2.6	1.4	3.24	2.95	3.1	1.2	.79	1.07	1.0
CK	-.29	-.2	-.2	-.3	-.08	-.26	0	-.1	-.24	-.55	-.6	-.3	-.54	-.74	-.7
CZ		.7	.4	-.1			1.7	.3		-.44	-.7	0.		-.16	-.1
CE		2.5	2.9	3.4	4.18	2.09	2.0	.8		2.72	2.8	1.9		1.32	1.3
length	1964			5yr					1981	1981	1981		1981		
levels	850-100			1000-50	945-65	945-65	850-100	850-100	1000-100	1000-100	1000-30		1000-100	1000-100	1000-30
coverage	20-Pole	NH	NH	NH	NH	NH	NH	NH	0-80	0-81	NH	SH	-80-0	-81-0	SH
comments		intgr. GFDL N20	intgr. GFDL N40		NMC observed	intgr. GISS	NCAR-A int.	NCAR-B int.	NMC			intgr. GISS	NMC		
period	← — —	— — — —	— — —	— — —	— — — —	January	— —	— — —	— —	— — —	— —	— —	— — —	— — —	→

A5. Integrated values of the energy budget terms found for different periods and areas for several authors.

	NH				SH				NH				
author year	Kruger 65	Newell 74	Tomatsu 79	Oriol 82	Newell 74	Oriol 82	Oort 64	Oort 64	Kruger 65	Oort 74	Peixoto 74	Tomatsu 79	Oriol 82
AZ		3000	2181	3458	3300	4228	3500	4000		3350	3700	1984	3654
AE		680 920	833	372	440 540	360	2000	1500		1560	739	884	516
KZ		280	726	497	450	786	500	800		360	464	719	577
KE		640	976	629	650	680	1000	700		880	703	960	707
CA	3.02	.8	3.09	1.74	.7 1.3	1.94	1.5	3.0	2.98	1.5		2.96	1.7
CK		-.30	-.45	-.57	-.22	-.63	-.3	-.4		-.3		-.43	-.5
CZ	-.74	-.17	-.44	-.21	-.08	-.27	.1	.1	-.66	-.2		-.40	-.2
CE	2.28		2.20	1.80		1.89	2.4	2.2	2.21	2.2		2.02	1.9
							compiled different authors						
length	Oct 58- Jul 63	5 yr	Oct 64- Sep 65	1980		1981			Oct 58- Jul 63	5 yr	5 yr	Oct 64- Sep 65	Aug 80- Jul 81
levels	850-200	1000- 100	925-10	1000- 30	1000- 100	1000- 30	all	all	850-200	1000-50	1000-50	925-10	1000-30
coverage	20-Pole	NH	20-75	NH	SH	SH	NH	NH	20-Pole	NH	NH	20-75	NH
comments							space- time	space		space- time			
period	← — — —	— — —	— autumn		— — —	— →	← — —	— —	— — — —	— — year — —		— — — —	— — →

A5. Contd.

	NH					SH		NH				SH	
author year	Kruger 65	Saltzmann 70	Newell 74	Tomatsu 79	Oriol 82	Newell 74	Oriol 82	Kruger 65	Newell 74	Tomatsu 79	Oriol 82	Newell 74	Oriol 82
AZ		2280	1900	1411	2392	2900	3679		3700	2054	3883	3600	5184
AE		780	550 630	599	462	360 420	299		650 950	866	521	510 680	340
KZ		560	150	362	269	340	572		480	714	615	510	1080
KE		990	500	600	505	570	573		670	942	721	670	650
CA	.72	1.7	.2 .3	.89	.53	.6 .9	1.18	3.04	.7 1.3	3.13	1.90	1.1 1.6	2.40
CK		-.7	-.19	-.22	-.26	-.33	-.65		-.35	-.35	-.51	-.30	-.74
CZ	-.30		-.07	-.17	.13	-.17	-.12	-.77	-.05	-.37	-.22	-.01	-.56
CE	.63	.6		.92	1.16		1.38	2.21		1.95	2.03		2.10
length	Oct 58-Jul 63		5 yr	Oct 64-Sep 65	1981	5 yr	1981	Oct 58-Jul 63	5 yr	Oct 64-Sep 65	1981	5 yr	1980
levels	850-200	all	1000-100	925-10	1000-30	1000-100	1000-30	850-200	1000-100	925-10	1000-30	1000-100	1000-30
cover-age	20-Pole	NH	NH	20-75	NH	SH	SH	20-Pole	NH	20-75	NH	SH	SH
comments													
Period	←			summer			→	←		spring			→

A5. Contd.

REFERENCES

Andrews, D.G.and M.E.McIntyre, 1976: Planetary waves in horizontal and vertical shear: the generalized E.P. relation and the mean zonal acceleration. J.Atmos.Sci., 33, 2031-2048.

Arpe, K.and E.Oriol, 1981: Energy calculations at ECMWF. Proceedings 6th Climate Diagnostic Workshop, Palisades, NOAA. p.285-291.

Baker,W.E.and E.C.Kung, 1977: Energetics diagnosis of the NCAR general circulation model. Mon.Wea.Rev., 105, 1384-1401.

Blackmon, M.L., J.M.Wallace, N.-C.Lau and S.L.Mullen, 1977: An observational study of the Northern Hemisphere wintertime circulation. J.Atmos.Sci., 34, 1040-1053.

Boer, G.J., 1975: Zonal and eddy forms of the available potential energy equations in pressure coordinates, Tellus, 27, 433-442.

Brown, J.A., 1964: A diagnostic study of tropospheric diabatic heating and the generation of available potential energy, Tellus, 16, 371-388.

Dopplick, T.G., 1971: The energetics of the lower stratosphere including radiative effects. Quart.J.Roy.Met.Soc., 97, 209-237.

Edmon,Jr. H.J., B.J.Hoskins, M.E.McIntyre, 1980: Eliassen-Palm cross sections for the troposphere. J.Atmos.Sci., 37, 2600-2616.

Eliassen, A. and E.Palm, 1961: On the transfer of energy in stationary mountain waves. Geofys.Publ., 22, 3, 1-23.

Hollingsworth, A., A.J.Simmons and B.J.Hoskins, 1976: The effect of spherical geometry on momentum transports in simple baroclinic flows. Quart.J.R.Met.Soc., 102, 901-911.

Hollingsworth, A. and G.Cats, 1981: Initialization in the Tropics. Workshop on tropical meteorology and its effects on medium range weather prediction at middle latitudes. ECMWF, pp.105-141.

Holopainen, E.O., 1970: An observational study of the energy balance of the stationary disturbances in the atmosphere. Quart.J.Roy.Met.Soc., 96, 626-644.

Kanamitsu, M., 1980: Some climatological and energy budget calculations using the FGGE-III-b analyses during January 1979. Dynamic Meteorology: Data Assimilation Methods. Ed.by L.Bengtsson, M.Ghil and E.Kallen. Applied Math.Sci., Vol.36, Springer Verl., New York, pp.263-318.

Kruger,A.F., J.S.Winston, D.A.Haines, 1965: Computations of atmospheric energy and its transformation for the Northern Hemisphere for a recent 5 year period. Mon.Wea.Rev., 93, 227-238.

Kung, E.C., 1967: Diurnal and long term variations of the kinetic energy generation and dissipation for a 5 year period. Mon.Wea.Rev., 95, 593-606.

Lau, N.-C. and A.H.Oort, 1981: A comparative study of observed Northern Hemisphere circulation statistics based on GFDL and NMC analyses. Part I: the time-mean fields. Mon.Wea.Rev., 109, 1380-1403.

Lau, N.-C. and A.H.Oort, 1982: A comparative study of observed Northern Hemisphere circulation statistics based on GFDL and NMC analyses. Part II: transient eddy statistics and the energy cycle. Mon.Wea.Rev., in press.

Lonnberg, P., 1980: Modifications to the operational analyses suite. Tech.Memo.No.15 ECMWF.

Lorenc, A., I.Rutherford, and G.Larser, 1977: The ECMWF analysis and data assimilation scheme. Analysis of mass and wind fields. ECMWF Tech.Rep.No.6.

Lorenc, A., 1981: Global 3-dimensional multivariate statistical interpolation scheme. Mon.Wea.Rev., 109, 701-721.

Lorenz, E.N., 1955: Available potential energy and the maintenance of the general circulation. Tellus, 7, 157-167.

Lorenz, E.N., 1967: The nature and theory of the general circulation of the atmosphere. WMO Publ.218. TP.115, Geneva.

Mak, M.-K., 1969: Laterally driven stochastic motions in the tropics. J.Atmos.Sci., 26, 41-64.

Manabe,S., J.Smagorinsky, J.L.Holloway, Jr., and H.M.Stone, 1970: Simulated climatology of a general circulation model with a hydrologic cycle. III.Effects of increased horizontal computational resolution. Mon.Wea.Rev., 98, 176-213.

Miller, A.J., 1970: The transfer of kinetic energy from the troposphere to the stratosphere. J.Atmos.Sci., 27, 388-393.

Miller, A.J., 1971: Kinetic energy and the quasi-biennial oscillation. Mon.Wea.Rev., 99, 912-918.

Miller, A.J., 1974: Periodic variation of atmospheric circulation at 15-16 days. J.Atmos.Sci., 31, 720-728.

Miller, A.J., W.Collins and D.Dubofsky, 1975: The NMC operational global energy program. NMC Office Note 109, 15p.

Miller, A.J. and C.M.Hayden, 1978: The impact of satellite derived temperature profiles on the energetics of NMC analyses and forecasts during August 1975 data system test. Mon.Wea.Rev., 106, 390-398.

Murakami, T., 1967: Vertical transfer of energy due to stationary disturbances induced by topography and diabatic heat sources and sinks. J.Meteor.Soc.Japan, 45, 205-230.

McIntyre, M.E., 1970: On the non-separable baroclinic parellel flow instability problem. J.Fluid Mech., 70, 2, 273-306.

Newell, R.E. and M.E.Richards, 1969: Energy fluxes and convergence patterns in the lower and midddle stratosphere during IQSY. Quart.J.R.Met.Soc., 95, 310-328.

Newell, R.E., D.G.Vincent, J.W.Kidson, T.G.Dopplick and D.Ferruzza, 1970: The energy blance of the global atmosphere. In the Global Circulation of the atmosphere. G.A.Corby, London, Roy.Met.Soc., -42-90.

Newell, R.E., J.W.Kidson, D.G.Vincent, G.J.Boer, 1972, 1974: The general circulation of the tropical atmosphere and interactions with extratropical latitudes: Vol.I and II. MIT Press, Cambridge, Mass.

Oort, A.H., 1964: On estimates of the atmospheric energy cycle. Mon.Wea.Rev., 92, 483-493.

Oort, A.H., 1971: The observed annual cycle in the meridional transport of atmospheric energy. J.Atmos.Sci., 28, 325-339.

Oort, A.H. and J.P.Peixoto, 1974: The annual cycle of the energetics of the atmosphere in a planetary scale. J.Geoph.Res., 79, 2705-2719.

Oort, A.H. and J.P.Peixoto, 1982: Global angular momentum and energy balance requirements from observations. Adv.in Geophy., 26.

Oort, A.H., and E.M.Rasmusson, 1970: On the annual variation of the monthly mean meridional circulation. Mon.Wea.Rev., 98, 423-442.

Oort, A.H., and E.M.Rasmusson, 1971: Atmospheric circulation statistics. NOAA Prof.Paper 5.

Oriol, E.P., 1080: Verification of fluxes and energetics for ECMWF forecasts. Proceedings XVIII Reunion Bienal RSEFQ Burgos, libro F, 10-13.

Oriol, E.P., 1980: Operational diagnostic calculations at ECMWF. Res.activities in atmospheric and ocean modelling. GARP num.exper.programme, Rep. 1, 9.10-11.

Oriol, E.P., 1981: Energetics operationally calculated at ECMWF. Res.activities in atmospheric and oceanic modelling. GARP num.exper.programme, Report 2, 8.1.

Oriol, E.P., 1981: El Ciclo energetico durante el invierno 1980-81. Proceedings IV Asamblea Geodesia y Geofisica (in press).

Oriol, E.P., 1982: El ciclo energetico de la atmosfera en las predicciones del ECMWF. Proceedings XIX Reunion Bienal RSEFQ Santander 9.9, 119-120.

Palmen, E. and C.W.Newton, 1969: Atmospheric circulation systems. International Geophysics Series, Vol.13. Ac.Press, N.Y., 603p.

Paulin, G. 1968: Spectral atmospheric energetics during January 1959. AFCRL-68-0476. Bedford, Mass.

Peixoto, J.P., N.E.Gaut and R.D.Rosen 1973 Kinetic energy conversions by horizontal and eddy processes from 5 years of hemispheric data. J.of Geoph.Res., 78, 2630-2649.

Peixoto, J.P., and A.H.Oort, 1974: The annual distribution of atmospheric energy on a planetary scale. J.Geophy.Res., 79, 2149-2159.

Reiter, E.R., 1969: Mean and eddy motions in the atmosphere. Mon.Wea.Rev., 97, 200-204.

Rosen, R.D., and D.A.Salstein, 1980: A comparison between circulation statistics computed from conventional data and NMC Hough Analyses. Mon.Wea.Rev., 108, 1226-1247.

Saltzman, B., 1957: Equations governing the energetics of the larger scales of atmospheric turbulence in the domain of wave number. J.of Meteorol., 14, 513-523.

Saltzman, B., 1970: Large-scale atmospheric energetics in the wave number domain. Rev. Geophys.Space Phys. 8, 289-302.

Savijarvi, H. 1981: Energy budget calculation from FGGE analyses and ECMWF forecasts. Proceedings International Conference on Preliminary FGGE data analysis and results. Bergen, pp.536-541. WMO, GARP.

Savijarvi, H., 1981: Winter and summer circulation statistics based on ECMWF operational analysis and forecasts. Tech.Memo.No.38, ECMWF.

Schilling, H.D., 1981: Persistent baroclinic outbursts related to long atmospheric waves. Proceedings IAMAP (in press).

Simmons, A.J. and B.J.Hoskins, 1978: The life cycles of some nonlinear baroclinic waves. J.Atmos.Sci., 35, 414-432.

Speth, P., 1975: The variability of the available potential energy, Meteorol.Rdsch., 28, 161-178.

Speth, P., 1978: The global energy budget of the atmosphere. Part I: The annual cycle of available potential energy and its variability throughout a ten year period (1967-1976). Beit.zur.Physik der Atmo., 51, 257-280.

Stone, P.H., S.Grow, and W.J.Quirk, 1977: The July climate nd a comparison of the January and July climates simulated by the GISS GCM, Mon.Wea.Rev., 105, 170-194.

Temperton, C., 1980: Design of the ECMWF normal mode initialization procedure. Seminar on data assimilation methods. ECMWF, 159-194.

Temperton, C., and D.Williamson, 1981: Normal mode initialization for a multi-level gridpoint model.Pt.1 Linear Aspects. Mon.Wea.Rev., 109, 4, p729-743

Tenenbaum, J., 1976: Spectral and spatial energetics of the GISS model atmosphere. Mon.Wea.Rev., 104, 15-30.

Tibaldi, S., and J.-F.Geleyn, 1981: The production of a new orography land-sea mask and associated climatological surface fields for operational purposes. ECMWF Tech.Memo.No.40.

Tomatsu, K., 1979: Spectral energetics of the troposphere and lower stratosphere. Adv.in Geophy., Vol. 21, Ac.Press, 289-405.

Wiin-Nielsen, A., 1967: On the annual variation and spectral distribution of atmospheric energy. Tellus, 19, 540-558.

Wiin-Nielsen, A., 1968: On the intensity of the general circulation of the atmosphere. Rev. of Geophys., 6, 559-579.

Williamson, D.L. and C.Temperton, 1981: Normal mode initialization for a multilevel grid-point model. Pt.2 Nonlinear aspects. Mon.Wea.Rev., 109, 4, 744-757.

ECMWF PUBLISHED TECHNICAL REPORTS

No. 1 A Case Study of a Ten Day Prediction

No. 2 The Effect of Arithmetic Precisions on some Meteorological Integrations

No. 3 Mixed-Radix Fast Fourier Transforms without Reordering

No. 4 A Model for Medium-Range Weather Forecasting - Adiabatic Formulation

No. 5 A Study of some Parameterizations of Sub-Grid Processes in a Baroclinic Wave in a Two-Dimensional Model

No. 6 The ECMWF Analysis and Data Assimilation Scheme - Analysis of Mass and Wind Fields

No. 7 A Ten Day High Resolution Non-Adiabatic Spectral Integration: A Comparative Study

No. 8 On the Asymptotic Behaviour of Simple Stochastic-Dynamic Systems

No. 9 On Balance Requirements as Initial Conditions

No.10 ECMWF Model - Parameterization of Sub-Grid Processes

No.11 Normal Mode Initialization for a multi-level Gridpoint Model

No.12 Data Assimilation Experiments

No.13 Comparison of Medium Range Forecasts made with two Parameterization Schemes

No.14 On Initial Conditions for Non-Hydrostatic Models

No.15 Adiabatic Formulation and Organization of ECMWF's Spectral Model

No.16 Model Studies of a Developing Boundary Layer over the Ocean

No.17 The Response of a Global Barotropic Model to Forcing by Large-Scale Orography

No.18 Confidence Limits for Verification and Energetics Studies

No.19 A Low Order Barotropic Model on the Sphere with the Orographic and Newtonian Forcing

No.20 A Review of the Normal Mode Initialization Method

No.21 The Adjoint Equation Technique Applied to Meteorological Problems

No.22 The Use of Empirical Methods for Mesoscale Pressure Forecasts

No.23 Comparison of Medium Range Forecasts made with Models using Spectral or Finite Difference Techniques in the Horizontal

No.24 On the Average Errors of an Ensemble of Forecasts

No.25 On the Atmospheric Factors Affecting the Levantine Sea

No.26 Tropical Influences on Stationary Wave Motion in Middle and High Latitudes

ECMWF PUBLISHED TECHNICAL REPORTS

No.27 The Energy Budgets in North America, North Atlantic and Europe Based on ECMWF Analyses and Forecasts

No.28 An Energy and Angular-Momentum Conserving Vertical Finite-Difference Scheme, Hybrid Coordinates, and Medium-Range Weather Prediction

No.29 Orographic Influences on Mediterranean Lee Cyclogenesis and European Blocking in a Global Numerical Model

No.30 Review and Re-assessment of ECNET - a private network with Open Architecture

No.31 An Investigation of the Impact at Middle and High Latitudes of Tropical Forecast Errors

No.32 Short and Medium Range Forecast Differences Between a Spectral and Grid Point Model. An Extensive Quasi-Operational Comparison

No.33 Numerical Simulations of a Case of Blocking: The Effects of Orography and Land-Sea Contrast

No.34 The Impact of Cloud Track Wind Data on Global Analyses and Medium Range Forecasts

No.35 Energy Budget Calculations at ECMWF. Part I: Analyses 1980-1981